



HAL
open science

Testing the Curie-de Gennes conjecture

Fatima Rida

► **To cite this version:**

Fatima Rida. Testing the Curie-de Gennes conjecture. Theoretical and/or physical chemistry. Université Grenoble Alpes, 2017. English. NNT : 2017GREAV061 . tel-01712692

HAL Id: tel-01712692

<https://theses.hal.science/tel-01712692>

Submitted on 27 Feb 2018

HAL is a multi-disciplinary open access archive for the deposit and dissemination of scientific research documents, whether they are published or not. The documents may come from teaching and research institutions in France or abroad, or from public or private research centers.

L'archive ouverte pluridisciplinaire **HAL**, est destinée au dépôt et à la diffusion de documents scientifiques de niveau recherche, publiés ou non, émanant des établissements d'enseignement et de recherche français ou étrangers, des laboratoires publics ou privés.

THÈSE

Pour obtenir le grade de

**DOCTEUR DE LA COMMUNAUTE UNIVERSITE
GRENOBLE ALPES**

Spécialité : **Chimie Physique Moléculaire et Structurale**

Arrêté ministériel : 25 mai 2016

Présentée par

Fatima Sobhi RIDA

Thèse dirigée par **Cyrille TRAIN (csv) Professeur (UGA)** et
codirigée par **Ghenadie NOVITCHI (csv), ingénieur de recherche
(cnrs)**.

Préparée au sein du **Laboratoire LNCMI- Laboratoire National
des Champs Magnétique Intenses**
dans **l'École Doctorale Chimie et Sciences du Vivant**

Tester la conjecture de Curie-de Gennes

Thèse soutenue publiquement le «**11 Octobre 2017**»,
devant le jury composé de :

Madame Anne MILET

Professeur, DCM-UGA, Président du Jury

Madame Jeanne CRASSOUS

Directeur de recherche, Institut des Sciences Chimiques de Rennes-
CNRS-Université de Renne 1, Examineur

Monsieur Narcis AVARVARI

Directeur de recherche, Laboratoire Moltech-Anjou- Université d'Angers,
Rapporteur

Monsieur Patrick ROSA

Chargé de recherche, ICMCB-CNRS- Université de Bordeaux, Rapporteur

Monsieur Geert RIKKEN

Directeur de recherche, LNCMI-CNRS, Grenoble et Toulouse, Membre
Invité



Acknowledgements

*“ On ne remarque jamais ce qui a été fait,
On ne peut voir que ce qu’il reste à faire .”*

M. Curie

This scientific report has been possible through the direct and indirect cooperation of various people and bears the imprint of their efforts on my work. Thereby, I take this opportunity to acknowledge the invaluable assistance of all those people who helped me in this project.

First and foremost, I would like to express my deepest appreciation and gratitude to my supervisor **Professor Cyrille TRAIN** for giving me a chance to work in LNCMI laboratory, also for his insight, advice, guidance, support and teaching me valuable things which might not be possible at any other place.

I would also like to thank my co-supervisor **Dr. Ghenadie NOVITCHI** for his guidance and teaching me valuable things during the first year of my PhD.

I would like to thank the director of LNCMI laboratory, **Dr. Geert RIKKEN** for being kind, ever-present to answer all my doubts and questions and giving valuable time to enhance my knowledge regarding this project. He has been very patient while dealing and carrying out experiments and guiding my doubts.

Generally, **Prof. Cyrille TRAIN** and **Dr. Geert RIKKEN** have encouraged and given me moral support and guided me in different matters regarding this project. They have been a huge source of knowledge and positive energy.

Furthermore, I would like to thank them for giving me the valuable opportunity to have a new engineering contract that allowed me to repeat the final experiments done during my PhD using E7 mixture of Liquid Crystal that delivered prior to my final defense.

Besides my supervisors, I would like to thank the rest of my thesis committee **Prof. Anne MILET**, **Dr. Jeanne CRASSOUS**, **Dr. Narcis AVARVARI** and **Dr. Patrick ROSA** for accepting our invitation to evaluate and judge my work done over the last three years.

I also wish to express my gratitude towards LNCMI-CNRS for providing lab facilities to conduct my experimental work project and **Professor Eric BEAUGNON** for allowing me to use the superconducting magnet several times.

I'm thankful for my colleagues, **Ivan BRESLAVETZ**, **Michael HAKL**, **Julien JOUSSET** and **Kevin PAILLOT** for their valuable advice, encouragement, help and support during my thesis. Also, to all the staff of lab for providing technical support, their kind help and co-operation throughout my study period.

Moreover, I would like to thank the **French National Research Agency (ANR)** for my PhD funding.

Acknowledgements

Thank you to my mother and father, who have always shown me an unswerving trust. Without their enthusiasm, their encouragement and their unwavering support, all this could not have been possible.

Sincere appreciation to my beloved sister **Nassima** and her family for their unconditional support and advice especially for coming from Switzerland to attend my final defense.

Thank you also to my brothers and my sister **Zeinab**.

Finally, I thank my friends who have contributed greatly to the completion of this thesis project.

Thanks to **Emna, Zeinab, Waad, Monika, Jacoub, Hiba, Tamara, Sanaa, Elissar, Amal, Rana, Roxana, Banan,** and **Maria** for sharing both good and hard moments of my thesis.

I address a particular thought **Mr. Alain BOURRET** for his help in improving my French language and also for attending my final defense with his wife **Danièle BOURRET**.

One page turns, another opens, thank you to everyone who contributed and made me make the right choices.

*“La patience et la persévérance
sont les source du succès”*

Fatima RIDA

Résumé (FR)	1
Abstract (EN)	3
Introduction (FR)	4
Introduction (EN)	7
CHAPTER I STATE OF THE ART	9
I. Abstract	9
I.1. Chirality	9
I.2. Problem of Homochirality	10
I.3. Historical Background.....	11
I.4. Discrete Symmetries (Parity, Time Reversal & Charge Conjugation)	12
I.5. The Reason behind Unsuccessful attempts of Pasteur’s Experiments.....	13
I.6. Breaking of the Symmetry in Different Aspects	14
I.6.a. Asymmetric Photochemistry	15
I.6.a.1. Circular Polarized Light	15
I.6.a.1.a. Photodestruction	15
I.6.a.1.b. Photoresolution	17
I.6.a.1.c. Asymmetric Photosynthesis	19
I.6.a.2. Magnetochiral Dichroism.....	20
I.6.b. Parity Violation in a Weak Nuclear Interaction	24
I.7. Curie de-Gennes conjecture (CdG).....	26
I.7.a. Historical Background.....	26
I.7.b. General Concepts of True and False Chirality.....	26
I.7.c. Representation of Falsely Chiral Influence using a Simple Example	28
I.7.d. Amplified Mechanisms Alone are not Sufficient to Explain the Origin of Homochirality.....	29
I.7.e. Incomplete Experimental Evidence for Falsely Chiral Influence.....	30
I.8. Main objective.....	33
References.....	34
CHAPTER II ENANTIO-SELECTIVE CRYSTALLIZATION	38
II. Abstract	38
II.1. General Description of MOF Compound	39
II.2. Motivation	40
II.3. Experimental Procedures	42
II.3.a. Synthesis of Ammonium Tris(oxalate)Chromate(III).....	42
II.3.b. Synthesis of 3-D Chiral Bimetallic Oxalate-Based Magnet	42
II.4. Characterization of the Chiral MOF.....	43
II.4.a. Powder X-ray Diffraction (PXRD)	43
II.4.b. Thermogravimetric Analysis (TGA)	44
II.5. Instrumentation and NCD Operating Principle.....	45
II.6. General Method	46
II.6.a. Sample Preparation	46
II.6.b. Resultant Spectra	47
II.6.b.1. 3-Dimensional NCD Spectrum.....	47
II.6.b.2. Single Frequency Measurements	48
II.6.b.3. 2-Dimensional NCD spectra	51
II.6.c. Global Method Used for NCD Data Analysis	52
II.6.d. Treatment Procedure	53
II.6.e. DAPI Test.....	54
II.6.f. Different Techniques Used to Study the Effect of External Forces	55

II.6.f.1. Crystallization in a Magnetic Field	55
II.6.f.1.a. Low Field	55
II.6.f.1.b. High Field	56
II.6.f.2. Crystallization in a High Speed of Rotation.....	57
II.6.f.2.a. First Rotatory Plates.....	57
II.6.f.2.b. Second Rotatory Plate	58
II.7. Results & Discussions	58
II.7.a. Evaluation the excess of lambda enantiomer.....	59
II.7.b. Crystallization of $(\text{NH}_4)_4[\text{MnCr}_2(\text{ox})_6]\cdot 4\text{H}_2\text{O}$ using Different Conditions	60
II.7.b.1. Crystallization of chiral MOF using D/L phenylalanine respectively.....	60
II.7.b.2. Crystallization of Chiral MOF using Tri-distilled Water.....	61
II.7.b.3. Crystallization of Chiral MOF using a New Treatment Method of Used Glassware at Different Temperature.....	61
II.7.c. Studying the effect of external forces on the ratio of Λ and Δ enantiomers	65
II.7.c.1. Crystallization in the presence of magnetic field	65
II.7.c.1.a. Low Field.....	65
II.7.c.1.b. High Field.....	68
II.7.c.2. Crystallization in the presence of rotational force.....	70
II.7.c.2.a. Unstable Rotation.....	70
II.7.c.2.b. Orbital and stable Rotation	71
II.8. General Conclusion	71
References.....	73
CHAPTER III MAGNETO-ELECTRIC ENANTIO-SELECTIVE CATALYSIS.....	75
III. Abstract.....	75
III.1. Atropisomerism of Biphenyl System	75
III.2. Estimation of the Strength of the Effect with an Atropisomeric Model	76
III.2.a. In the Absence of an Externally Applied Magnetic and Electric Fields	76
III.2.b. In the Presence of Magnetic and Electric Fields.....	77
III.3. General Properties and Motivation for using Racemic Atropisomeric Based Nematic Liquid Crystals ...	79
III.4. General and Experimental Methods	81
III.4.a. Typical Structure of Sandwich type LC cell	81
III.4.b. Fabrication of Liquid Crystal Cells using Different Methods	82
III.4.b.1. Mechanical Rubbing	82
III.4.b.1.a. On Glass using Diamond Papers.....	82
III.4.b.1.b. On PVA Polymer Layer using Optical Tissue	83
III.4.b.2. Magnetic Field Alignment.....	84
III.4.c. Experimental Setup.....	85
III.5. Results and Discussion	87
III.5.a. Mechanical rubbing	87
III.5.a.1. On Glass using Diamond Papers	87
III.5.a.1.a. Observation Under Microscope	87
III.5.a.1.b. Optical Measurements under the Effect of Magnetic and Electric Fields.....	87
III.5.a.2. On PVA Polymer Layer using Optical Tissue.....	88
III.5.a.2.a. Observation Under Microscope	88
III.5.a.2.b. Optical measurements under the Effect of Magnetic and Electric Fields.....	89
III.5.b. Static Magnetic Field	90
III.5.b.1. Evolution of Averaging R and α in Time	90
III.5.b.2. Frequency Dependence.....	91
III.5.b.3. Linear Dependence of the Combined E and B on the e.e. of NLCs.....	92
III.6. General Conclusion and perspectives	94
References.....	95
General conclusion (EN).....	97

Table of contents

Conclusion Générale (FR)	99
Perspectives (EN)	102
Perspectives (FR)	103

Résumé (FR)

“La vie ne produit pas de corps symétrique”

L. Pasteur

Briser la symétrie-miroir est un sujet fascinant qui revêt un rôle crucial en physique, en chimie et en biologie.

Le but ultime de cette étude est de démontrer expérimentalement la conjecture de Curie de-Gennes. Cette hypothèse a été proposée pour la première fois par P. Curie 1894 et plus tard développée par De-Gennes. Elle indique qu'il est possible de générer une dissymétrie (excès énantiomérique (e.e.)) en soumettant un mélange racémique à l'influence combinée de champs magnétique et électrique colinéaires. Une telle influence modifie la cinétique du système : selon l'orientation relative des champs magnétique et électrique, l'un des énantiomères est formé plus rapidement que l'autre en raison d'une énergie d'activation inférieure (E_a). Une telle influence a été ultérieurement appelée « faussement chirale » par Barron.

Pour démontrer expérimentalement cette conjecture, deux expériences différentes ont été développées :

- 1) La cristallisation énantiosélective d'un réseau de coordination chiral sous des influences physiques externes (champ magnétique ou force de rotation) par diffusion lente. Un petit e.e. est supposé être créé puis amplifié par la croissance des cristaux à l'interface solvant/vapeur d'éthanol. Dans cette expérience, nous avons constaté que la démonstration de conjecture de Curie de Gennes est difficile à atteindre en raison de la forte dispersion de la moyenne des valeurs du e.e. obtenues et de la faiblesse de l'effet attendu.
- 2) La création d'un e.e. dans un atropisomère racémique d'un cristal liquide à base de biphényle en appliquant des champs magnétique et électrique (anti) parallèles. Un arrangement supramoléculaire hélicoïdal des molécules de biphényles dans la phase nématique augmentera le signal lié à la présence d'un e.e. à un niveau mesurable. Au cours de cette seconde expérience, nous avons observé expérimentalement un e.e. des dérivés à base de biphényle induit par une combinaison (anti)parallèle de champs magnétique et électrique. Cet excès dépend linéairement du produit des champs magnétique et électrique et l'ordre

de grandeur des résultats observés expérimentalement correspond aux estimations théoriques. Compte tenu des résultats obtenus, sous réserve d'ultimes vérifications, cette expérience constitue une démonstration expérimentale convaincante de la conjecture Curie de Gennes.

Abstract (EN)

“La vie ne produit pas de corps symétrique”

L. Pasteur

Mirror symmetry breaking is an ever-fascinating topic that plays a crucial role in physics, chemistry, and biology.

The ultimate goal of this study is to demonstrate experimentally the so-called Curie de-Gennes conjecture. It was proposed for the first time by P. Curie (1894) and later developed by de-Gennes. It stipulates that it is possible to generate dissymmetry (enantiomeric excess (e.e.)) by submitting a racemic mixture to the combined influence of collinear magnetic and electric fields. Such influence modifies the kinetics of the system: depending on the relative orientation of the magnetic and electric fields, one of the enantiomers is formed faster than the other because of a lower activation energy (E_a). This influence was later named by Barron as « falsely chiral ». To demonstrate this conjecture, two different experiments were developed:

- 1) The enantioselective crystallization of a chiral metal-organic framework under external physical influence (magnetic field or rotation force) by slow diffusion. The small e.e. is expected to be created and amplified by crystal growth at the interface aqueous solution / ethanol-saturated vapors. In this experiment, we have found that the Curie de-Gennes conjecture demonstration is difficult to achieve due to high dispersion of the average of the observed e.e. and the weakness of the expected effect.
- 2) Creating an e.e. in a racemic atropisomeric biphenyl based liquid crystal by applying (anti)parallel magnetic and electric fields. The helical twisting power of biphenyls molecules in the nematic phase will enhance the dichroic signal related to the expected e.e. to a measurable level.

During this second experiment we have experimentally observed an e.e. in biphenyl-based nematic liquid crystals induced by (anti)parallel combination of magnetic and electric fields. This excess was linearly dependent on the product of magnetic and electric fields and, within one order of magnitude, its absolute value corresponds to the theoretical estimation. Ultimate checks shall confirm that these results constitute a convincing experimental demonstration of the Curie de Gennes conjecture.

Introduction (FR)

“Il n’est pas d’effet sans causes”

&

“Il n’est pas de causes sans effets”

P. Curie[1]

La vie terrestre utilise globalement la version L des acides aminés (configuration gauche). Cette propriété est étroitement liée à l'homochiralité de la vie [2]. La raison de la préférence d'un énantiomère sans traces de l'acide aminé droit (D) "non naturel" a stimulé les efforts, pendant longtemps, pour comprendre son origine.

En 1848, Louis Pasteur [3] était l'un des premiers chercheurs qui ont découvert le concept d'énantiomorphisme par la séparation manuelle des cristaux d'acide tartrique L et D, puis il a démontré que des solutions correspondantes tournent le plan de polarisation vers la direction gauche ou droite.

La production d'un excès énantiomérique (e.e.) sans intervention d'un produit chimique est nécessaire pour justifier l'homochiralité de la vie. De nombreuses tentatives ont été faites pour produire des produits énantiomériquement enrichis à partir de précurseurs achiraux ou racémiques sans l'intervention de réactifs chimiques ou de catalyseurs chiraux. Pasteur [4] a essayé de produire des cristaux chiraux dans un champ magnétique après la découverte par Faraday de polarisation rotatoire induite par le champ magnétique.

Les résultats négatifs obtenus ne l'ont pas découragé à essayer des expériences apparentées, telles que l'induction d'une activité optique en effectuant des réactions dans une centrifugeuse [5]. Toutes ces expériences n'ont pas abouti à former un excès énantiomérique (e.e.) à partir de précurseurs achiraux. Pasteur a conclu que seulement un phénomène cosmique encore inconnu ou des forces asymétriques peuvent expliquer la dissymétrie observée dans les substances naturelles. En 1894, Pierre Curie [1] a réexaminé les expériences de Pasteur sur les forces chirales dans la nature. Il a proposé que la combinaison énantiomorphe des champs magnétiques et électriques colinéaires crée une influence qui pourrait conduire à une énantiosélectivité. En 1970, De Gennes [6] a déclaré que dans une telle situation, la production d'excès énantiomérique dans le système s'appuie sur la vitesse de transition entre le deux énantiomère plutôt que sur l'équilibre lui-même.

Briser la symétrie en utilisant cette chiralité fondamentale est en principe possible; cependant, elle n'a toujours pas été suffisamment prouvée expérimentalement [7],[8].

Cette thèse est consacrée à démontrer expérimentalement la conjecture Curie-de Gennes, en présence d'une influence fausse chirale. Deux expériences différentes ont été développées pour examiner l'hypothèse de Curie :

- La première est la cristallisation énantiosélective d'un métal organique chiral $(\text{NH}_4)_4[\text{MnCr}_2(\text{ox})_6].4\text{H}_2\text{O}$ par diffusion lente sous le champ magnétique ou sous une force de rotation élevée. Cet effet est renforcé par la croissance des cristaux à l'interface solvant/vapeur d'éthanol.
- La deuxième est basée sur le déplacement de l'équilibre atropisomérique des biphenyls sous l'effet combiné du champ électrique et magnétique. En utilisant les biphenyls sous forme d'un cristal liquide nématique, le comportement collectif permet d'amplifier un très petit excès énantiomérique dans une rotation optique mesurable. Le travail sur cette expérience a été réalisé avec la collaboration, le suivi et la coopération de Dr. Geert RIKKEN- directeur du laboratoire LNCMI.

Au cours de ma thèse, j'ai travaillé sur deux sujets connexes. Le premier sujet est la synthèse de complexes de métal hétéroleptique dont l'équilibre entre les configurations *trans*, *A-cis* et *Δ -cis* a déjà été étudié par RMN [9] puisque nous avons initialement prévu d'utiliser ces molécules pour tester la conjecture Curie-de Gennes [10]. Nous avons finalement changé d'avis pour utiliser des systèmes plus prometteurs.

Néanmoins, les propriétés magnétiques de ces molécules ont été soigneusement étudiées au laboratoire. J'ai également synthétisé des molécules fluorées chirales pour la détection d'énantiomères par RMN (S. Krämer, LNCMI). La mauvaise description de la synthèse de l'un des précurseurs dans la publication de C. Lui *et al.* a conduit à de nombreux essais infructueux [11]. Enfin, le retrait de l'article correspondant a permis S. Krämer de se concentrer sur le développement en cours de l'expérience réalisée et de la tester sur des produits commerciaux [12]. Afin d'éviter une présentation variée et désordonnée, ces deux sujets ne seront pas présentés et ce rapport sera uniquement consacré à la présentation des résultats directement liés à la démonstration expérimentale de la conjecture Curie-de Gennes.

Ainsi, ce manuscrit sera divisé en trois chapitres :

Le premier sera consacré à donner des définitions essentielles à propos de la chiralité et à rappeler l'état de la technique concernant la production d'excès énantiomériques sous des influences physiques.

Le deuxième chapitre décrit nos efforts pour générer un e.e. contrôlé par cristallisation sous champ magnétique ou par rotation de l'échantillon.

Les expériences sur l'atropisomérisation des molécules de biphényle sous les champs électriques et magnétiques sont présentées dans le troisième chapitre. Enfin, le manuscrit contient les conclusions et les perspectives de la thèse.

Introduction (EN)

“Il n’est pas d’effet sans causes”

&

“Il n’est pas de causes sans effets”

P. Curie[1]

Terrestrial life utilizes only the left-handed version of amino acids, a pattern that is known as the homochirality of life [2]. The reason for preference of one enantiomer with no traces of “unnatural” D-amino acid has stimulated long-standing efforts to understand its origin.

In 1848, Louis Pasteur [3] was one of the first researchers to discover the concept of enantiomorphism by the manual separation of the left- and right-handed tartaric acid crystals (sodium-ammonium double salt). He then found that the corresponding solutions rotate the plane of polarization of light at sodium D line in opposite directions.

In order to reproduce the production of an enantiomeric excess (e.e.) without the intervention of any resolved chemical needed to justify the homochirality of life, numerous attempts were done starting from achiral or racemic precursors submitted to physical influences. Following Faraday’s discovery of magnetically-induced optical activity, Pasteur [4] tried to grow chiral crystals in a magnetic field. The negative results did not discourage him from trying related experiments, such as attempts to induce optical activity by performing reactions in a centrifuge [5]. Since all these attempts failed to form measurable e.e. from achiral precursors, Pasteur concluded that only a still unknown cosmic phenomenon or asymmetric forces could explain the dissymmetry observed in the natural substances.

In 1894, using symmetry arguments, Pierre Curie [1] re-examined Pasteur’s experiments on chiral forces in nature and proposed that the combination of collinear magnetic and electric fields creates an influence that should be able to lead to an e.e.. In 1970, De Gennes [6] stated that, in such a situation, the production of e.e. relies on different transition rates toward the two enantiomers rather than a modification of the equilibrium itself. This possibility is known as the Curie-de Gennes conjecture. Up to now, their prediction is still not fully supported experimentally [7],[8]. This thesis was mostly devoted to convincingly demonstrate experimentally the Curie de-Gennes conjecture. Two different experiments were developed towards this goal:

- The enantioselective crystallization of a chiral metal-organic framework at the interface between an aqueous solution and ethanol-saturated vapors by slow diffusion of ethanol under

the high magnetic field or rotation force. The production of a measurable e.e. should be favored by crystal growth.

- The atropisomerization of biphenyl molecules in a liquid crystalline phase under the combined effect of electric and magnetic fields. The detection of the expected e.e. by optical rotation measurements is favored by the large helical twisting power (HTP) of the chiral biphenyls mixture taken in its nematic liquid crystalline phase. The work on this experiment was carried out under the guidance, collaboration, and continuous active participation of the director of LNCMI laboratory- Dr. Geert RIKKEN.

Moreover, during the past three years, I have been working on two related subjects. The first one is the synthesis of heteroleptic metal complexes whose equilibrium between the *trans*, *A-cis* and *Δ-cis* configurations was previously studied by NMR [9]. I undertook this synthetic work because we initially intended to use these molecules to test the Curie-de Gennes conjecture[10]. We finally switched to more promising systems. Nonetheless, the magnetic properties of these molecules were thoroughly studied in the laboratory. I also spent some time in synthesizing chiral fluorinated molecules for detection of enantiomers by NMR (S. Krämer, LNCMI). The poor description of the synthesis of one of the precursors [11] led to many unfruitful tries. Finally the withdrawal of the corresponding paper led S. Krämer to concentrate on the still ongoing development of the set-up and, though they are expected to be less efficient [12], to test it on commercial products. In order to avoid a miscellaneous and messy presentation, these two subjects will not be presented in this report.

Accordingly, this manuscript will be solely devoted to the presentation of the results directly related to the experimental demonstration of the Curie-de Gennes conjecture. It will be divided into three chapters:

The first one will give essential definitions about chirality and recall the state of the art about the production of enantiomeric excess under physical influences.

The second chapter will describe our efforts in generating a controlled e.e. by crystallization under magnetic field or by rotating the sample.

The experiments on the atropoisomerisation of biphenyl molecules under electric and magnetic fields will be presented in a third chapter. Finally, some conclusions and perspectives will be presented.

Chapter I State of the Art

I. Abstract

“La vie est fonction de la dissymétrie de l’univers”

L. Pasteur [4]

There are many unsolved problems concerning the origin of life. One of them is related to the enantioselection of one set of optical isomers over the other. That’s why, several processes could be postulated to explain origin of the optical activity on the Earth.

In this introductory chapter, the origin of chirality, problem of homo-chirality and an overview of the various methods reported to control molecular chirality will be illustrated. In the second part of this chapter, the history of the Curie-de Gennes conjecture and the consequences of this proposal in terms of symmetry arguments are discussed. Finally, the main goals of the currently presented research are given.

I.1. Chirality

The term chirality originates from Greek word “χειρ” (Kheir) which means “hand” [13]. It was previously defined by Pasteur as dissymmetry and latter Lord Kelvin replaced it by the term chirality “I call any geometrical Equz, or group of points, *chiral*, and say that it has chirality, if its image in a plane mirror, ideally realized, cannot be brought to coincide with itself” [4], [14], [15]. In other words, chirality means that a system exists in two forms, that are non-superimposable mirror images of each other, called enantiomers. This characteristic is independent of the orientation of the objects, and it is easily recognized. For example, our hands are chiral, hence the name.

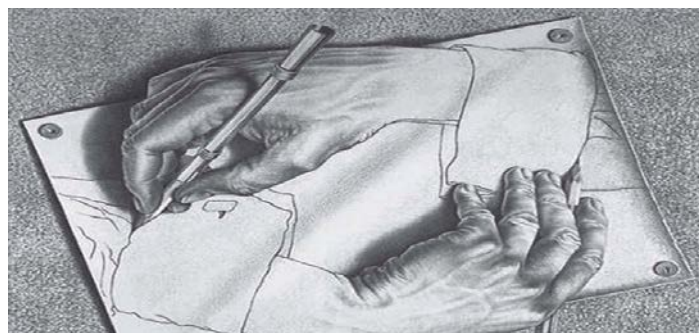


Figure I-1 Chirality status represented as defined by Pasteur and Lord Kelvin.

The simple question rose by G. H. Wagnière [16] in accordance to Figure I-1 “If the right hand draws the left hand, and the left hand draws the right hand then how did it start?” triggers many speculations.

I.2. Problem of Homochirality

A scientific topic directly related to these speculations is the single-handedness (homochirality) of biological molecules. This subject has attracted scientists since Pasteur's first manual separation of the enantiomorphic crystals of a tartrate salt more than 150 years ago [17]. Generally, all life on Earth is homo-chiral: only L-amino acids are present in proteins, and only D- sugars form backbones of DNA and RNA (Figure I-2).

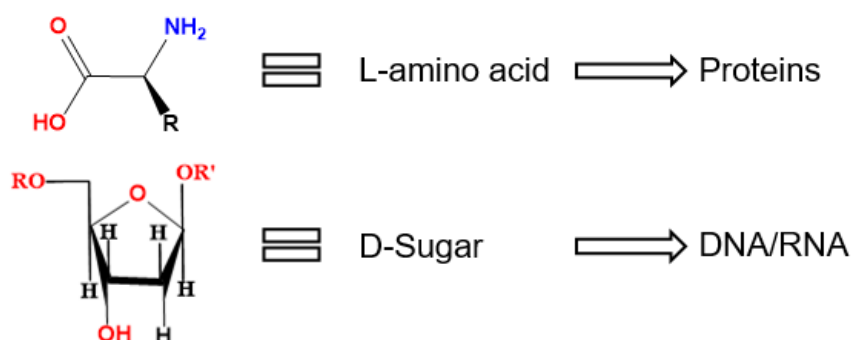


Figure I-2 Homochirality in aminoacids and sugars.

One of the big enigmas in biology, chemistry and physics is figuring out the reason of the preference of one enantiomer over the other in the macromolecules, with no traces of “un natural” D-amino acid and L- sugar. However, synthesizing these compounds in the laboratory without further care usually yields a racemic mixture of both enantiomers, e.g. an equimolar mixture of left- and right-handed molecules [18].

I.3. Historical Background

The science of the early XIXth century was influenced by the correlation between physical properties and the symmetry of optically active molecules [19]. The French mineralogist René Just Haüy noted that the electrical polarity is manifested only in geometrically dissimilar ends of some crystals, such as the tourmaline prism. He also observed that few crystals possess small faces named later hemihedral faces where the crystal exhibits half the number of planes required for the symmetry of the holohedral form [4], [20], [21]. These small faces eliminate the center and planes of symmetry of the basic holohedral hexagonal crystal showing that the structure of crystals is chiral as shown clearly in Prelog's (1976) photograph (Figure I-3) [22].

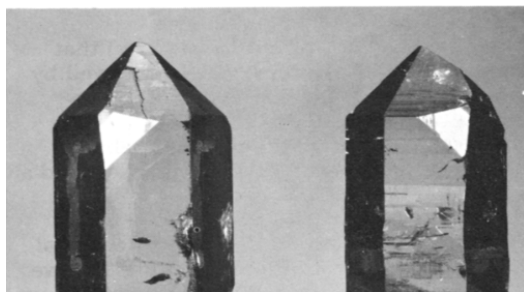


Figure I-3 D and L- Quartz crystals showing very prominent minor faces [22].

In 1811, Arago observed colors in plane-polarized light transmitted through the optical axis of a quartz crystal placed between crossed polarizers. One year later, Biot established that the colors originated due to the rotation of the plane of polarized light. In addition, he found that quartz crystals existed in two forms that rotates the plane of polarization in the opposite direction [21], [23], [24]. Later, J. W. F. Herschel showed that all the crystals of quartz which possess the same hemihedral structure presented a rotatory power (CPL) of the same sign. After a while, the chemist Auguste Laurent and Gabriel Delafosse developed this work, but the real diffusion of the term dissymmetry was done by Louis Pasteur [19]–[21]. He denoted the presence of right and left shapes in a certain class of hemihedry crystals for instance, a pair of crystals of sodium ammonium (2R,3R)- and sodium ammonium (2S,3S)- tartrates. These crystals were separated manually to find that in a solution they provoke opposite rotations of linearly polarized light [3], [4], [25]. Based on this observation, Pasteur introduced for the first time the term “molecular dissymmetry” anticipating what is now called chirality. This also led him to wonder about the dissymmetric forces which govern natural principles which was

difficult to answer with precision “La dissymétrie, je la vois partout dans l’univers” (Pasteur 1883) [4].

Pasteur was the first researcher who tried to generate dissymmetry by using external forces. The first experiment was done in Strasbourg where he tried to induce handedness in crystals by growing them in Ruhmkorff powerful magnets following Faraday’s discovery in 1846 of magnetically-induced optical rotation. However, the magnetic field did not have any effect on the optical activity. Nonetheless, these negative results did not discourage him to try such experiments. In Lille, he attempted to create the dissymmetry by growing plants in artificial environment such as, Heliostat, in which the sun rise in the west and set in the east. Moreover, Pasteur attempted to induce optical activity by running the reaction in clockwork mechanism to reverse the direction of earth rotation. All these attempts were negative [4], [5], [20], [21]. Pasteur concluded that only a still unknown cosmic phenomenon or asymmetric force can explain the dissymmetry observed in the natural substances [26].

I.4. Discrete Symmetries (Parity, Time Reversal & Charge Conjugation)

A discrete symmetry is a symmetry that describes non continuous changes in a system. In our work, we consider three different discrete symmetry operations which are: parity, time reversal and charge conjugation [19],[27].

- Parity: represented by the operator P which inverts the coordinates of all particles in a system through the coordinate origin (x,y,z) into $(-x,-y,-z)$.
- Time Reversal: represented by the operator T which reverses the motions of all particles in the system (t into $-t$).
- Charge Conjugation: represented by the operator C which interconverts particles and antiparticles (q into $-q$).

All these symmetries (P , T & C) hold for quantum mechanics and electrodynamics and we will assume for the remainder that physics is invariant under P , T and C but as shown in Table I.1, specific physical quantities are not necessarily invariant under these three symmetry operations.

Table I-1 Behavior of E, B and L under the main symmetry operations (P, T and C).

Physical Quantity \ Symmetry operations	Electric field (E)	Magnetic field (B)	Angular momentum (L)	E.B
P	-	+	+	-
T	+	-	-	-
C	-	-	+	+

Table I-1 represents the behavior of E, B, L and combination of EB under the main symmetry operation P, T and C which is very important to be mentioned before explaining the concept of Curie de-Gennes conjecture.

I.5. The Reason behind Unsuccessful attempts of Pasteur's Experiments

In 1994, Zadel *et al.* reported one paper entitled as "Enantioselective Reactions in a Static Magnetic field". A huge enantiomeric excess (20-98%) of aryl ethanol's was obtained to be linear with the applied magnetic field (0.2 to 1.2T) (Figure I-4), but the sign of the e.e. was arbitrary and independent of the sign of the magnetic field. [28].

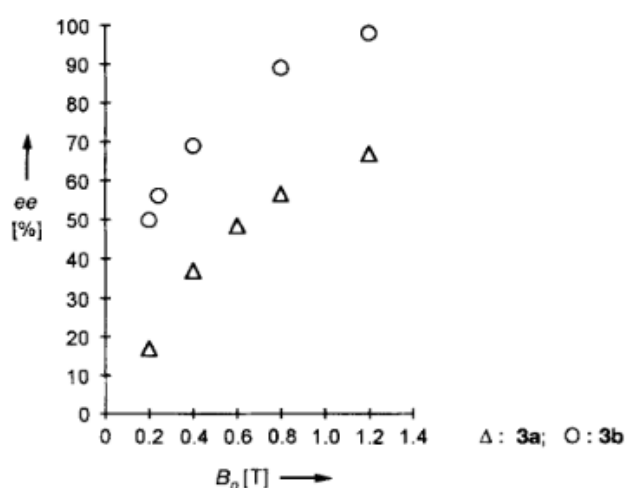


Figure I-4 Enantiomeric excess of (R) or (S)-1-phenylethanol (3a) and -1-(2-naphyl)ethanol (3b) as function of the static magnetic field [28].

These impressive results have astonished the chemical community since they contradict Pasteur's experiments regarding the effect of magnetic field in chiral mixtures. Later, Ben L. Feringa *et al.* decided to repeat this experiment in their laboratory, but they were unsuccessful in reproducing the results previously obtained which has later lead to retract Zadel paper [29].

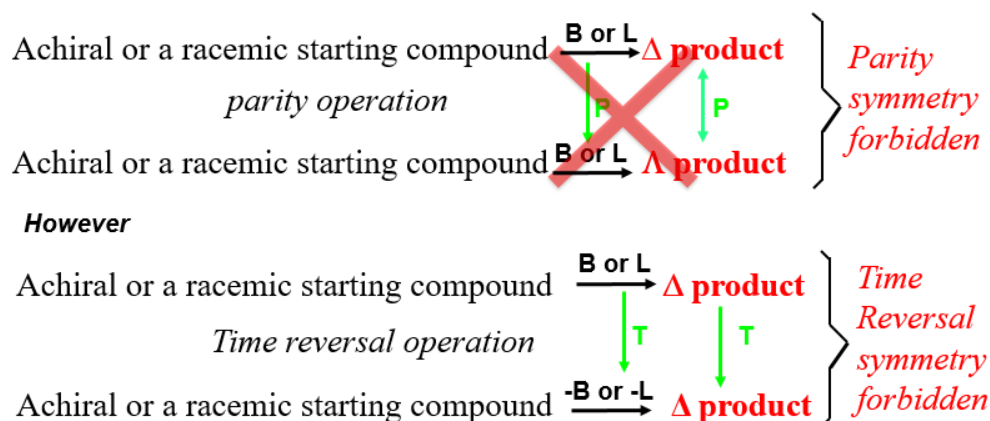


Figure I-5 No effect of space inversion on magnetic field nor on angular momentum (rotation).

By using the fundamental symmetry arguments on experiments of Pasteur or Zadel *et al.* using rotation or magnetic field to know why these experiments were condemned to fail, it appears that both \vec{B} (magnetic field) and \vec{L} (angular momentum) are interconverted by \hat{T} but not by \hat{P} (Figure I-5). However, the fact that the B and L are time-odd axial vectors and their signs are reversed by \hat{T} are not enough to break the symmetry and generate an e.e. of one of the two enantiomers. Accordingly, following the scheme above, the application of a magnetic field or rotational force alone is not breaking space reversal symmetry and, therefore, is not compatible with the generation of any e.e. [24].

I.6. Breaking of the Symmetry in Different Aspects

Pasteur's experiments and his conclusions regarding the chiral forces responsible for breaking the symmetry was broadened and re-examined later by many researchers. To reach homochirality, a chiral selective process was required at some stage in the early evolution of life on Earth to generate an initial e.e. that would then be amplified by regular enantioselective chemical processes.

Various theories have been proposed to explain how homo-chirality might have been initially started [18]. I have selected the main theories for generating the initial e.e. and sorted them according to the nature of the chiral influence involved.

I.6.a. Asymmetric Photochemistry

Circular polarized light (CPL) and magnetochiral dichroism are examples of truly chiral influences, in the sense defined by Barron [30] (refer to page 26). They can produce an enantiomeric enhancement in a racemic mixture or in the reaction products starting from achiral starting materials. CPL can favor in distinguishing between two enantiomers because a chiral medium interacts differently with RCPL and LCPL at a given wavelength. According to this difference we can expect that the photochemistry of chiral molecules will be sensitive to the choice of polarization. Photochemistry with unpolarized light can also be enantioselective through the magneto-chiral dichroism [2]. In this case the relative orientation of light and magnetic field determines the handedness of the result.

I.6.a.1. Circular Polarized Light

Circularly polarized light (CPL) is one of the most studied chiral physical sources that have been proposed to achieve enantiomeric imbalance in molecular system [25]. In 1897, Van't Hoff was one of the first researchers to suggest the possibility of asymmetric photochemistry with CPL[32]. This proposal has been widely used later by many researchers to develop 3 different approaches to use CPL for enantio-differentiating reactions: photodestruction, photoresolution and asymmetric photosynthesis.

I.6.a.1.a. Photodestruction

Asymmetric photodestruction is the most common method for the preparation of enantioenriched compounds using CPL. In such experiments, one enantiomer should be slightly sensitive and more quickly destroyed, therefore creating a different rate of photodestruction for the two enantiomers which leads to e.e.. This process is irreversible [33], [34]. In 1895, Cotton studied the interaction of CPL with optically active molecules. He found that the right-handed CPL is absorbed in a different way than left-handed CPL (circular dichroism) [35]. Asymmetric

photodegradation was demonstrated experimentally for the first time by Kuhn and Braun in 1929 [36]. In this experiment, a racemic mixture of the ethyl-2-bromopropionate was submitted to photochemical destruction by the action of CPL.

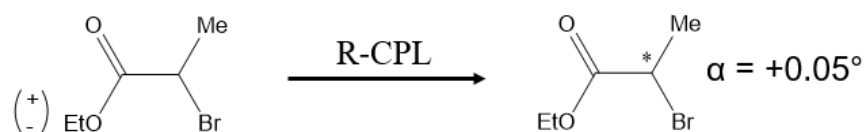


Figure I-6 The first photodestruction of (\pm)-ethyl-2-bromopropionate

The obtained product showed a small excess of (+)-ethyl-2-bromopropionate witnessed by a very small optical activity ($\alpha = +0.05^\circ$) when right- CPL was used (Figure I-6).

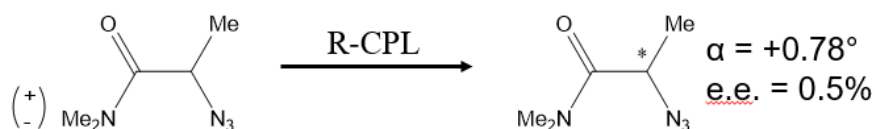


Figure I-7 Photodestruction of (\pm)-2-azido-N,N-dimethyl propanamide.

After one year, Kuhn and Knopf [37] succeeded again in carrying out irradiation experiment with right- and left-CPL at 300 nm on the racemic mixture of (\pm)-2-azido-N,N-dimethyl propanamide ($\text{CH}_3\text{HCN}_3\text{CON}(\text{CH}_3)_2$) dissolved in n-hexane. A stronger optical activity of the corresponding chiral compounds was observed with α being worth $+0.78^\circ$ and -1.04° respectively when their experiments were conducted up to a 40% extent of reaction. Generally, they found that the CPL-induced preferential decomposition of one of the two enantiomers depends on the handedness of CPL (Figure I-7).

To obtain quantitative results, a study of the asymmetric decomposition of a racemic camphor was chosen as a good substrate due to its high g factor and it's easy to do the photochemistry of these types of molecules (Figure I-8) [38].

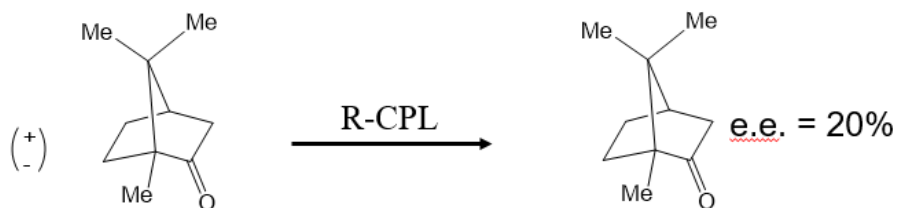


Figure I-8 Photochemical synthesis of optically active camphor starting from (\pm)-camphor.

In this experiment, it was demonstrated that the optical purity (20%) has achieved during photolysis of a racemate with 290-370 nm CPL which is dependent on the Kuhn anisotropic factor (g). This factor is equal to the ratio between the difference in molar extinction coefficient for the two enantiomers ($\Delta\epsilon$) (circular dichroism value) and the average extinction coefficient $\epsilon = 1/2 (\epsilon_{lCPL} + \epsilon_{rCPL})$. This anisotropy factor g was previously called the dissymmetric factor and is given by (Equation I-1).

$$g = \frac{\epsilon_l - \epsilon_r}{\epsilon} = \frac{\Delta\epsilon}{\epsilon} = \frac{2 \Delta\epsilon}{\epsilon_l + \epsilon_r} \quad \text{Equation I-1}$$

Generally, they deduced that there is a proportional relationship between the obtained optical purity and the advancement of the reaction. Furthermore, high optical purity of 20% was isolated after prolonged photolysis by circularly polarized light [38].

Later, the application of asymmetric photolysis method on racemic organic molecules such as amino acids became very popular [32], [39], [40].

I.6.a.1.b. Photoresolution

The second approach is partial photoresolution which is known as deracemization process of photochemically interconvertible enantiomers. In contrast with the previous case, this is a reversible process.

For example, Stevenson and Verdick [41] succeeded in performing an enantiodifferentiating reaction with circularly polarized light in the visible region (546 nm), namely a partial photoresolution of the racemic aqueous solutions of tris(oxalato)chromate(III) (Figure I-9).

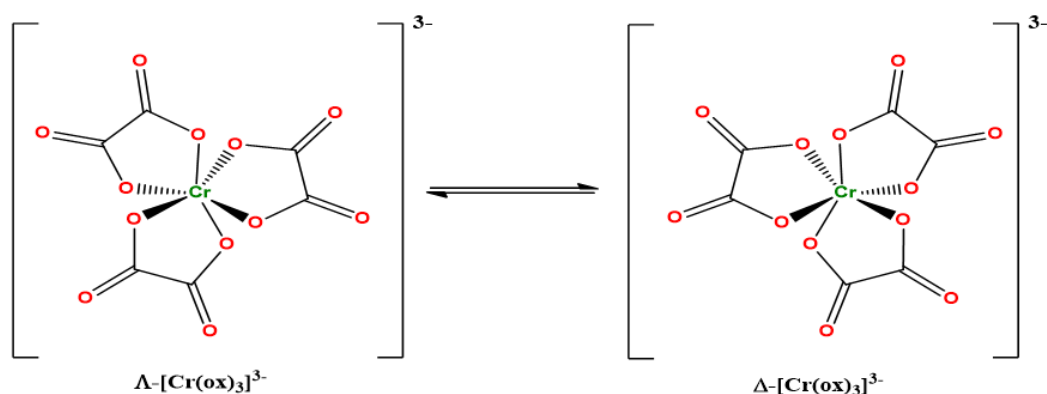


Figure I-9 Λ (left-handed screw axis) and Δ (right-handed screw axis) enantiomers for $[\text{Cr}(\text{ox})_3]^{3-}$ complex in equilibrium.

The CPL excites one of the two enantiomers of tris(oxalato)chromate(III) more and from this excited state racemization takes place. The other enantiomer, which is less absorbing, will accumulate in solution until a steady-state is reached leading to the plateau observed in Figure I.10.

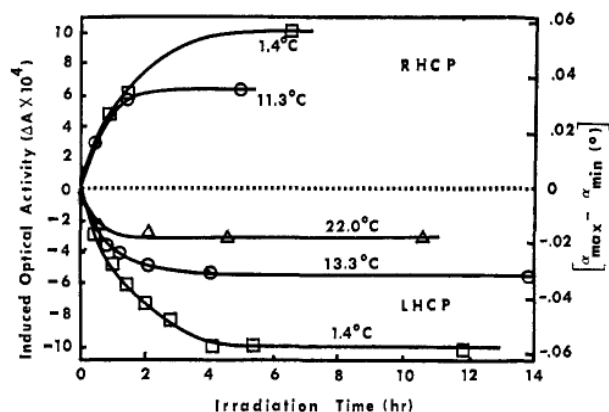


Figure I-10 Photoresolution of trioxalatochromate(III) in both right- and left-handed circular polarized light at 546 nm (2.6×10^{-2} M) [41].

This figure represents the observed optical rotation of trioxalatochromate(III) as a function of irradiation time (r-CPL and l-CPL) and for different temperatures. It can be seen that the optical activity decreases with decreasing irradiation time and increasing temperature (thermal isomerization). For this system, the photochemical reaction is reversible and the steady-state is reached [41], [42].

I.6.a.1.c. Asymmetric Photosynthesis

In the field of asymmetric photosynthesis, it is possible to start from achiral or prochiral molecules where the irradiation of these molecules with CPL preferentially converts the ground state into an excited state with a certain chirality that can lead to a preference for the formation of one enantiomer depending on the handedness of CPL [33]. One of the early attempt to examine the idea of using CPL as a mean of performing absolute asymmetric synthesis was an irradiation of an asymmetrically substituted triphenylmethyl radical. However, the attempt was unsuccessful [43]. Helicenes molecules have received attention, long time ago, as a suitable system to demonstrate the concept of asymmetric photosynthesis due to their intense optical rotatory power for instance, the specific rotation of hexahelicene is equal to 3640° [23], [44].

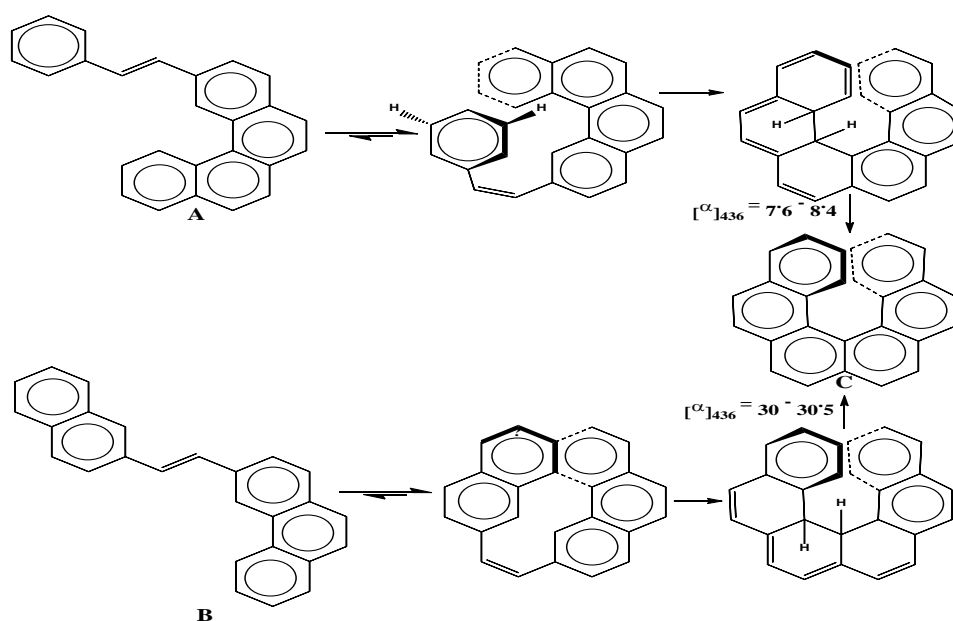


Figure I-11 Asymmetric photosynthesis of hexahelicene using CP light [33].

The only known examples of asymmetric photochemical synthesis using CPL was done by groups of Kagan and Calvin independently [45], [46]. The principle is represented in Figure I-11. The optically active hexahelicene (**C**) was obtained by two independent methods. When the two planar 1-(2-benzo[*c*]phenanthryl)-2-phenylethene (**A**) and 1-(2-naphthyl)-2-(2-phenanthryl)-ethene (**B**) were irradiated with (left /right) CPL in the wavelength range 310-410 nm in the presence of iodine as an oxidant, a hexahelicene (**C**) was obtained via a dihydrohelicene intermediate. The first method, gives a low specific rotation $[\alpha]_{436} = + 7.8-8.4^\circ$ (0.2% optical yield). In comparison, the second method leads to a much higher specific rotation, $[\alpha]_{436} = + 30^\circ$ (0.8% optical yield) [33], [47]. The positive optical rotation indicates that the M-

hexahelicene enantiomer was favored upon irradiation by left-CPL, whereas, the mirror-image (P-hexahelicene) was obtained by irradiation with right-CPL.

Circularly polarized light acts as a chiral activator to excite the ground state molecules to an excited state with a certain helical sense, which gives a specific optical rotation in the final products.

I.6.a.2. Magneto-chiral Dichroism

Photochemical asymmetric synthesis using linearly polarized light in the presence of a magnetic field was reported as early as 1939 [19],[28]. The obtained products exhibit a slight enantiomeric excess; however, the results were shown to be irreproducible [48]. A new nonreciprocal magneto-optical effect was evidenced by V. A. Markelov et al. who observed a difference in the refractive index between light propagation parallel and antiparallel to the magnetic field in a lithium-iodate (LiIO_3) crystal [49], [50]. Later G. Wagnière and A. Meier showed, by the quantum mechanical model of chiral dynamics, that static magnetic field parallel to the direction of propagation of an incident light beam causes a small shift in the value of the absorption coefficient of a chiral molecule. The increment in the absorption coefficient has the same sign for left and right circular polarized light, and which also occurs with linearly polarized light. This means that the shift is quite independent of the polarization characteristic of the light beam [51]. This conclusion made them propose that the same effect should occur with arbitrary or unpolarized light [52]. In summary, they showed that the shift changes sign either replacing the chiral molecule by its mirror image, or reversing the relative direction of magnetic field with respect to the direction of propagation of the incident light [53]. This phenomenon was named as magnetic field-induced absorption difference (MIAD) [51]. Later on, the name of this phenomenon was changed to magneto chiral dichroism MChD [54].

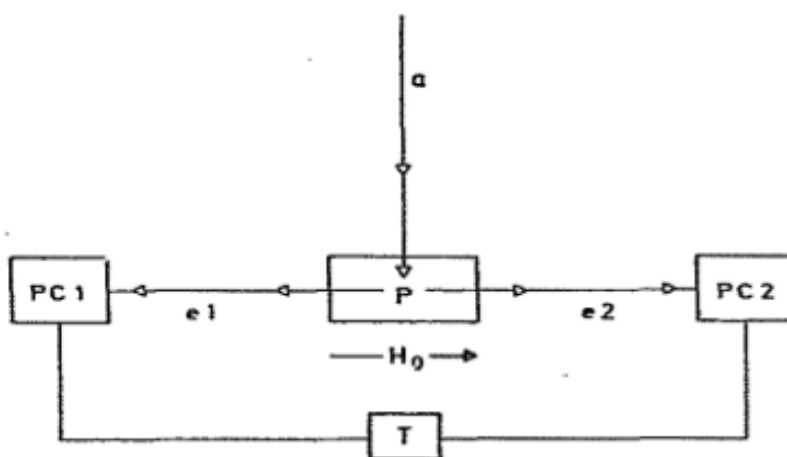


Figure I-12 The first proposed configuration of magneto-chiral luminescence effect [54].

Figure I-12 represents a simple experimental arrangement suggested to detect magneto-chiral effect in emission using two emitted beams (e_1 & e_2), the first one is antiparallel and the second one is parallel to the applied field (H_0). Additionally, two photon counters (PC_1 & PC_2), simultaneously connected to the external trigger (T) to count the number of the incident photon for a certain time period, were used to detect the small difference in intensity. In order to detect rapidly the small relative difference ratio $(I_1 - I_2) / (I_1 + I_2)$, the noise-to-signal ratio of each counter should be less than the relative difference intensity ratio $(I_1 - I_2) / (I_1 + I_2)$. According to their estimation any variation in the intensity of the exciting beam (a) or in the temperature of the sample, will affect both beams in the same way which lead to change the value of the relative difference [54]. In general, a small difference in intensity is very difficult to detect and required controlled conditions to be reproducible.

A convincing experimental demonstration for magneto-chiral luminescence anisotropy using static magnetic field was first published in 1997 by G. Rikken and E. Raupach [55]. In this experiment, unpolarized light from a mercury lamp produces a small difference in the intensity of emission of enantiopure $[Eu((+)tfc)_3]$ or $[Eu((-)tfc)_3]$ ($tfc^- = \text{tris}(3\text{-trifluoroacetylcamphorato})$) complexes, when the luminescence was measured in the direction parallel (I_1) and antiparallel (I_2) to the applied magnetic field. The $\text{tris}(3\text{-trifluoroacetyl-}\pm\text{-camphorato})\text{europium(III)}$ complex was chosen for this experiment because it has a very strong chiral transitions in the region of ${}^5D_0 \rightarrow {}^7F_J$ Eu^{3+} emission (where $J=1; 2$) especially in dimethyl sulfoxide which yielded the strongest CPE (circularly polarized emission) spectra in comparison to other solvents [53], [56]. The developed experimental setup used to measure the difference in

luminescence intensity in both directions of the field was based on the suggested experimental arrangement (Figure I-12) proposed by Wagnière to observe magnetochiral dichroism in emission [54].

$$g = \frac{\frac{\partial}{\partial B}(I_1 - I_2)B}{I_1 + I_2}, \quad I_1 = I_{B\uparrow\uparrow k} \text{ \& } I_2 = I_{B\uparrow\downarrow k} \quad \text{Equation I-2}$$

The values of interest is the magneto-chiral anisotropy (g) which provides whether or not magneto-chiral optical effect in a particular emission band is measurable for a given instrumental sensitivity (Equation I-2).

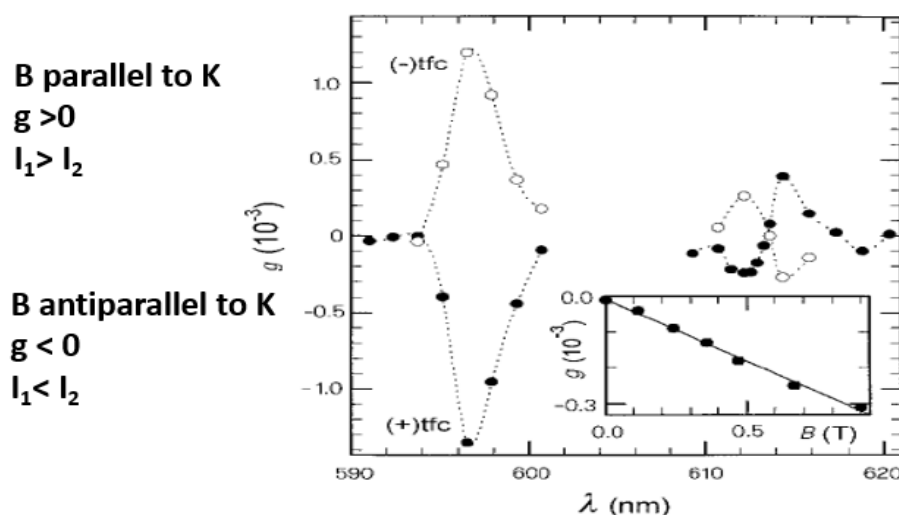


Figure I-13 Magneto-chiral luminescence anisotropy (g) of $(Eu((\pm))tfc)_3$ complexes, dissolved in deuterated dimethyl sulfoxide as function of luminescence wavelength [55].

The experimental result for magneto-chiral luminescence anisotropy (g) for the two enantiomers were shown in Figure I.13 of the important results obtained is the reversing of the sign of g for the two enantiomers. Moreover, the value of magneto-chiral anisotropy (g) of $Eu((+))tfc)_3$ complex is linearly dependent on the strength of the applied magnetic field.

These results together with enantio-selectivity confirm convincingly the existence of a magneto-chiral effect in emission.

As for NCD that allowed to obtain e.e. by irradiation with CPL, the observation of MChD is an open door to try and obtain e.e. by photochemistry with unpolarized light under magnetic field. This possibility was demonstrated by Rikken *et al.* using tris(oxalato)chromate(III) in solution

(Figure I-9) [2]. This octahedral complex (Δ/Λ -[Cr(ox) $_3$] $^{3-}$) was selected for this study because it is labile in aqueous solution and spontaneously dissociates and re-associates [2]. Additionally, a significant magneto-chiral dichroism is expected in chiral, paramagnetic complexes containing transition metals such as Cr(III) [53].

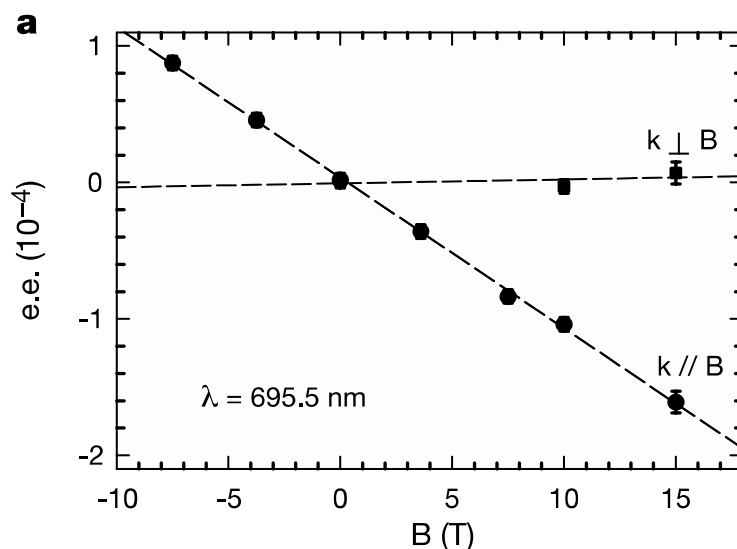


Figure I-14 Photoresolution of a chiral system (*rac*)-[Cr(ox) $_3$] $^{3-}$ in aqueous solution with unpolarized light in a magnetic field [2].

The authors show that, when the tris(oxalato)chromate(III) complex is irradiated with an unpolarized laser beam travelling parallel to a static magnetic field, a small enantiomeric excess (e.e.) was observed. It is linear with the scalar product $\vec{k} \cdot \vec{B}$ and the proportionality factor is about $\text{e.e.}/B = 1.0 \times 10^{-5} \text{ T}^{-1}$. Reversing the magnetic field direction resulted in the detection of an equal concentration of the mirror-image enantiomer. For perpendicular fields, no significant e.e. was observed (Figure I-14). In summary, the authors showed an enrichment of the solution in the less absorbing enantiomer of the tris(oxalato)chromate(III) by irradiation of unpolarized light under static magnetic field, the handedness of major enantiomer being determined by the sign of the $\vec{k} \cdot \vec{B}$ scalar product.

After the publication of these original data, many researchers tried to repeat the same experiment using different targets, for example, Yuichi Kitagawa *et al.* reported the first observation of magneto-chiral photochemistry in organic compounds using chiral J-aggregates of water-soluble porphyrins [57]. Later, Yangyang Xu *et al.* published new experimental observation of the same effect of helical polydiacetylene (PDA) assemblies from initially wholly achiral diacetylene (DA) monomers [58].

All these experiments provide convincing arguments that magneto-chiral photochemistry is a robust process that might have played an important role in the origin of biological homochirality.

I.6.b. Parity Violation in a Weak Nuclear Interaction

The parity is conserved if a physical process behaves in the same way in the mirror world as it does in our real world. In a simple way, the law of nature are invariant under reflection, that is to say nature is mirror symmetric [59]. However, the Parity Non Conservation (PNC) or Parity Violation (PV), defined as the breakdown of mirror-image symmetry, occurs when the process behaves differently in the mirror world.

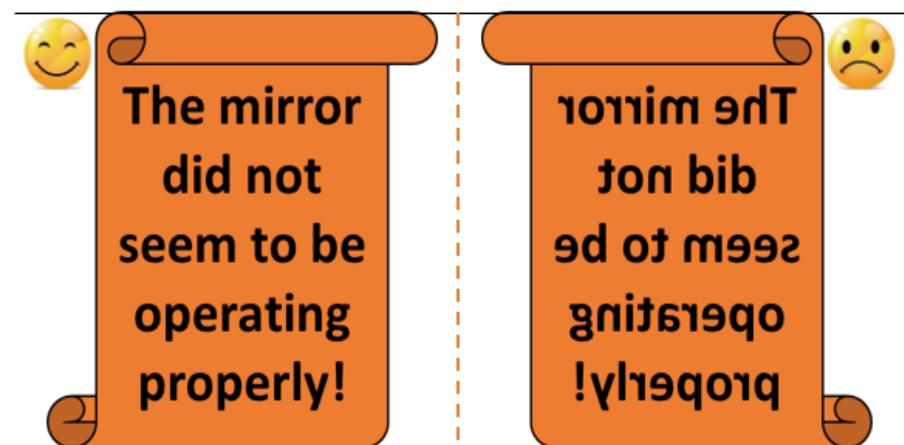


Figure I-15 Two non-superimposable mirror images.

In Figure I-15 we can see clearly that the written text in the mirror world is not familiar to us. This means that the mirror will not always reflect the real image, that is to say not all reactions or experiments obey to the law of conservation of parity. Prior to 1956, the parity was believed to be conserved in all physical systems. However, Lee and Yang published that there is no existing evidence to support parity conservation in weak interaction. Additionally, they proposed several experiments to check whether the parity is conserved or not [60].

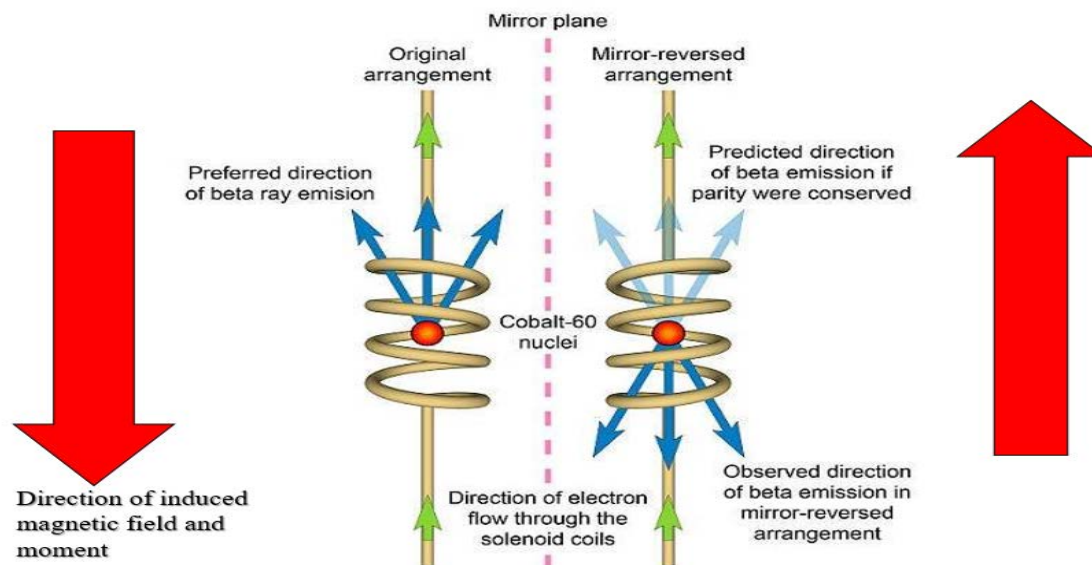


Figure I-16 Parity Non Conservation during β -decay simplified in this figure and downloaded from [Wikipedia Wu Experiment](#) [61].

One year later, the first experimental evidence for parity violation was observed in the case of ^{60}Co β -decay experiment by Wu *et al.* [62]. An illustration of Wu's experiment is shown in Figure I-16. The red balls represent cobalt 60 nuclei cooled at a temperature of about 0.01 K to reduce atomic vibrations. They were placed in a solenoid to magnetically align the atomic nuclear moments along the direction of the magnetic field. In order for parity to be conserved electrons should then be emitted parallel and anti-parallel to the magnetic field, but a large asymmetry in the β emission was observed: the emission of electrons is more favored in the direction opposite to the magnetic field, thus verifying experimentally that parity is violated at the level of weak interactions [61], [63]. After publication of this fundamental experimental evidence of mirror image symmetry breaking in β -decay experiment, Zelodvich proposed in 1958 the possibility to have parity violation effect in atomic physics of a weak electron-nucleon interaction induced by neutral currents [64]. Furthermore, PV effect is also operative in molecules. In this case, measuring a small energy difference (ΔE_{PNC}) between two enantiomers lead to demonstrate experimentally the Parity Violation (PV) effect in chiral molecules [63]. However, this value is expected to be very small according to numerical calculations of ΔE_{PNC} which is equal to 10^{-16} kJ/mol. Additionally, for the time being, there is a contradiction, where either there is no clear experimental evidence for a connection between PNC and biomolecular homochirality [65] nor the reverse [66]. Despite several attempts with an amplification to measure Parity Violation Energy Difference (PVED), this difference has not been measured yet at the molecular level [67].

I.7. Curie de-Gennes conjecture (CdG)

I.7.a. Historical Background

In 1894 Pierre Curie re-examined Pasteur's experiments on chiral forces and showed that magnetic field alone could not generate dissymmetry because it breaks time-reversal symmetry (T-) whereas generating an e.e. breaks parity (P-).

P. Curie, inspired by the Wiedemann effect, proposed that the combination of magnetic and electric fields, namely the parallel and the antiparallel alignment of the fields, could be considered as a mean to generate an enantiomeric excess. Wiedemann experiment states that if we take a piece of wire, magnetize it in the direction of its length and then let the current pass through, the wire will twist. The wire has itself cylindrical symmetry group, namely the coherent elements of symmetry of a circular cylinder. For the twisting phenomenon to take place, it is necessary that some symmetry elements are missing, in other words that some dissymmetry items appear, so that the final symmetry is lowered to be compatible with the production of a twist. The introduction of a magnetic field (the wire is magnetized) and an electric field in the same direction (the wire is carrying a current) will introduce the necessary conditions for the manifestation of torsion. According to Curie, it is "the dissymmetry that creates the phenomenon" [1].

Later, in 1970 De Gennes [6] extended Curie's hypothesis stating that the combination of E and B can produce an enantiomeric excess (e.e.) that relies on different transition rates towards two enantiomers rather than the equilibrium itself. Following the complementary contributions of the two researchers, this proposal was called the Curie-de Gennes conjecture.

I.7.b. General Concepts of True and False Chirality

Recently, Barron has introduced the concept of 'true' and 'false' chirality to remove the confusion that existed since Pasteur's time concerning the nature of physical influences able to induce absolute enantio-selection [68]. The main concept of 'true' and 'false' chirality are represented in Table I-2.

Table I-2 True and false chirality as defined by Barron [68].

Type of chirality	True chirality	False chirality
General Definition		
Common feature	System existing in two enantiomeric states interconverted by space inversion.	
Different feature	The two enantiomers cannot be interconverted by time reversal combined with any spatial rotation. For example, collinear magnetic field with an unpolarized light (magneto-chiral photochemistry).	The two enantiomers can be interconverted by time reversal combined with a spatial rotation. For example, Collinear magnetic and electric fields (Curie de-Gennes conjecture effect).
Symmetry arguments for both examples [69]		
Common feature	<p>k (wavevector of light) is a polar vector and B is an axial vector, parallel and antiparallel are interconverted by P</p>	<p>E is a polar vector and B is an axial vector, parallel and antiparallel are interconverted by P:</p>
Different features	<p>k is the time-odd and B is the time-odd, thus parallel and antiparallel arrangements of B and k are not interconverted by T so that the combined PT is non-invariant overall:</p>	<p>E is the time-even and B is the time-odd, so parallel and antiparallel arrangements are interconverted not only by P but also by time reversal T so that it is PT invariant overall:</p>
	Thermodynamically controlled	Kinetically controlled

I.7.c. Representation of Falsely Chiral Influence using a Simple Example

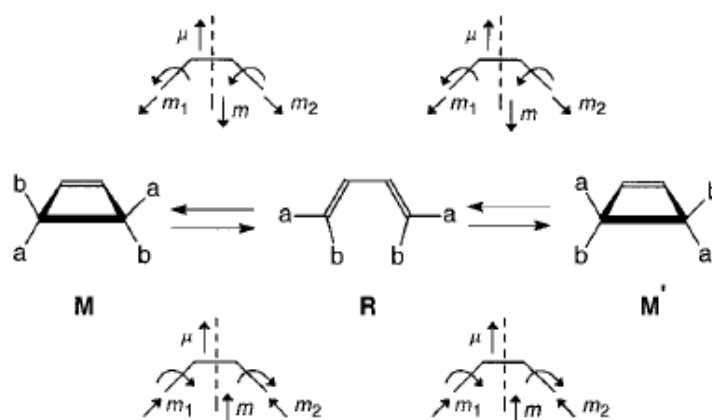


Figure I-17 The conrotatory interconversion of butadiene and the two enantiomeric chiral cyclobutenes in the presence of false chiral influence [33], [70].

To illustrate falsely chiral influence, the conrotatory ring closure of a substituted butadiene to produce a chiral cyclobutenes has been proposed by Barron as a simple theoretical example of how collinear magnetic and electric fields can generate a difference in potential energy profiles where the final state of both enantiomers will remain strictly degenerate [70]. There are two possible mechanisms to convert cyclobutene into butadiene or vice versa which are defined as conrotatory and disrotatory. However, enantiomeric chiral cyclobutenes can only be achieved through a conrotatory ring closing mechanism by which thermal electro-cyclic reactions occur [71]. During the entire process the molecules preserve the twofold proper rotation axis C_2 possessed by **R**, **M** and **M'** throughout the reaction. When the electric density starts to accumulate between the ends of 1,3-butadiene through the transition state, the symmetry arguments show that there will be an electric dipole moment (μ) parallel to C_2 axis. Moreover, μ will have the same magnitude and sense during the whole process. By choosing **a** to be a bulky group such as phenyl and **b** a hydrogen atom, the rotational motion of these groups (**a** & **b**) will generate transient magnetic moments **m** (**m**₁ & **m**₂) collinear to the local rotational axes. Figure I-17 show that the forward (**M**→**R**→**M'**) and backward (**M'**→**R**→**M**) reactions are parallel ($\vec{\mu}, \vec{m}$) and antiparallel ($\vec{\mu}, -\vec{m}$) arrangements of transient electric and magnetic moments respectively, where the sign of the magnetic moment (+/- **m**) depends on the sense of rotation which are represented in the transition states [23], [33], [70].

In general, the electric field will partially align the molecules while the parallel and antiparallel arrangements of μ and **m** will generate different energies in the entire process.

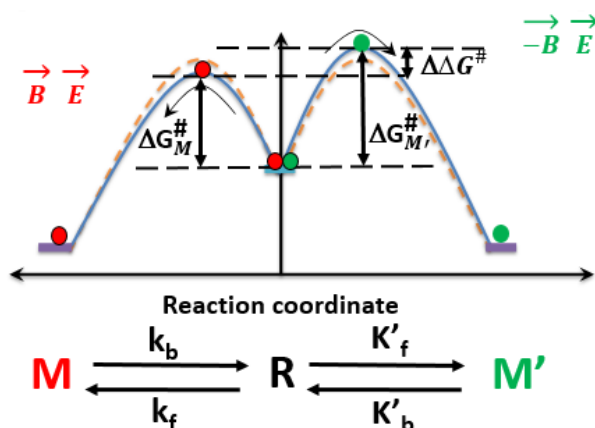


Figure I-18 Potential energy profiles for the conrotatory interconversion of two enantiomeric chiral cyclobutenes [72].

As shown in Figure I-18, the breakdown of microscopic reversibility in the chemical process appeared as a different potential energy profiles for forward and backward direction of reactions which involve two different enantiomers in the presence of time-noninvariant enantiomorphous for example, collinear electric and magnetic fields [72].

On the other hand, M and M' enantiomers remain strictly isoenergetic. However, this influence can modify asymmetrically the activation energy barriers where $\Delta G_{M/M'}^\ddagger$ are the activation energies for the formation of M and M' enantiomers respectively and the difference between them is represented by $\Delta\Delta G^\ddagger$. In addition, the rate constant ($k_b \neq k_b'$ & $k_f \neq k_f'$) will be also modified which leads to an enantiomeric excess (M or M') in process under kinetic control [24]. Clearly a falsely chiral influence consisting of a parallel combination of magnetic field and electric field (\vec{E}, \vec{B}), will interact differently to antiparallel arrangement ($\vec{E}, -\vec{B}$). These transient pairs of moments can thus develop an enantiomeric excess of one enantiomer over the other in a controlled manner depending on the type of combination (parallel or anti-parallel).

I.7.d. Amplified Mechanisms Alone are not Sufficient to Explain the Origin of Homochirality

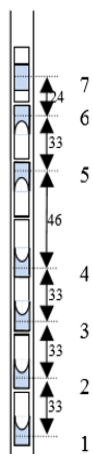
In 1953, F. C. Frank [73] proposed theoretically a new approach concerning asymmetric amplification in autocatalysis. He suggested that the origin of single chirality can in principle be obtained from achiral starting materials where the formed enantiomer catalyzes its own formation and at the same time suppresses the formation of its mirror image. Frank concluded that spontaneous asymmetric synthesis is a natural property of life, which may be present in

simpler autocatalytic systems. The first experimental proof of this proposal was found by Soai *et al* [74]. However, this method requires adding willingly a small excess of single chiral enantiomer to achieve controlled total symmetry breaking at the end of the process. Moreover, this approach does not give any information concerning the origin of the existing imbalance from the beginning, as well as, the origin of homochirality itself. Recently, Cristobal Viedma [75] successfully extended Frank's concept to nonlinear autocatalysis-recycling process to obtain what is now known as "Viedma ripening". In this experiment, a saturated solution containing symmetric mixture of both crystals D and L NaClO₃ was prepared, and then the solution was strongly agitated using glass balls in an isothermal evaporation process. The difference in crystal size between two types of crystal was achieved by intensive grinding and stirring. Over a period of several days, unknown initial e.e. is amplified exponentially to an enantiopure end state, but, of course, the obtained handedness was uncontrolled (L or D randomly). The reason behind the breaking of first enantiomer into clusters more than the other to have 100 % e.e. of second enantiomer is not obvious (chiral sign of the crystallization products of NaClO₃). These types of experiments, mostly autocatalysis mechanism, are still used as one of the amplification mechanisms.

I.7.e. Incomplete Experimental Evidence for Falsely Chiral Influence

To account for the origin for a small e.e. from the beginning, more experiments were done using external forces. Micali *et al.*[7] have recently shown how the combined rotational motion and effective gravity induce enantioselection. They demonstrated experimentally how a small chiral perturbation (rotation, magnetic alignment and levitation) during the early stage of the aggregation process of an achiral molecular building block tris-(4-sulfonatophenyl)phenylporphyrin (TPPS₃), in which the porphyrins stack on the top of one another through $\pi - \pi$ interactions to form supramolecular helices [7], [8] (120 > time > 30 minutes) is sufficient to achieve chiral selection. The full aggregation process requires three days to be completed in the absence of any bias. Additionally, it is reported previously that stirring of TPPS₃ solutions during the assembly process can cause mirror symmetry breaking [76].

Table I-3 Used values at the different z positions.



Number of vials	z(mm)	B(z) (Tesla)	$G_{\text{eff}}(G_n)$	B^2/G_{eff} (T^2S^2/m)	
7	103	12.96	-0.004	-3968.60	→ $G_{\text{eff}} \leq 0$ Near zero G_{eff} or levitation
6	79	15.92	-1.142	-22.62	} $Z > 0$ Inverted effective gravity $G_{\text{eff}} < 0$
5	46	22.33	-1.360	-37.36	
4	0	25	1	63.71	→ $Z = 0$ Normal gravity $G_{\text{eff}} = G_n$
3	-33	23.81	23.16	23.16	} $Z < 0$ Enhanced effective gravity $G_{\text{eff}} > G_n$
2	-66	18.62	8.98	8.98	
1	-99	13.39	8.74	8.74	

The samples of a porphyrin (TPPS₃) solution are subjected to a spinning motion (L) and a magnetic field (B) that depends on their position within the magnet. This leads to a magnetic levitation force resulting in an enhanced, normal, or inverted effective gravity G_{eff} compared with the normal value of G_n (Table I-3).

The gravitational vector (\vec{G}) combined with rotation or spinning fluid (\vec{L}) has exactly the same symmetry as \vec{E} and \vec{B} [77]. Both systems are examples of false chirality. Thus, in order to demonstrate experimentally falsely chiral influence, the effect should increase when the magnitude of these vectors ($(\vec{E} \vec{B})$ or $(\vec{G}_{\text{eff}} \vec{L})$) is increase. However, Micali *et al.* showed an inverse dependence on G_{eff} as shown in figure I-19 (c).

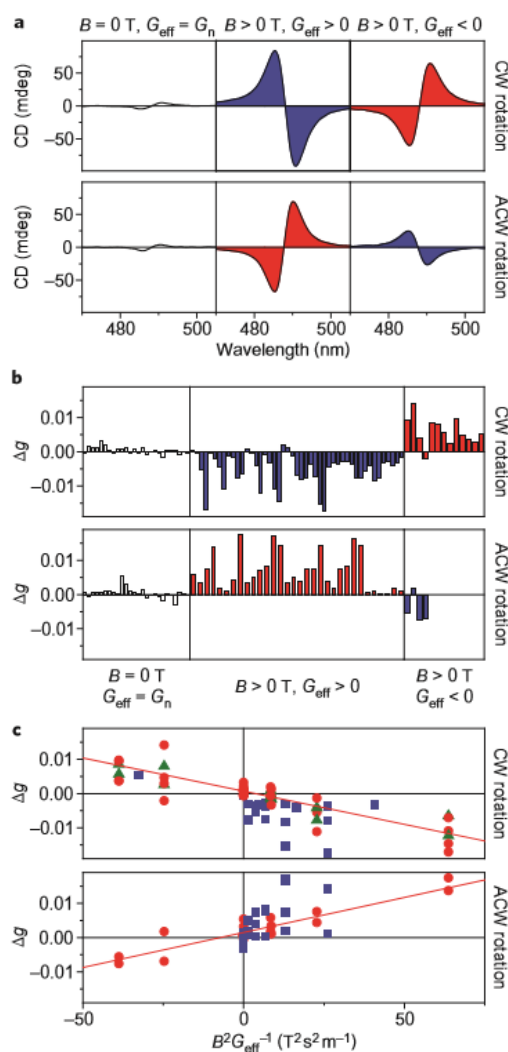


Figure I-19 Selection of supramolecular chirality in the presence of rotation, magnetic and levitation forces [7].

Figure I-19: (a) represents the effect of rotation (CW and ACW) combined with effective gravity ($G_{\text{eff}} < 0$ and $G_{\text{eff}} > 0$) on the CD spectra of the final TPPS₃ aggregates.

Figure I-19 (b) shows the measured chirality parameter ($\Delta g = g_{(491\text{nm})} - g_{(486\text{nm})}$) where g is the ratio of the CD to the conventional absorption ($g = \Delta A/A$) for clockwise and anticlockwise (Equation I-1). In the presence of magnetic field the handedness was inverted by inverting the rotation direction under the same gravity ($G_{\text{eff}} < 0$ or $G_{\text{eff}} > 0$). It shows that the chiral sign depends on the relative directions of the rotational and gravitational forces.

Figure I-19 (c) presents the variation of Δg as function of $B^2 G_{\text{eff}}^{-1}$ for CW and ACW rotation at $t = 30$ minutes (green triangle), $t = 60$ minutes (red circles) and $t = 120$ (blue square). The red lines represents the linear fits to the data points for $t = 60$ minutes with a slope determined by the spinning sense. We can see clearly that the values of Δg are increasing with the increase

of $B^2G_{\text{eff}}^{-1}$ factor rather than the opposite. They attribute the $1/G_{\text{eff}}$ dependence to the influence of the actual chiral hydrodynamic flow. However, this did not change the symmetry arguments for falsely chiral influence. The interpretation is not consistent with the Curie de-Gennes conjecture and the symmetry analysis can be more complicated due to the combined effect of different experimental factors on the symmetry as the rotation, magnetic field and gravity which makes it harder to resolve the single effect of each parameter.

Additionally, there are stochastic and wide distribution of Δg values. According to given information, we consider that their demonstration of Curie-de Gennes conjecture is not totally unambiguous. A clear demonstration is therefore still awaits.

I.8. Main objective

The question of the origin of the homochirality of biomolecules is considered closely related to the problem of the origin of life itself. Though the effect of circularly polarized light or unpolarized light associated with magnetic field can be viewed as the origin of homochirality, an attractive hypothesis that remains to be fully examined is the possibility to generate an e.e. using falsely chiral influences. This will be the focus of my work, e.g. the use of falsely chiral influences obtained by combining magnetic, electric fields and/or rotational force to generate e.e.. Furthermore, working on this demonstration was facilitated in our laboratory due to the availability of different needed requirements such as superconducting magnet and the setup in LNCMI- Toulouse built solely for this objective which is magneto-electric enantioselective optical measurements.

It's also interesting for us to work on an issue previously proposed by pioneer in this field such as Pierre Curie and de-Gennes which is later confirmed by others. That's why we have aimed to demonstrate experimentally Curie de-Gennes conjecture effect, however, the small expected e.e. makes these studies very challenging, conclusive results would indeed bring a definitive answer to a hundred years old conjecture.

References

- [1] P. Curie, "Sur la symétrie dans les phénomènes physiques, symétrie d'un champ électrique et d'un champ magnétique," *J Phys Theor Appl*, vol. 3, no. 1, pp. 393–415, 1894.
- [2] G. L. J. A. Rikken and E. Raupach, "Enantioselective magnetochiral photochemistry," *Nature*, vol. 405, no. 6789, pp. 932–935, juin 2000.
- [3] L. Pasteur, "Mémoire de L. Pasteur sur la relation qui peut exister entre la forme cristalline et la composition chimique et sur la cause de la polarisation rotatoire," *Séances Acad Sci*, pp. 535–538, 1848.
- [4] L. Pasteur, "La dissymétrie moléculaire," *Conférence Faites À Société Chim. Paris*, pp. 24–37, Le décembre 1883.
- [5] S. F. Mason, "Origins of biomolecular handedness," *Nature*, vol. 311, no. 5981, pp. 19–23, Sep. 1984.
- [6] M. P.-G. de Gennes, "Sur l'impossibilité de certaines synthèses asymétriques," *Simple Views Condens. Matter 3rd Ed. Ed. GENNES PIERRE-GILLES Publ. World Sci. Publ. Co Pte Ltd*, vol. t. 270, pp. 505–507, 1970.
- [7] N. Micali, H. Engelkamp, P. G. van Rhee, P. C. M. Christianen, L. M. Scolaro, and J. C. Maan, "Selection of supramolecular chirality by application of rotational and magnetic forces," *Nat. Chem.*, vol. 4, no. 3, pp. 201–207, Mar. 2012.
- [8] L. D. Barron, "Chirality: Spin and gravity give a helping hand," *Nat. Chem.*, vol. 4, no. 3, pp. 150–152, Mar. 2012.
- [9] F. Riblet, G. Novitchi, R. Scopelliti, L. Helm, A. Gulea, and A. E. Merbach, "Isomerization Mechanisms of Stereolabile tris- and bis-Bidentate Octahedral Cobalt(II) Complexes: X-ray Structure and Variable Temperature and Pressure NMR Kinetic Investigations," *Inorg. Chem.*, vol. 49, no. 9, pp. 4194–4211, mai 2010.
- [10] Ghénadie Novitchi, ShangDa Jiang, Sergiu Shova, Fatima Rida, Ivo Hlavička, Milan Orlita, Wolfgang Wernsdorfer, Rana Hamze, Cyril Martins, Nicolas Suaud, Nathalie Guihéry, Anne-Laure Barra and Cyrille Train, "From Positive to Negative Zero Field Splitting in a Series of Strongly Magnetically Anisotropic Mononuclear Metal Complexes," *Inorg. Chem.*, vol. 56, pp. 14809–14822, Nov. 2017.
- [11] C. Liu, H. Ma, J. Nie, and J. Ma, "Retracted: A Facile Synthetic Route to New Fluorinated Building-Blocks of 1-Fluoroalkynes and 1-Fluorodiyne," *Chin. J. Chem.*, vol. 30, no. 1, pp. 47–52, Jan. 2012.
- [12] P. Garbacz, J. Cukras, and M. Jaszuński, "A theoretical study of potentially observable chirality-sensitive NMR effects in molecules," *Phys. Chem. Chem. Phys.*, vol. 17, no. 35, pp. 22642–22651, Aug. 2015.
- [13] J. Sarfati, "Origin of life: the chirality problem," *J. Creat.*, vol. 12, no. 3, pp. 263–266, 1998.
- [14] D. Balcells Badia, F. Maseras Cuní, and G. Ujaque Pérez, *A Computational approach to the synthesis of chiral sulfoxides*. Universitat Autònoma de Barcelona, 2006.
- [15] Baron William Thomson Kelvin, *Baltimore Lectures on Molecular Dynamics and the Wave Theory of Light*. C.J. Clay and Sons; Publication agency of the Johns Hopkins University, 1904.
- [16] G. H. Wagnière, *On Chirality and the Universal Asymmetry: Reflections on Image and Mirror Image*. John Wiley & Sons, 2008.
- [17] D. G. Blackmond, "The Origin of Biological Homochirality," *Cold Spring Harb. Perspect. Biol.*, vol. 2, no. 5, May 2010.
- [18] M. Gargaud, R. Amils, and H. J. Cleaves, "Homochirality," in *Encyclopedia of Astrobiology*, pp. 759–760, 2011.

- [19] L. D. Barron, "An introduction to chirality at the nanoscale," in *chirality at the Nanoscale: Nanoparticles, Surfaces, Materials and More*, John Wiley & Sons, pp. 1-24, 2009.
- [20] L. Pasteur, *Recherches sur la dissymétrie moléculaire des produits organiques naturels, par M. L. Pasteur, ... Leçons professées à la Société chimique de Paris le 20 janvier et le 3 février 1860*. Impr. de C. Lahure, 1860.
- [21] H. D. Flack, "Louis Pasteur's discovery of molecular chirality and spontaneous resolution in 1848, together with a complete review of his crystallographic and chemical work," *Acta Crystallogr. A*, vol. 65, no. Pt 5, pp. 371-389, Sep. 2009.
- [22] V. Prelog, "Chirality in chemistry," *Science*, vol. 193, no. 4247, pp. 17-24, Jul. 1976.
- [23] A. Guijarro and M. Yus, *The Origin of Chirality in the Molecules of Life*. 2008.
- [24] L. D. Barron, "Fundamental Symmetry Aspects of Molecular Chirality," in *New Developments in Molecular Chirality*, P. G. Mezey, Ed. Springer Netherlands, pp. 1-55, 1991.
- [25] H. Kitzerow and C. Bahr, *Chirality in Liquid Crystals*. Springer Science & Business Media, 2006.
- [26] A. Julg, "Origin of the L-Homochirality of Amino-Acids in the Proteins of Living Organisms," in *Molecules in Physics, Chemistry, and Biology*, Springer, Dordrecht, pp. 33-52, 1989.
- [27] L. D. Barron, "Chirality and life," *Space Sci Rev*, vol 135, p.p. 187-201, 2008.
- [28] G. Zadel, C. Eisenbraun, G.-J. Wolff, and E. Breitmaier, "Enantioselective Reactions in a Static Magnetic Field," *Angew. Chem. Int. Ed. Engl.*, vol. 33, no. 4, pp. 454-456, Mar. 1994.
- [29] B. L. Feringa, R. M. Kellogg, R. Hulst, C. Zondervan, and W. H. Kruizinga, "Attempts to Carry Out Enantioselective Reactions in a Static Magnetic Field," *Angew. Chem. Int. Ed. Engl.*, vol. 33, no. 14, pp. 1458-1459, Aug. 1994.
- [30] L. D. Barron, "True and false chirality and absolute asymmetric synthesis," *J. Am. Chem. Soc.*, vol. 108, no. 18, pp. 5539-5542, Sep. 1986.
- [31] K. Rijeesh, P. K. Hashim, S. Noro, and N. Tamaoki, "Dynamic induction of enantiomeric excess from a prochiral azobenzene dimer under circularly polarized light," *Chem. Sci.*, vol. 6, no. 2, pp. 973-980, Jan. 2015.
- [32] J. J. Flores, W. A. Bonner, and G. A. Massey, "Asymmetric photolysis of (RS)-leucine with circularly polarized ultraviolet light.," *J. Am. Chem. Soc.*, vol. 99(11), pp. 3622-3625, 1977.
- [33] Ben L. Feringa and Richard A. van Delden RA, "Absolute Asymmetric Synthesis: The Origin, Control, and Amplification of Chirality," *Angew. Chem. Int. Ed Engl.*, vol. 38, no. 23, pp. 3418-3438, Dec. 1999.
- [34] R. D. Richardson, M. G. J. Baud, C. E. Weston, H. S. Rzepa, M. K. Kuimova, and M. J. Fuchter, "Dual wavelength asymmetric photochemical synthesis with circularly polarized light," *Chem. Sci.*, vol. 6, no. 7, pp. 3853-3862, Jun. 2015.
- [35] V. Schurig, *Differentiation of Enantiomers II*. Springer, 2014.
- [36] W. Kuhn and E. Braun, "Photochemische Erzeugung optisch aktiver Stoffe," *Naturwissenschaften*, vol. 17, pp. 227-228, Apr. 1929.
- [37] W. Kuhn and E. Knopf, "Photochemische Erzeugung optisch aktiver Stoffe," *Naturwissenschaften*, vol. 18, pp. 183-183, Feb. 1930.
- [38] H. B. Kagan, G. Balavoine, and A. Moradpour, "Can circularly polarized light be used to obtain chiral compounds of high optical purity?," *J. Mol. Evol.*, vol. 4, no. 1, pp. 41-48, Mar. 1974.
- [39] A. G. Griesbeck and U. J. Meierhenrich, "Asymmetric photochemistry and photochirogenesis," *Angew. Chem. Int. Ed Engl.*, vol. 41, no. 17, pp. 3147-3154, Sep. 2002.

- [40] U. Meierhenrich, *Amino Acids and the Asymmetry of Life: Caught in the Act of Formation*. Springer, 2008.
- [41] K. L. Stevenson and J. F. Verdick, "Partial photoresolution. Preliminary studies on some oxalato complexes of chromium(III)," *J. Am. Chem. Soc.*, vol. 90, no. 11, pp. 2974–2975, May 1968.
- [42] N. A. P. Kane-Maguire and C. H. Langford, "Partial Photoresolution of Some Chromium (III) Complexes of Phenanthroline and Bipyridine Using Circularly Polarized Laser Irradiation," *Can. J. Chem.*, vol. 50, no. 20, pp. 3381–3383, Oct. 1972.
- [43] G. Karagunis and G. Drikos, "Zur Stereochemie der freien Triarylmethylradikale. Eine total asymmetrische Synthese," *Naturwissenschaften*, vol. 21, no. 33, pp. 607–607, Aug. 1933.
- [44] H. Isla and J. Crassous, "Helicene-based chiroptical switches," *Comptes Rendus Chim.*, vol. 19, no. 1, pp. 39–49, Jan. 2016.
- [45] W. J. Bernstein, M. Calvin, and O. Buchardt, "Absolute asymmetric synthesis. III. Hindered rotation about aryl-ethylene bonds in the excited states of diaryl ethylenes. Structural effects on the asymmetric synthesis of 2- and 4-substituted hexahelicenes," *J. Am. Chem. Soc.*, vol. 95, no. 2, pp. 39–49, 1973.
- [46] H. Kagan, A. Moradpour, J. F. Nicoud, G. Balavoine, and G. Tsoucaris, "Photochemistry with circularly polarized light. Synthesis of optically active hexahelicene.," *J. Am. Chem. Soc.*, vol. 93, no. 9, pp. 2353–2354, 1971.
- [47] H. Kagan, A. Moradpour, J. F. Nicoud, G. Balavoine, R. H. Martin, and J. P. Cosyn, "Photochemistry with circularly polarised light. II) Asymmetric synthesis of octa and nonahelicene.," *Tetrahedron Lett.*, vol. 12, no. 27, pp. 2479–2482, Jan. 1971.
- [48] R. Dan and M. Valer, "Attempted synthesis of optically active asymmetric spirans." *Bul. Chim., Soc. Chim. Romania*, vol. 1, pp. 18-24, 1939 .
- [49] V. A. N. Markelov, M. A. Novikov and A. A. Turkin, "Experimental observation of a new nonreciprocal magneto-optical effect," *JETP Lett.*, vol. 25, no 9, pp. 378-380, 1977.
- [50] G. L. J. A. Rikken and E. Raupach, "Pure and cascaded magnetochiral anisotropy in optical absorption," *Phys. Rev. E* 58, 5081 (1998).
- [51] G. Wagnière and A. Meier, "Difference in the absorption coefficient of enantiomers for arbitrarily polarized light in a magnetic field: A possible source of chirality in molecular evolution.," 1983.
- [52] C. A. Mead, A. Moscovitz, H. Wynberg, and F. Meuwese, "The influence of an electric and magnetic field in chemical reactions," *Tetrahedron Lett.*, vol. 18, no. 12, pp. 1063–1064, 1977.
- [53] L. D. Barron and J. Vrbancich, "Magneto-chiral birefringence and dichroism," *Mol. Phys.*, vol. 51, no. 3, pp. 715–730, 1984.
- [54] G. Wagnière, "Magneto-chiral dichroism in emission. Photoselection and the polarization of transitions - ScienceDirect," *Chem. Phys. Lett.*, vol. 110, no. 5, pp. 546–551.
- [55] G. L. J. A. Rikken and E. Raupach, "Observation of magneto-chiral dichroism," *Nature*, vol. 390, no. 6659, pp. 493–494, décembre 1997.
- [56] H. G. Brittain and F. S. Richardson, "Circularly polarized emission studies on the chiral nuclear magnetic resonance lanthanide shift reagent tris(3-trifluoroacetyl-d-camphorato)europium(III)," *J. Am. Chem. Soc.*, vol. 98, no. 19, pp. 5858–5863, 1976.
- [57] Y. Kitagawa, H. Segawa, and K. Ishii, "Magneto-Chiral Dichroism of Organic Compounds," *Angew. Chem.*, vol. 123, no. 39, pp. 9299–9302.
- [58] Y. Xu, G. Yang, H. Xia, G. Zou, Q. Zhang, and J. Gao, "Enantioselective synthesis of helical polydiacetylene by application of linearly polarized light and magnetic field," *Nat. Commun.*, vol. 5, p. ncomms6050, Sep. 2014.

- [59] L. S. Rodberg and V. F. Weisskopf, "Fall of Parity," *Science*, vol. 125, no. 3249, pp. 627–633, Apr. 1957.
- [60] T. D. Lee and C. N. Yang, "Question of Parity Conservation in Weak Interactions," *Phys. Rev.*, vol. 104, no. 1, p. 254, 1956.
- [61] H. Klus, "Quantum Field Theory of the Weak Nuclear Force," *The Star Garden*, 01-Jan-2009.
- [62] C. S. Wu, E. Ambler, R. W. Hayward, D. D. Hoppes, and R. P. Hudson, "Experimental Test of Parity Conservation in Beta Decay," *Phys. Rev.*, vol. 105, no. 4, pp. 1413–1415, 1957.
- [63] N. Saleh, "Parity Violation effects in chiral molecules," in *Chiral complexes: from fundamental chirality to helicene chemistry, (Doctoral dissertation)*, pp. 13–28.
- [64] Y. B. Zel'dovich, "Parity nonconservation in the first order in the weak-interaction constant in electron scattering and other effects," *Sov Phys JETP*, vol. 9, pp. 682–683, 1959.
- [65] R. Wesendrup, J. K. Laerdahl, R. N. Compton, and P. Schwerdtfeger, "Biomolecular Homochirality and Electroweak Interactions. I. The Yamagata Hypothesis," *J Phy Chem*, vol. 107, no. 34, pp. 6668–6673.
- [66] A. Szabó-Nagy and L. Keszthelyi, "Demonstration of the parity-violating energy difference between enantiomers," *Proc. Natl. Acad. Sci.*, vol. 96, no. 8, pp. 4252–4255, Apr. 1999.
- [67] J. Crassous *et al.*, "Search for resolution of chiral fluorohalogenomethanes and parity-violation effects at the molecular level," *Chemphyschem Eur. J. Chem. Phys. Phys. Chem.*, vol. 4, no. 6, pp. 541–548, Jun. 2003.
- [68] L. D. Barron, "True and false chirality and absolute asymmetric synthesis," *J. Am. Chem. Soc.*, vol. 108, no. 18, pp. 5539–5542, Sep. 1986.
- [69] M. Avalos, R. Babiano, P. Cintas, J. L. Jiménez, J. C. Palacios, and L. D. Barron, "Absolute Asymmetric Synthesis under Physical Fields: Facts and Fictions," *Chem. Rev.*, vol. 98, no. 7, pp. 2391–2404, Nov. 1998.
- [70] L. D. Barron, "Reactions of chiral molecules in the presence of a time-non-invariant enantiomorphous influence: a new kinetic principle based on the breakdown of microscopic reversibility," *Chem. Phys. Lett.*, vol. 135, no. 1,2, pp. 1–8, 1987.
- [71] R. Hoffmann and R. B. Woodward, "Conservation of orbital symmetry," *Acc. Chem. Res.*, vol. 1, no. 1, pp. 17–22, Jan. 1968.
- [72] L. D. Barron, "Can a Magnetic Field Induce Absolute Asymmetric Synthesis?," *Science*, vol. 266, no. 5190, pp. 1491–1492, 1994.
- [73] F. C. Frank, "On spontaneous asymmetric synthesis," *Biochim. Biophys. Acta*, vol. 11, pp. 459–463, Jan. 1953.
- [74] K. Soai, T. Shibata, H. Morioka, and K. Choji, "Asymmetric autocatalysis and amplification of enantiomeric excess of a chiral molecule," *Nature*, vol. 378, no. 6559, pp. 767–768, Dec. 1995.
- [75] C. Viedma Molero, "Chiral Symmetry Breaking During Crystallization: Complete Chiral Purity Induced by Nonlinear Autocatalysis and Recycling," *Phys. Rev. Lett.*, vol. 94, no. 10.1103/PhysRevLett.94.065504, pp. 65504–1, 2005.
- [76] J. M. Ribó, J. Crusats, F. Sagués, J. Claret, and R. Rubires, "Chiral Sign Induction by Vortices During the Formation of Mesophases in Stirred Solutions," *Science*, vol. 292, no. 5524, pp. 2063–2066, Jun. 2001.
- [77] R. C. Dougherty, "Chemical geometrodynamics: gravitational fields can influence the course of prochiral chemical reactions," *J. Am. Chem. Soc.*, vol. 102, no. 1, pp. 380–381, Jan. 1980.

Chapter II Enantio-selective Crystallization

II. Abstract

“ Lorsque certaines causes produisent certains effets, les éléments de symétrie des causes doivent se retrouver dans les effets produits.”

Et

“ Lorsque certains effets révèlent une certaine dissymétrie, cette dissymétrie doit se retrouver dans les causes qui lui ont donné naissance.”
P. Curie

MOF (Metal Organic Framework) with the formula $(\text{NH}_4)_4[\text{MnCr}_2(\text{ox})_6]\cdot 4\text{H}_2\text{O}$ is an interesting compound to be tested under Curie de-Gennes conjecture effect because, during the crystallization process, starting from racemic or achiral materials chiral single crystals are formed *at the interface* between an aqueous solution and ethanol-saturated vapor.

Surprisingly, without any controlled source of chirality, aqueous solution of $(\text{NH}_4)_4[\text{MnCr}_2(\text{ox})_6]\cdot 4\text{H}_2\text{O}$ yields a random distribution of Λ and Δ crystals with an excess of Λ enantiomer in most of the crystallization processes that were made. This observation led us to the conclusion that this excess might originated from the association of earth rotation or magnetic field, together with the crystallization *at the interface* and could therefore be a manifestation of the Curie-de Gennes conjecture. This chapter describes our endeavors to give a scientific confirmation of this intuition.

The first part of this chapter is devoted to our efforts to explore other possible origins of the observed enantiomeric excess and get rid of them. A large number of crystallization experiments of this MOF at 15 °C using harsh cleaning procedures leads to a vanishingly small overall excess of Λ enantiomer.

Using these cleaning conditions, crystallizations in a high speed rotation or high magnetic field yield an overall excess of Λ and Δ enantiomers that depend on the rotation or field orientation. Nevertheless, the distribution of the results is so large that these experiments cannot be considered as a definitive demonstration of the Curie-de Gennes conjecture.

II.1. General Description of MOF Compound

Metal-Organic Frameworks (MOFs) are compounds that contain metal ions or clusters bridged by organic ligands to form infinite structures in one-, two- or three-dimensions. Most of the time, MOF is reserved to 3D coordination networks whereas “coordination networks” is used whatever the dimensionality of the network. They form a class of nanoporous materials with huge surface area, regularity and flexibility [1], [2].

Recently, a compound having formula $(\text{NH}_4)_4[\text{MnCr}_2(\text{ox})_6]4\text{H}_2\text{O}$ was obtained by reacting ammonium tris(oxalato)chromate(III) and manganese(II) chloride in water. Large needles shaped single crystals were obtained by slow diffusion of ethanol. The compound crystallizes in two enantiomorphous space groups, $P6_522$ and $P6_122$. Experimentally, without any obvious source of chirality, an excess of single crystals crystallizing in the $P6_522$ space group has been observed [3].

Moreover, quartz has an important role since the discovery of the optical activity in chiral crystals. It was one of the first material used by J. B. Biot in 1815 [4]. Our target is based on Metal Organic Quartz-like Framework (MOQF) because it has a hexagonal symmetry and its optical activity depends on its crystal structure and thus when it dissolves in water it loses its optical activity.

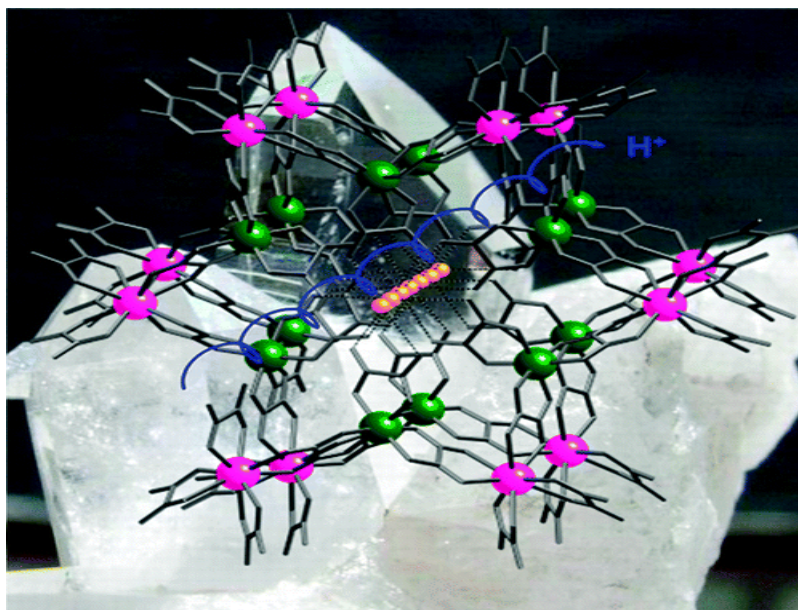


Figure II-1 Perspective fragment of the 3-D anionic bimetallic coordination networks of $(\text{NH}_4)_4[\text{MnCr}_2(\text{ox})_6]4\text{H}_2\text{O}$ [3].

The structure of this chiral MOF is represented in Figure II-1. In the MOF, each manganese(II) ion (purple balls) is surrounded by four bidentate oxalate ligands whereas chromium(III) ion (green balls) is bound to three bidentate oxalate ligands. One of these ligands is directed towards co-crystallized water molecules along the helical axis while the two others bridge chromium(III) and manganese(II) ions in a bis-bidentate way. Accordingly, each manganese(II) is linked to four chromium(III) by bridging oxalate ligands [3], [5].

It is worth mentioning that this compound is a proton conductor. In Figure II-1, blue helix represents the pathway of the proton transfer through hydrogen bonds between non bridging oxalate ligand and proton bearing molecules, ammonium cations and water molecules represented as orange balls. Moreover, it exhibits a long range ferromagnetic ordering at low temperature below $T_c = 3.0\text{K}$ due to the host anionic network [3]. Briefly, the oxalate ligand is one of the most studied ligand in molecular magnetism which controls the coupling between two spin centers depending on its coordination mode [6]–[11], for instance, Cr(III)-Mn(II). Moreover, oxalate-based chiral MOF forms open networks capable of hosting guest cation (H^+ , H_3O^+ or NH_4^+). This property can be exploited to design multifunctional materials [3].

II.2. Motivation

The advantage of this system is that the final compound is obtained through the crystallization process by slow diffusion of more volatile solvent **at the interface**. In principle, when the vapor

of the more volatile solvent diffuses **at the interface** of the second vial which is containing the racemic aqueous solutions, the volume (water + ethanol) in the latter increases, the concentration decreases. But, at the same time, the solubility of the MOF in the water/ethanol mixture dramatically decreases. Therefore, the crystallization of $(\text{NH}_4)_4[\text{MnCr}_2(\text{ox})_6]\cdot 4\text{H}_2\text{O}$ occurs **at the interface** between aqueous solution and ethanol vapor interfaces (Figure II-2).

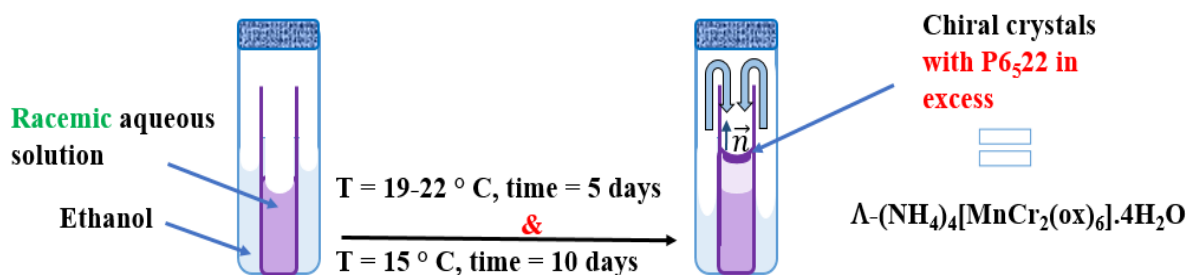


Figure II-2 Crystallization of chiral MOF compound by vapor diffusion method.

In correlation to what was mentioned in chapter I, the collinear magnetic (time odd-axial vector) and electric (time-even polar vector) fields generate spatial dissymmetry as proposed by Pierre Curie [12]. In this experiment, we were inspired by Curie's proposal, since in this crystallization experiment, there is the association of a time-even polar vector (\vec{n}) which is normal to the interface and time odd-axial vectors ((\vec{L}) or (\vec{B})). Moreover, with the crystallization process, we expect the effect to be amplified by crystal growth.

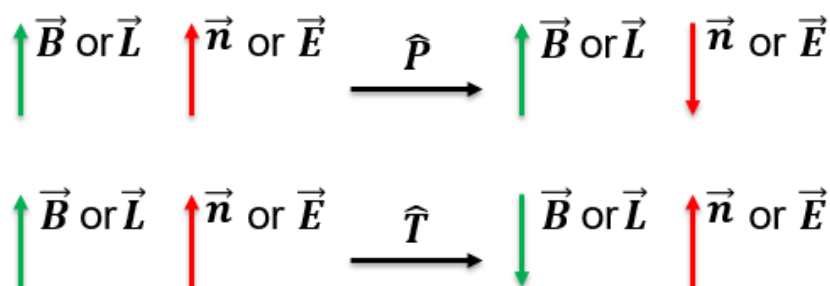


Figure II-3 False chirality of a parallel combination of a different vectors and their transformation under the operation of parity P and time reversal T .

As illustrated previously, a parallel set of electric and magnetic field ($\vec{B} \vec{E}$) gives under space inversion different sets of field with antiparallel orientation ($-\vec{B} \vec{E}$), which are not superimposable on the original set. Additionally, both set of fields can be interconverted by the time reversal operator. The combination of ($\vec{n} \vec{L}$) and ($\vec{n} \vec{B}$) follows exactly the same argument regarding to the effect of parity and time reversal as shown in the Figure II-3.

That's why we expected the possibility of obtaining enantioselective crystallization of MOF compound by a combination of external forces (\vec{B} or \vec{L}) and crystals growing **at the interface** (\vec{n}) under falsely chiral influence.

II.3. Experimental Procedures

II.3.a. Synthesis of Ammonium Tris(oxalate)Chromate(III)

3.8g (27 mmol) of ammonium oxalate monohydrate was mixed with 11.17g (87.5 mmol) of oxalic acid dihydrate in 150mL of water, resulting in a white opaque suspension. The solution was mixed with a magnetic stir rod and heated up to 80 °C for 30 minutes. 3.3g (13 mmol) of ammonium dichromate was then added slowly. The resulting mixture turned dark green and the reaction was carried out until CO₂ vapors disappeared. The solution volume was reduced to 10 ml in order to favor crystal formation. The concentrated solution was slowly evaporated at room temperature. Dark green-black crystals were formed. The total yield was 98 % (~ 10.34 g). The overall reaction writes as follow:



II.3.b. Synthesis of 3-D Chiral Bimetallic Oxalate-Based Magnet

0.42 g (1 mmol) of the ammonium tris(oxalato)chromate(III), $(\text{NH}_4)_3[\text{Cr}(\text{C}_2\text{O}_4)_3] \cdot 3\text{H}_2\text{O}$ was dissolved in 1mL of water. Then 0.1 g (0.5 mmol) of $\text{MnCl}_2 \cdot 4\text{H}_2\text{O}$ dissolved in 0.8 mL of water was added to the $(\text{NH}_4)_2[\text{Cr}(\text{C}_2\text{O}_4)_3] \cdot 3\text{H}_2\text{O}$ solution. The resulting solution was stirred for 30 minutes. After that, two vials were used: a wide one and a narrow one that will fit inside the wider one. 0.2 mL per vial of the racemic aqueous solution is placed in the inner vial and ethanol solvent is placed in the wider one. After some time the more volatile solvent (ethanol) starts to diffuse slowly towards the interface of aqueous solution as shown in the (Figure II-2). After several days large violet prismatic single crystals of $(\text{NH}_4)_4[\text{MnCr}_2(\text{ox})_6] \cdot 4\text{H}_2\text{O}$ were obtained. The time of crystallization depends on the temperature of crystallization process: for example at 15°C, it takes 10 days while at room temperature (19-23 °C), 5 days are sufficient (Figure II-2). The overall reaction writes as follow:



Elemental Analysis: Calculated for $C_{12}H_{24}Cr_2MnN_4O_{28}$ (831.3 g/mol): C, 17.34; H, 2.91; N, 6.74. Found: C, 17.21; H, 2.65; N, 6.89; IR spectra were measured between 400 and 4000 cm^{-1} using a Nicolet Fourier Transform Infra-Red iS50 FT-IR Spectrometer: 3090s, 3150s [$\nu(N-H)$ & $\nu(O-H)$]; 1707s, 1670s, 1639s [$\nu(C=O)$]; 1400vs, 1259s [$\nu(C-O)$].

II.4. Characterization of the Chiral MOF

II.4.a. Powder X-ray Diffraction (PXRD)

Powder X-ray diffraction patterns were recorded using a Bruker D5000R diffractometer. PXRD analyses are essential to determine crystal structure of the expected product.

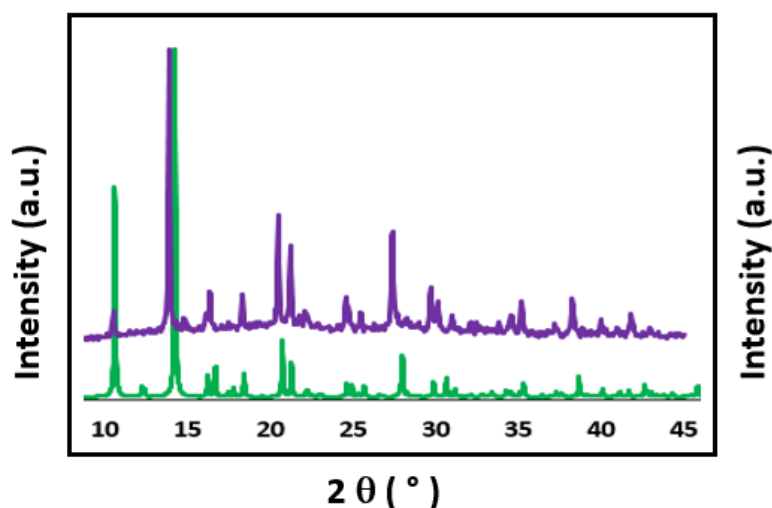


Figure II-4 Overlay of powder x-ray diffraction pattern for chiral MOF at RT (violet spectra) and calculated pattern from single-crystal XRD measured at 200 K (green spectra).

As can be seen in Figure II-4, it appears that the experimental powder diffractogram of the chiral MOF agrees with the powder diffraction patterns calculated from the corresponding single-crystal X-ray structure [3]. However, there is small shift in the peaks of the violet spectra towards left because the single-crystal X-ray experiment was done at 200 K while the experimental PXRD was performed at room temperature. Accordingly, because of thermal contraction due to the variation of the temperature, all the Bragg peaks are shifted to lower value of diffraction angle.

II.4.b. Thermogravimetric Analysis (TGA)

TGA measurements were performed with a METTLER TOLEDO TGA/DSC star^e System. It measures the amount and the rate (velocity) of change in the mass of a sample as a function of temperature and time in a controlled atmosphere. The measurements are used primarily to determine the thermal or oxidative stabilities of MOF as well as their compositional properties. The technique can provide information about decomposition, vaporization, and absorption etc.

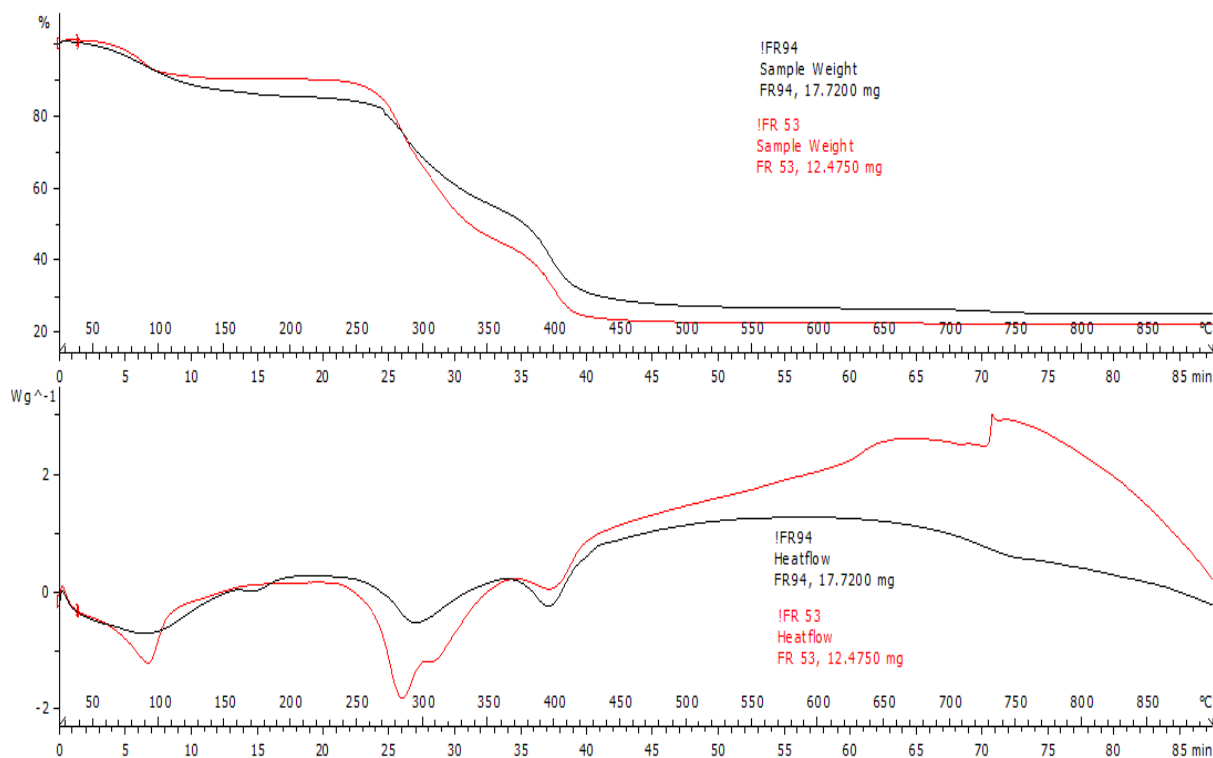


Figure II-5 TGA of $(\text{NH}_4)_4[\text{MnCr}_2(\text{ox})_6].4\text{H}_2\text{O}$ (black spectra) and tris(oxalato)chromate(III) (red one).

TGA data in Figure II-5 indicates that the loss of H₂O molecules (10%) in the first step in the temperature range 50-100°C. The sharp weight loss (60%) after 300°C is due to structural decomposition in the framework which is in agreement with the reported chromium salt (red curve) [13], [14] but here in the end we expected to get manganese and chromium oxides (red spectra) instead of only chromium oxide as the final product of TGA (red spectra).

II.5. Instrumentation and NCD Operating Principle

Natural Circular dichroism (NCD) spectroscopy measures differences in the absorption of left- and right-handed circularly polarized light (ΔA) as a function of the wavelength [15]:

$$\Delta A(\lambda) = A(\lambda)_{LCPL} - A(\lambda)_{RCPL} \quad \text{Equation II-1}$$

This measured difference gives important data regarding the structure, absolute configuration of the molecule of interest. NCD spectra were recorded with a JASCO Model J-1500 spectropolarimeter (Figure II-6A), using PMT (photomultiplier tube) detector and either halogen or xenon lamps. All measurements were performed in a visible region.

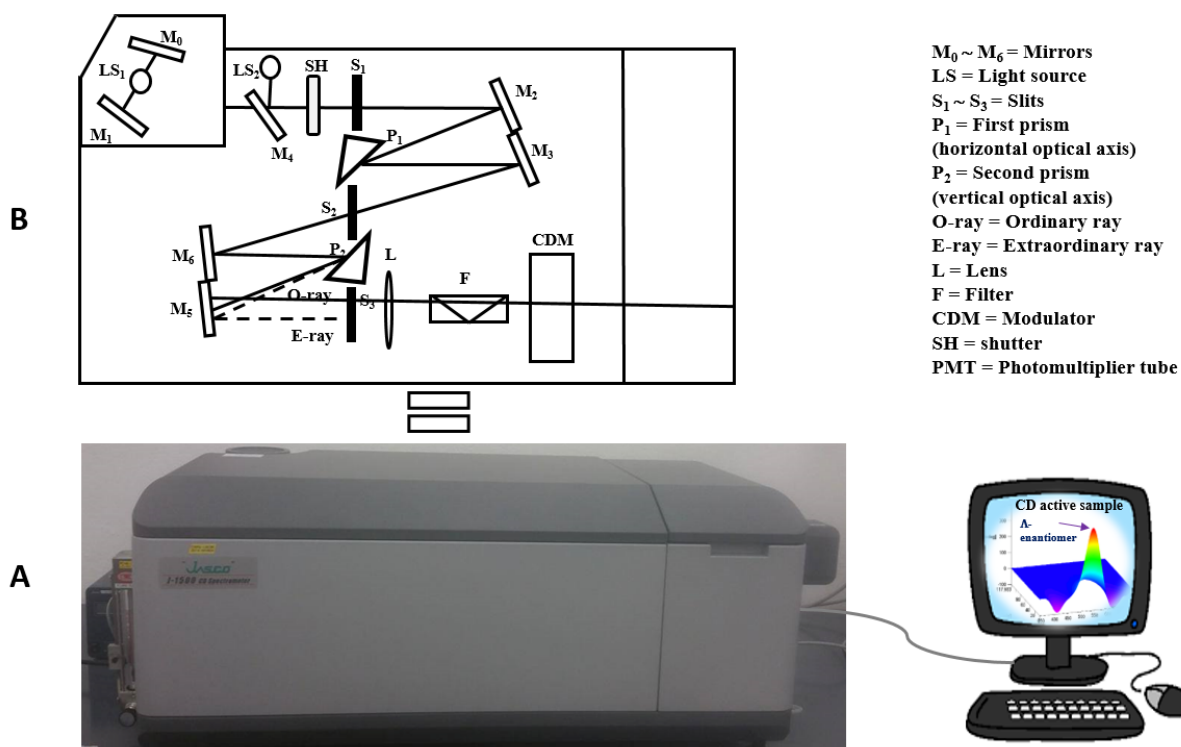


Figure II-6 High performance CD spectrometer (Model J-1500) for versatile measurements and its optical system (redrawn from JASCO tutorial).

Figure II-6B represents the optical system of CD spectrometer where xenon or halogen lamps were used as a light source (LS_1). The monochromator is a double quartz prism monochromator (P_1 & P_2). At the entrance of this monochromator, there is a shutter (SH) which prevents light from passing through the monochromator when the instrument is idle. As a white light passes through the first prism, it splits into its component wavelengths and the wavelength is selected by the intermediate slit (S_2). Through this intermediate slit, the mixture of horizontally polarized

light of the selected wavelength and vertically polarized light will pass through it. Then, the second prism (P_2) separates out the contaminating vertically polarized beam, as well as stray light (extraordinary ray). Only the ordinary ray (solid line) will be passing through exit slit (S_3), lens (L) and polarizing filter (F). So that, the monochromator and polarized filter output is linearly polarized monochromatic light. Finally, the linearly polarized light is passed through a photoelastic modulator that converts it into alternatively left- and right- circularly polarized light (LCPL & RCPL) which passes through the sample.

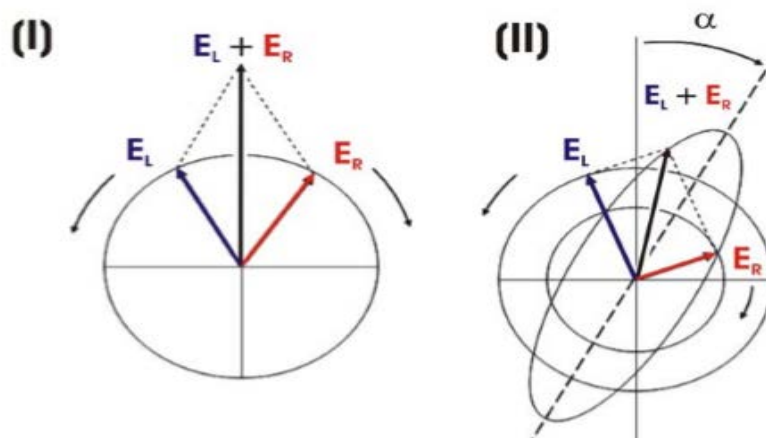


Figure II-7 Behaviors of the field vectors of left (blue) and right (red) circularly polarized light and their position (black), before (I) and after (II) passage through the optically active sample [16].

Figure II-7 represents how right and left circularly polarized light combined before and after passing through the optically active sample. In I the two waves have the same amplitude, the result is plane polarized light. However, in II the amplitude of two waves is different, the result is elliptically polarized light with a $(E_R + E_L)$ and b $(E_R - E_L)$ as their major and minor axes. The resulting LCPL and RCPL of unequal intensities reached the detector (PMT). A lock-in detection monitors the NCD signal of the sample. Sweeping the wavelength finally lead to the NCD spectrum [17], [18].

II.6. General Method

II.6.a. Sample Preparation

Given that in all the samples we have prepared, both enantiomers were present with a different ratios and they were randomly distributed in each badge. So, the solid NCD measurements

would require huge amount of measurement of each sample. We have thus defined a protocol to perform quantitative NCD measurements in solution instead of solid NCD measurements. The collected single crystals from each individual experiment were dissolved in 10 mL of water and this volume was measured by using a volumetric flask. It is very important to do these measurements as soon as possible after the dissolution of the MOF because the chiral species remaining in solution, that is tris(oxalato)chromate(III), has to be racemized in time. All NCD spectra are collected in high transparency quartz cells with path length of 1 cm.

II.6.b. Resultant Spectra

II.6.b.1. 3-Dimensional NCD Spectrum

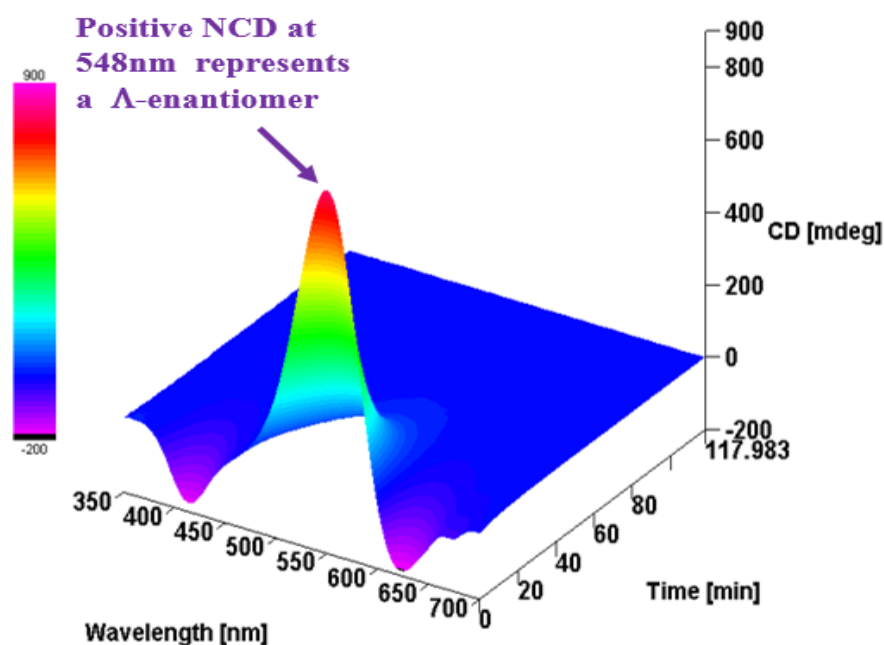


Figure II-8 Three dimensional NCD (3D-NCD) spectrum of chiral tris(oxalato)chromate(III) in solution.

Figure II-8 represents the 3D NCD signal of the chiral tris(oxalato)chromate(III) obtained after the dissolution of the MOF in water. This type of measurement allows simultaneous acquisition of up to three data channels including NCD, wavelength, and time. It shows the variation of NCD as function of wavelength and time where the maximum positive NCD signal appearing

at highest absorption band (548 nm) corresponds to the Λ enantiomer of tris(oxalato)chromate(III).

In order to determine numerically the racemization rate and $t_{1/2}$, a single frequency NCD measurements of the most intense band (548 nm) for different single crystals were performed.

II.6.b.2. Single Frequency Measurements

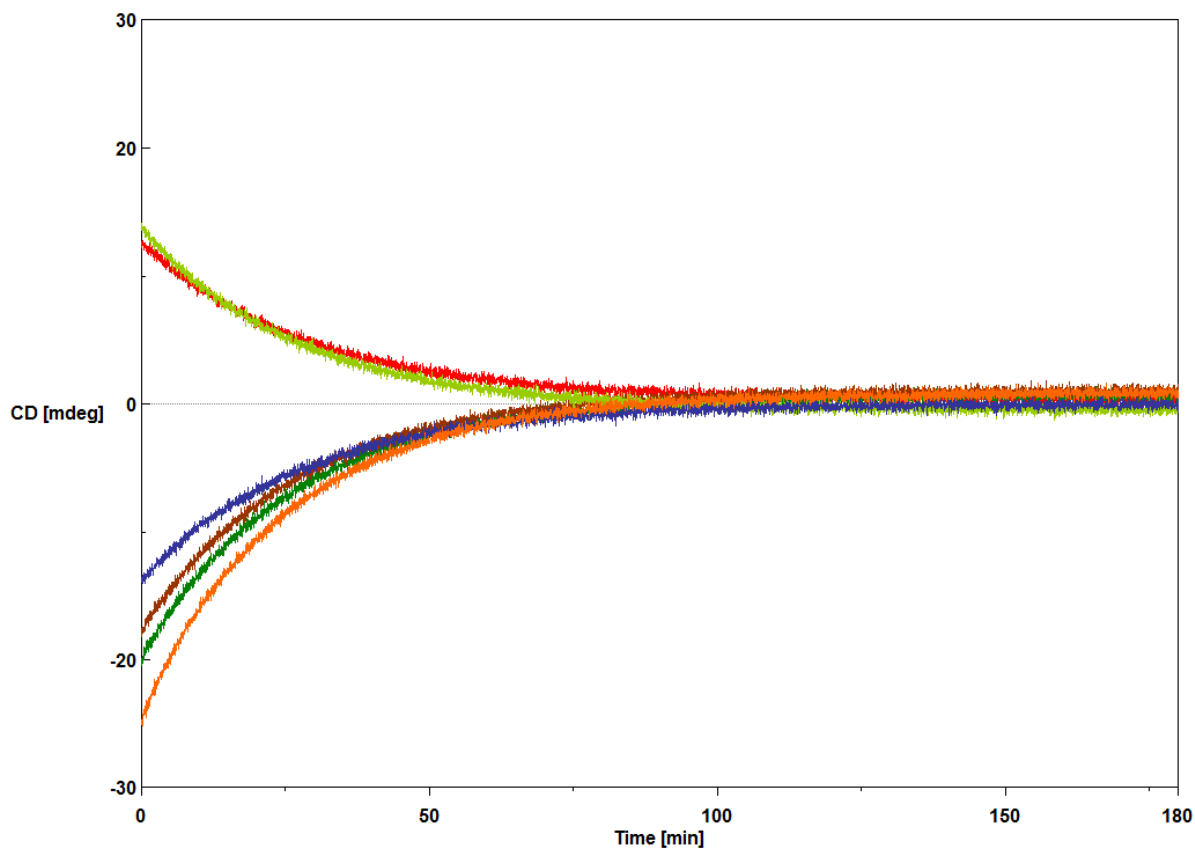


Figure II-9 NCD decay for different single crystals as function of time at 548 nm.

Figure II-9 shows the rate of racemization of different single crystals where the y-axis represents CD decay as function of time.

Clearly, in this figure it can be seen that the rate of change in the CD signal is proportional to the percentage of the optical purity of single crystals is decreasing with time. The curve is much steeper at the beginning and as time progresses, the curve approaches a horizontal line. Thus, this graph evidently shows that the optically active tris(oxalato)chromate(III) compounds is racemized completely after one hour.

According to this figure, positive CD signal represents the Λ enantiomer whereas negative signal represents the Δ enantiomer. Moreover, the curves with different colors represents the different measurements for six single crystals of different weight.

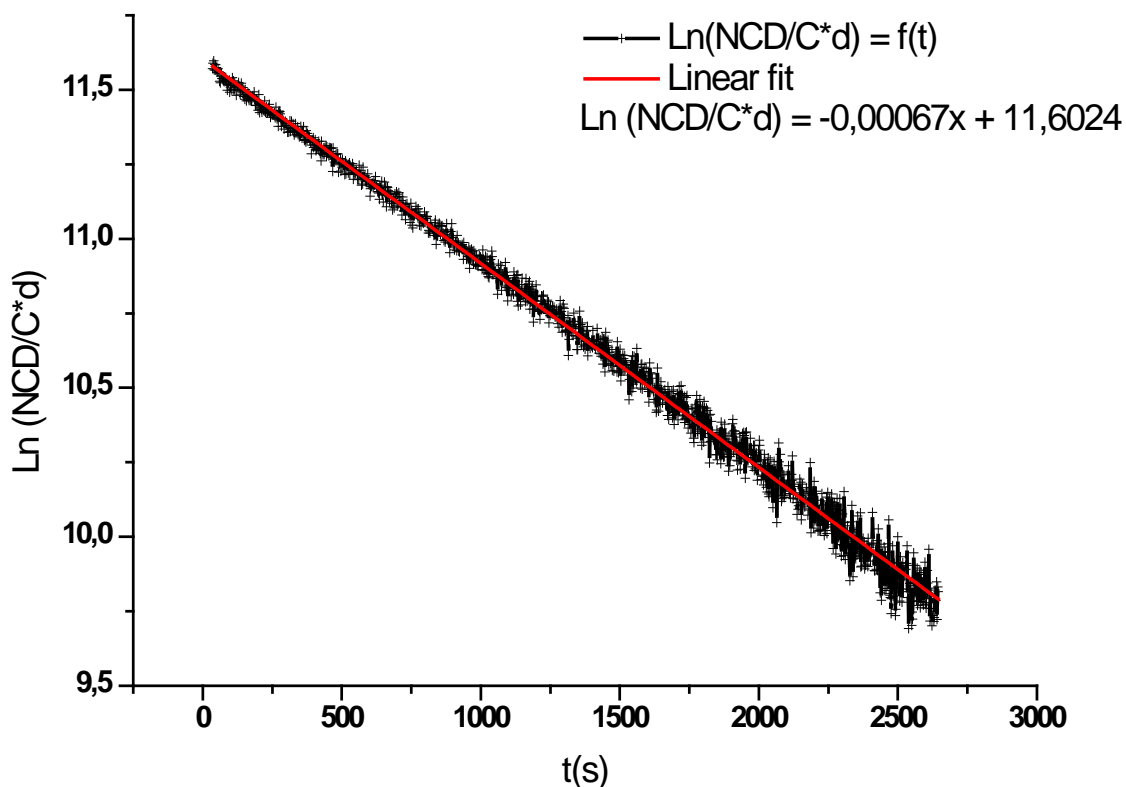


Figure II-10 First-order plot of $\ln(NCD/C \cdot d)$ versus time.

In order to determine the value of $t_{1/2}$, the obtained data from NCD spectrometer was used to make a new plot of $\ln NCD/C \cdot d$ with respect to time, where NCD is the signal of optical activity of tris(oxalato)chromate(III), C is the concentration of tris(oxalato)chromate(III) obtained from the dissolution of one single crystal in water and d is the path length of the micro cuvette that was used for these measurements.

Figure II-10 represents one plot out of 6 that we have made. All the plots we have performed give a straight line. This means that our system exhibit first-order kinetics and the graphical methods allow the determination of the rate constant (k). So that, the slope of this plot should be equal to $-k$ which is equal to $0,00067 \text{ sec}^{-1}$ and half-life time $t_{1/2} = \ln(2)/k$ equal to 17 minutes.

Table II-1 Values of rate constant k and half-life time.

Crystal / Sample number	k (s⁻¹)	t_{1/2} (min)
1	0,00055	21
2	0,00067	17
3	0,00069	17
4	0,00069	17
5	0,00066	17
6	0,00059	20

Kinetic parameters of the first-order (kinetic constant k) and the corresponding half-life time $t_{1/2}$ for all chosen single crystals are reported in Table II-1. These values were similarly obtained to the example shown above. We notice from this table that there is a good agreement for all chosen single crystals where the values of k and $t_{1/2}$ vary slightly in all measurements.

Generally, the kinetic data, the spontaneous decay of NCD) and rate of racemization as a function of time of tris(oxalato)chromate(III) is well understood, well-described and has been verified by numerous measurements. The racemization rate is independent of the intensity of initial NCD signal. The half-life, $t_{1/2}$, is the amount of time required for half of the initial NCD in a sample to racemize which is ranged between 17 and 21 minutes. This type of measurement demonstrates that the tris(oxalato)chromate(III) in solution loses its optical activity after some times (average of $t_{1/2} = 18$ minutes), which means preparing the samples for liquid NCD measurements rapidly will not affect the final results.

II.6.b.3. 2-Dimensional NCD spectra

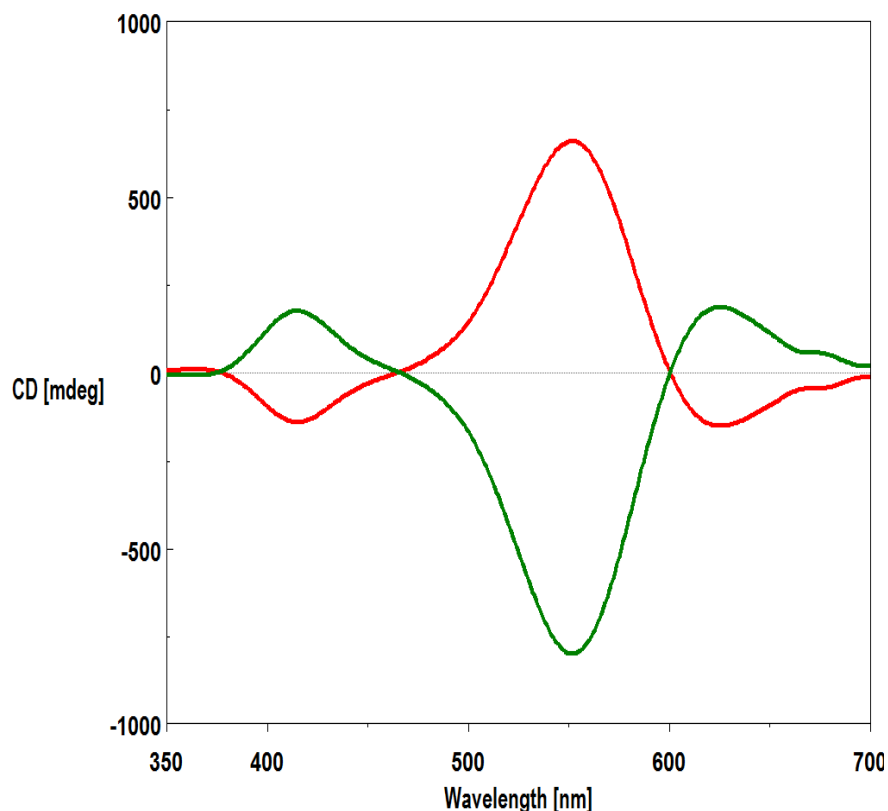


Figure II-11 2D- NCD spectra of Λ (red curve) and Δ (green curve) polymers.

Figure II-11 represents the NCD spectra of two different samples of chiral tris(oxalato)chromate(III) dissolved in water. The two NCD bands with opposite sign and different intensities (Λ - and Δ -(NH_4)₄[$\text{MnCr}_2(\text{ox})_6$].4 H_2O) are observed. These two spectra are mirror images of each other.

Using 2D-NCD measurement is preferable over 3D-NCD since the kinetic properties of tris(oxalato)chromate(III) do not change from one sample to another as demonstrated in the previous part. Moreover, it is fast where it only takes 5 minutes to measure a sample.

For these reasons, we will stick to this type of measurement and only consider the values at 548 nm.

II.6.c. Global Method Used for NCD Data Analysis

Our NCD spectrometer measures NCD in terms of ellipticity of the polarization which is abbreviated as (θ), usually expressed in millidegrees [19]. This value is originated from the magnitudes of the electric field vectors E_L and E_R using the rules of trigonometry (Equation II-2).

$$\tan \theta = \frac{E_R - E_L}{E_R + E_L} = \frac{b}{a} \quad \text{Equation II-2}$$

Where E_R and E_L are the electric field amplitudes of the right- and left- circularly polarized light. When θ is given in radian and the values of the ellipticity is low, $\tan\theta$ is equal to θ [17]. Additionally, there is a simple numerical relationship between ΔA and ellipticity (θ) (Equation II-3).

$$\theta[\text{degrees}] \approx 32.98 \Delta A \quad \text{Equation II-3}$$

In general, literature data are mostly reported in molar circular dichroism ($\Delta\varepsilon$) which is equal to:

$$\Delta\varepsilon = \frac{\theta}{32980lC} \quad \text{Equation II-4}$$

Where l in cm, C in mol/L or (mmol/cm³), θ in millidegrees and $\Delta\varepsilon$ in L/mol.cm or (cm²/mmol). However, in our case we used an alternative way to express results. As previously mentioned, that we have a fast racemization in solution and in some vials a very small amount of crystals is formed. Weighting them to determine the concentration would lead to enormous errors. This is why I proposed to introduce the following method which does not require concentration calculations.

As a first step, normalized NCD values (nNCD) were calculated using Equation II-5, where the ellipticity, that we called NCD values obtained from NCD spectrometer at 548 nm, were divided by absorption (A) at the same wavelength.

$$nNCD = \frac{NCD}{A} = \frac{\theta}{A} \quad \text{Equation II-5}$$

In each experiment, a large number of samples are considered. So that mass normalized frequency is calculated for each individual sample using the following formula:

$$Freq_i = \frac{m_i}{m_{total}} \quad \text{Equation II-6}$$

Where m_i is the mass of MOF compound in each individual sample divided by total mass obtained from all the samples of the experiment performed in the same conditions.

Then, the average of nNCD is calculated which is equal to the summation of nNCD values multiplied by mass normalized frequency (Equation II-6). The value of mass was taken into account because the amount of obtained product is not same in all samples.

$$nNCD_{average} = \sum_{i=1}^N nNCD_i \times freq_i \quad \text{Equation II-7}$$

The standard deviation (SD) in each experiment was calculated. SD of N experiments is equal to square root of the variance (V) and given by (Equation II-8).

$$SD = \sqrt{V} = \sqrt{(\sum_{i=1}^N freq_i \times nNCD_i^2) - nNCD_{average}^2} \quad \text{Equation II-8}$$

II.6.d. Treatment Procedure

The details of the procedure used to treat the surfaces of the vials that we used for crystallization process are the following:

- Introduce all the glassware used in the crystallization process into the oven (**250 ° C**) for 2 hours after washing them with distilled water.
- Put them in a concentrated sodium hydroxide solution (**14 mol/L**) for 30 minutes.
- Rinse all glassware in bi-distilled water several times to be sure that all traces of sodium hydroxide are removed.

Later this method was slightly modified where all the glassware used in the crystallization process were introduced twice into the oven (**250 ° C**) before and after using a concentrated solution of NaOH.

II.6.e. DAPI Test

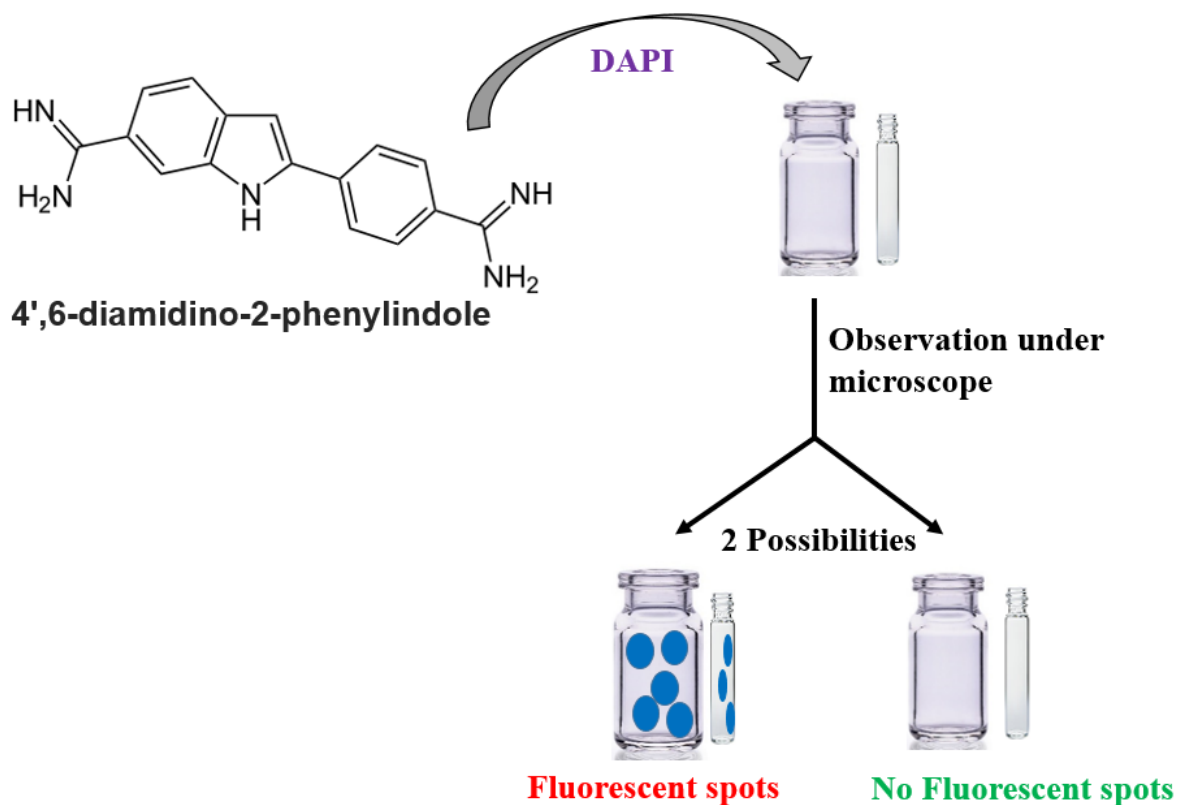


Figure II-12 Testing the purity of vials using DAPI test.

DAPI (4,6-diamino-2-phenylindole) test is a test allowing us to check the presence of bacteria, virus, biofilm at the surface and bottom of the used vials for crystallization process. DAPI is a fluorescent stain that binds strongly to A-T rich regions of DNA, and it has the ability to pass through an intact cell membrane. Figure II-12 illustrates how we identify whether the used vials present traces of DNA or not. After adding DAPI inside the vials, if the treatment procedure is quite enough to clean the vials, the observation under microscope should not show any fluorescent spots. However, if the DNA traces are left behind after the cleaning procedure, the observation under microscope will show fluorescent spots on the whole surface of the vial.

II.6.f. Different Techniques Used to Study the Effect of External Forces

II.6.f.1. Crystallization in a Magnetic Field

II.6.f.1.a. Low Field

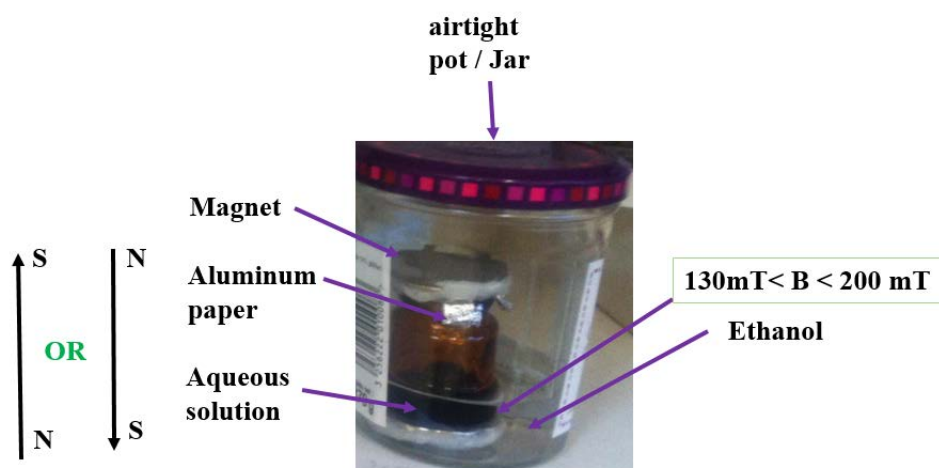


Figure II-13 Experimental setup for crystallization process using small Neodymium magnet.

To investigate the effect of magnetic field, a first setup was built (Figure II-13) where the sample in a small brown glass vial is placed between two NdFeB magnets of 5mm height and 35mm diameter are used. The magnetic field at the interface where the crystallization process takes place has been measured using a Gauss meter and was found to be **130-200 mT**. The experiment is performed at room temperature and the direction of the field is marked and identified before crystallization process. Aluminum paper was used to allow the diffusion of ethanol vapor and the magnets were covered with parafilm to prevent the interaction with ethanol.

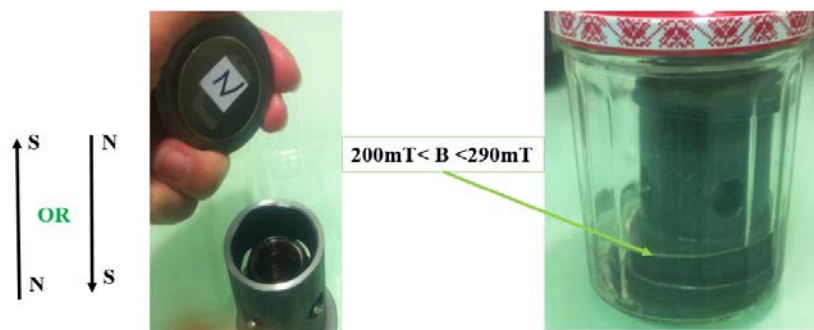


Figure II-14 Experimental setup for crystallization process using small Neodymium magnet and iron tubes.

To increase the magnetic field, iron tubes were designed in our laboratory specifically for this purpose (Figure II-14). Same experimental was setup as shown in previous figure with only one difference which is crystallization process occurred inside iron tubes where two NdFeB are used again. The strength of the field is ranged between **200** and **290 mT**.

II.6.f.1.b. High Field

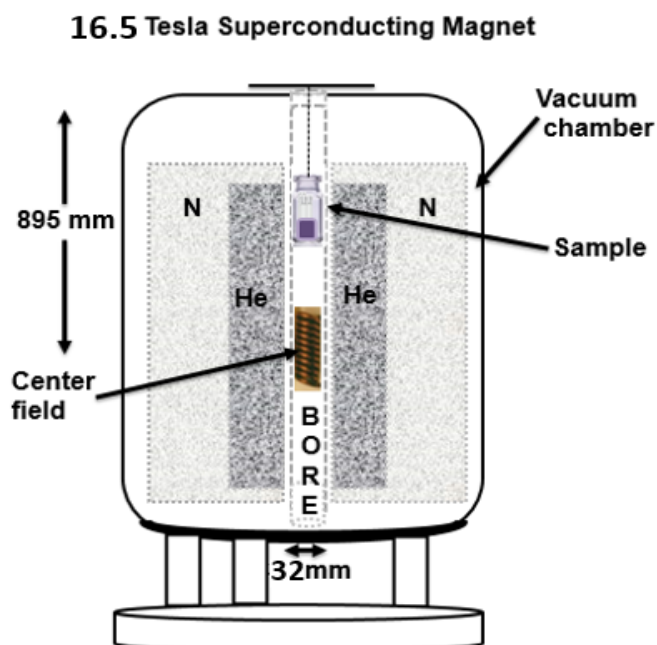


Figure II-15 Schematic of a 16.5 Tesla superconducting magnet (SCM) with vertical bore.

Figure II-15 shows the scheme of Oxford Instrument (16.5 Tesla) superconducting magnet (SCM) that we used for crystallization process. A SCM is an electromagnet made up of coils of superconducting wire. The superconducting coils are immersed in liquid helium (boiling point $\cong 4.2$ K) in an inner dewar, which is also surrounded by an outer dewar containing liquid nitrogen at 77 K. This type of magnet produces a high magnetic field, up to 16.5 Tesla. The cryogenic tanks of liquid helium & nitrogen are wrapped around a central column known as the magnetic bore and the diameter of this bore is of only 32mm. The sample to be crystallized is introduced into the magnet via the top of the bore and is placed at the central magnet field (B_0) at a depth of 895 mm from the top, where the strength of the field is very high and most homogeneous. The general conditions for crystallization in SCM are: crystallization time is 7 days, temperature inside the magnet is 15 °C, and the magnetic field is **12 Tesla**; moreover, a maximum of three samples was placed inside this magnet.

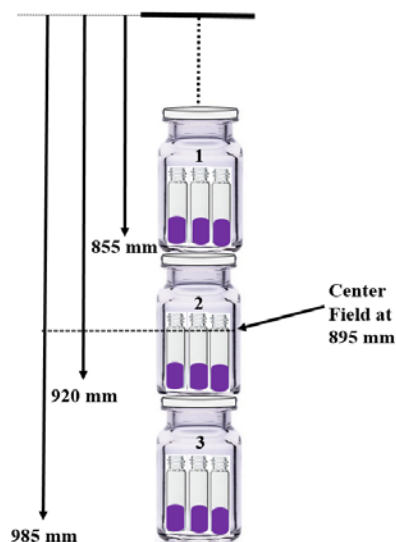


Figure II-16 Three large cylindrical vessels placed one over the other inside the SCM.

Here we are still using a SCM; however, in this experiment, we have used 3 big vials in place of one put above each other (Figure II-16) where the number of the samples is increased to 9 samples per experiment, and these vials were placed at the different positions inside the magnet.

II.6.f.2. Crystallization in a High Speed of Rotation

II.6.f.2.a. First Rotatory Plates

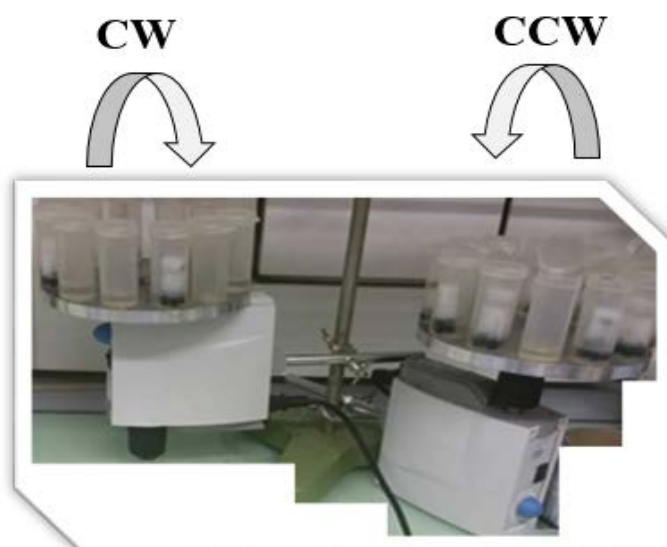


Figure II-17 First experimental setup used to study the effect of rotation.

The induction of chirality by means of rotating the samples in both directions clockwise (CW) and counterclockwise (CCW) is represented in Figure II-17. In this experiment I have built a

setup containing two rotatory plates: one rotates CW and the other rotates CCW and 12 plastic vials are fixed symmetrically at the edge of these rotatory plates. In each plastic vial, we placed 4 small glass vials. Moreover, the crystallization processes were performed at room temperature where the process is finished after 5 days, and the magnitude of angular velocity is **240 rpm**.

II.6.f.2.b. Second Rotatory Plate



Figure II-18 Experimental setup for crystallization process using rotatory plate inside the fridge.

Figure II-18 represents the recent rotatory plate that we used for crystallization process. In this experiment, the crystallization process was done inside the fridge at temperature $15\text{ }^{\circ}\text{C}$ where the process is finished after 10 days, the magnitude of angular velocity is **109 rpm**. At the same time, many samples (up to 24) were prepared under exactly the same conditions with only one difference where the sample is not rotated during the crystallization process in order to study the effect of rotation. These samples were used as blank samples.

II.7. Results & Discussions

As we mentioned previously, MOF compound with the formula $(\text{NH}_4)_4[\text{MnCr}_2(\text{ox})_6]\cdot 4\text{H}_2\text{O}$ is crystallized in a chiral hexagonal space groups ($P6_522$ and $P6_122$). Experimentally, an excess of lambda enantiomer ($P6_522$) is often observed [3]. The generation of e.e. from achiral or racemic precursors during the course of the crystallization is still an unpredictable and unexplained phenomenon [20].

It is crucial to find the origin of this enantiomeric excess and settle conditions where it is suppressed before undertaking experiments under controlled magnetic field or rotational force. In turn, this was the source of inspiration because we believe that earth rotation or earth magnetic field associated to \vec{n} was at the origin of the observed effect; therefore, I decided to increase the field or the rotation speed using different setups in order to increase the e.e.

The work on this chapter involves three mutually interconnected approaches: the first approach is to emphasize quantitatively the general method used for crystallization process. The second approach is based on studying different factors to know the source of the excess that appeared at the end of crystallization process in order to get rid of them. While the third one is based on studying the effect of external forces such as, rotation and magnetic fields on the enantioselectivity of chiral MOF. The last two approaches were done in parallel.

II.7.a. Evaluation the excess of lambda enantiomer

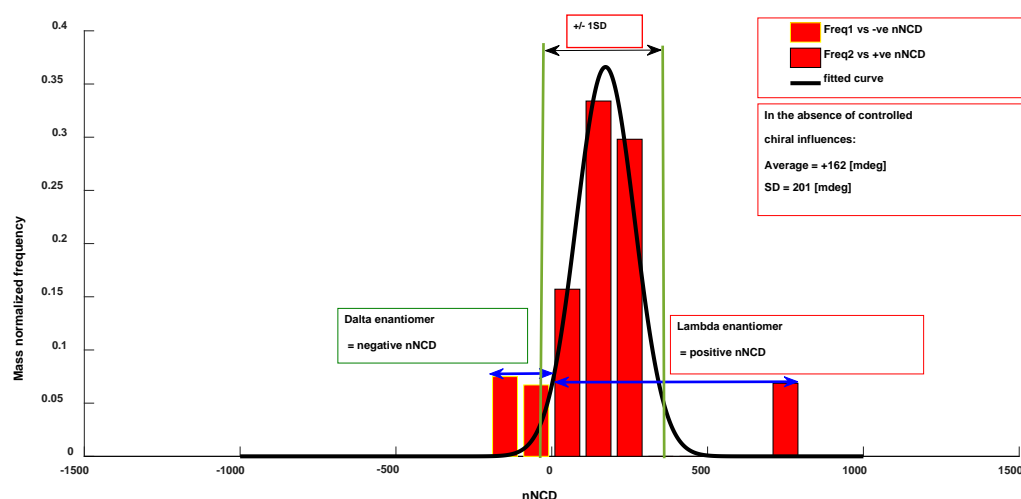


Figure II-19 Mass normalized frequency versus normalized NCD values.

We have done many experiments in the absence of any volunteer chiral perturbation during the crystallization process.

To present results more effectively, we plotted a histogram with normal distribution. Figure II-19 represents a statistical distribution of normalized NCD values for Δ and Λ enantiomers where no chiral perturbation was introduced during crystallization process.

However, the standard deviation, 201 [mdeg], is greater than the average nNCD estimated from the normal distribution (black curve) which is equal to +162 [mdeg]. Therefore, the results

shown in Figure II-19 appear as manifestation of some kind of chiral bias that gives every time, as an average, excess of Λ -enantiomer. So, where does this initial chiral bias come from?

II.7.b. Crystallization of $(\text{NH}_4)_4[\text{MnCr}_2(\text{ox})_6]\cdot 4\text{H}_2\text{O}$ using Different Conditions

As a first step of my work, I have searched for the origin of this chemical bias. So I have checked whether there is some chiral bias in the starting material such as tris(oxalato)chromate(III) or in the solvent that we used for crystallization process. Positively, nothing was detected which means a zero NCD.

After that, I proposed that there is a biological origin of this chiral bias, but since we do not know their origin, several tests were done.

II.7.b.1. Crystallization of chiral MOF using D/L phenylalanine respectively

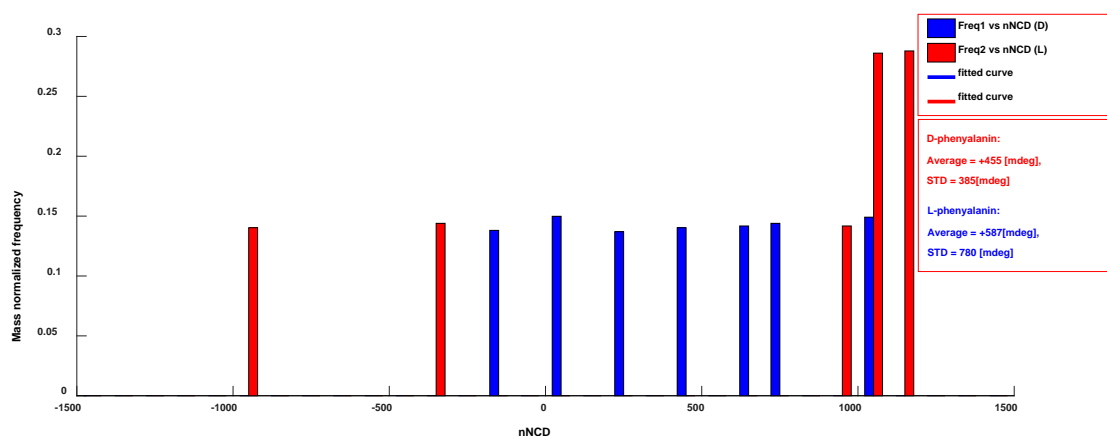


Figure II-20 Mass normalized frequency versus normalized NCD values for crystallization of $(\text{NH}_4)_4[\text{MnCr}_2(\text{ox})_6]\cdot 4\text{H}_2\text{O}$ using D and L phenylalanine separately.

First test was done by adding willing D and L phenylalanine separately to the aqueous solution of $(\text{NH}_4)_4[\text{MnCr}_2(\text{ox})_6]\cdot 4\text{H}_2\text{O}$ with a concentration equals to $1.667 \cdot 10^{-3} \text{ mol}\cdot\text{L}^{-1}$. This was done to study the effect of chiral impurities that may come from the atmosphere or from the material that we are using for crystallization process [21], [22]. Figure II-21 shows that the chiral sign of the used amino acid (D & L) did not affect the enantioselectivity of chiral MOF (statistical distribution of nNCD). In both cases, two types of enantiomers are obtained with the same unknown type of bias that favors the formation of lambda enantiomer in excess.

The normal distribution is not drawn in some figures due to high dissymmetric dispersion of the obtained nNCD values, low number of samples and high standard deviation.

II.7.b.2. Crystallization of Chiral MOF using Tri-distilled Water

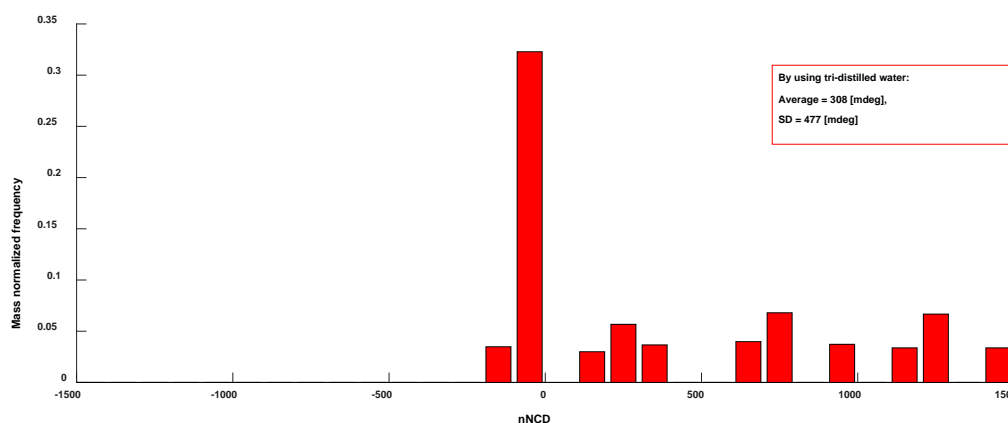


Figure II-21 Mass normalized frequency versus normalized NCD values for crystallization of $(\text{NH}_4)_4[\text{MnCr}_2(\text{ox})_6]\cdot 4\text{H}_2\text{O}$ using tri-distilled water.

In general, bacteria form the largest number of living organisms on the planet and are habitable in all types of environments. Some kinds of bacteria such as Cyanobacteria are aquatic which means that they live in the fresh water and can manufacture their own food [23]. These bacteria have gained a lot of attention in recent years because of their application in the production of chiral compounds. Here in this experiment, the crystallization process were performed in a very pure and fresh distilled water placed in glass bottles (bi- or tri-distilled water) due to the fact that the storage of water in plastic bottles might form bacteria with time [24]. In Figure II-21, we can see that the nNCD values appear to have been fairly and randomly distributed through the region, and the same type of bias is present as in the previous experiments with an average value equal to +308 [mdeg].

II.7.b.3. Crystallization of Chiral MOF using a New Treatment Method of Used Glassware at Different Temperature

The third test is checking the purity of vials that we are using for crystallization process. Prof. Brucker who has an experience in cell biology, organic material and material interfaces suggested the way to identify whether the bacteria, virus, biofilm etc. exist in our vials using a fluorescent stain called DAPI. The purity of vials cleaned using a classical method (water and

ethanol) was checked by Dr. Nicola Glade. According to his observation, he found microscopically small fluorescent cells at the edge and bottom of the vials (Figure II-22).

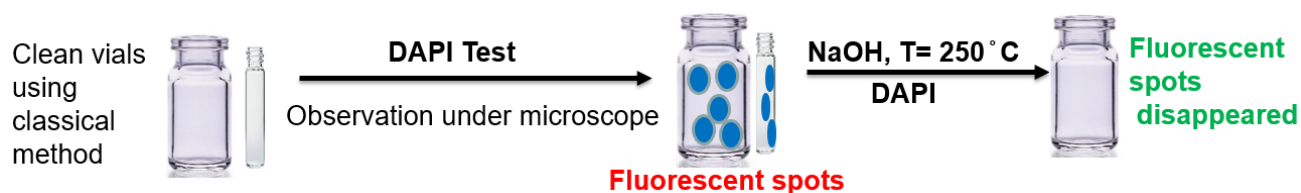


Figure II-22 Testing the purity of vials using DAPI test.

This observation means that there is something of natural origin that, owing to the homochirality of life, is present as a single enantiomer on our vials. The next important step is to define and test an appropriate treatment to get rid of these chiral contaminants. Once again we turned ourselves to methods used in biology. We selected a general method known to destroy some kinds of bacteria, bio-films or biological debris. Moreover, we followed the treatment procedure described previously (page 53), after that, we have repeated the purity test using DAPI, no fluorescent spots appeared.

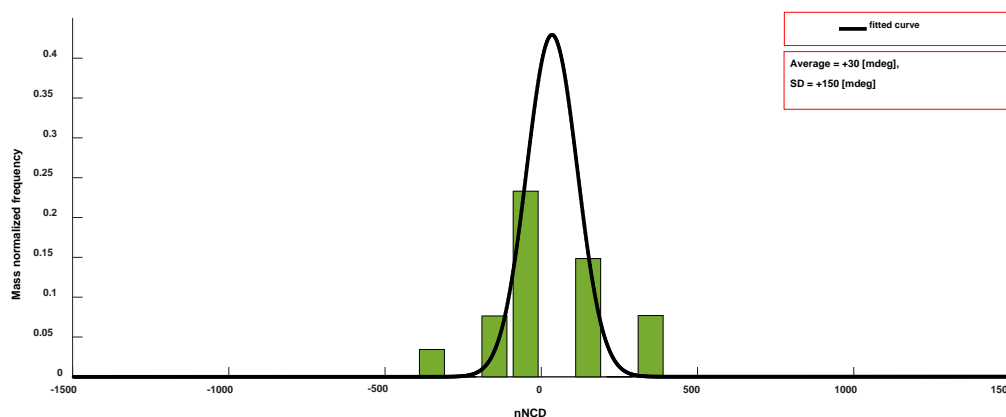


Figure II-23 Mass normalized frequency versus normalized NCD values for crystallization of $(\text{NH}_4)_4[\text{MnCr}_2(\text{ox})_6]\cdot 4\text{H}_2\text{O}$ using treatment procedure at 15°C .

In this experiment, we follow the treatment procedure but with heating all glassware in the oven at 250°C only once before putting them in a concentrated solution of sodium hydroxide. The crystallization procedure was done at 15°C because we have found that the temperature inside the coil of superconducting magnet is less than room temperature ($\cong 15^\circ\text{C}$). Finally, the statistical distribution of normalized mass frequency as function of normalized NCD and its normal distribution represents a clear evidence that the shift to the right has almost disappeared with an average quite close to zero ($+30$ [mdeg]), and the standard deviation is equal to 150 [mdeg].

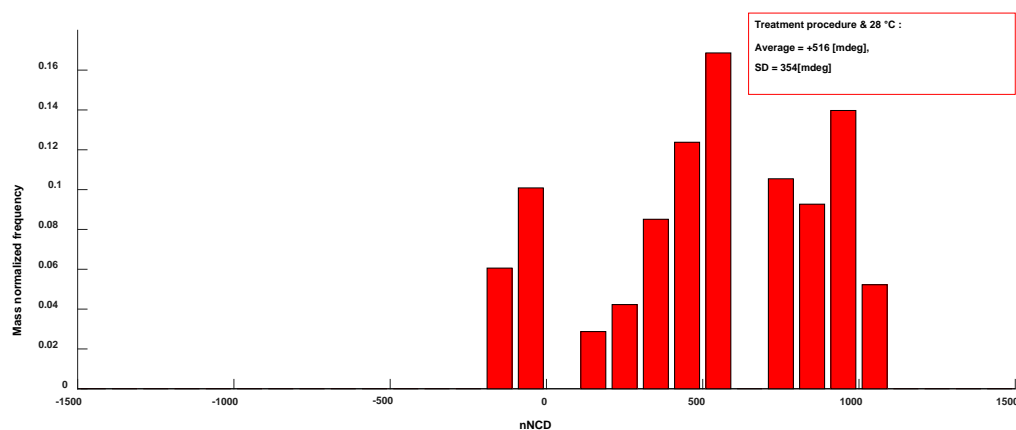


Figure II-24 Mass normalized frequency versus normalized NCD values for crystallization of $(\text{NH}_4)_4[\text{MnCr}_2(\text{ox})_6]\cdot 4\text{H}_2\text{O}$ using treatment procedure at 28 °C.

To have a total validity for the treatment procedure at different conditions, crystallization process was done at RT or slightly above. In this experiment, many samples were prepared exactly as mentioned in previous part with only one difference which is the temperature.

Herein, the crystallization process was done at 28 °C. The results show that even using treatment procedure, is not sufficient to suppress this bias which is represented in Figure II-24 by excess of positive nNCD (+516 [mdeg]).

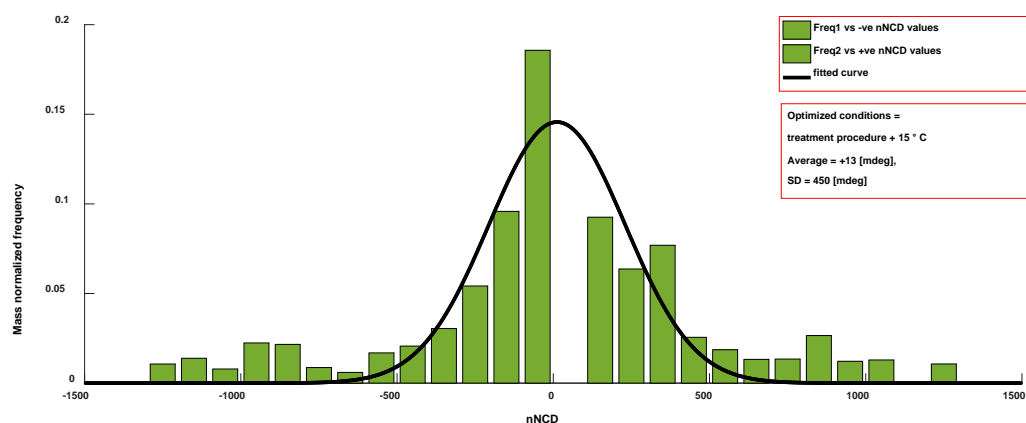


Figure II-25 Mass normalized frequency versus normalized NCD values for crystallization of $(\text{NH}_4)_4[\text{MnCr}_2(\text{ox})_6]\cdot 4\text{H}_2\text{O}$ using optimized conditions.

We repeated crystallization process using the optimized conditions: modified treatment procedure which includes heating of all glassware up to 250 °C for 2 hours twice before and after immersing them in a concentrated solution of NaOH and crystallization at a temperature of 15 °C to check whether the results will be reproducible or not. Figure II-25 represents the same results obtained previously (Figure II-23), but here more experiments were done, and the

normal distribution is fitted better than before with more dispersion of nNCD data (SD = 450 [mdeg]) and 13 [mdeg] as an average.

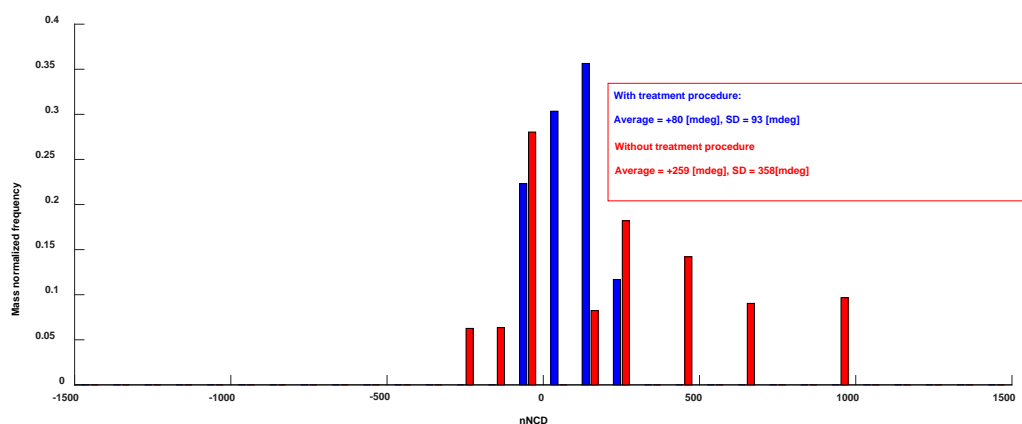


Figure II-26 Mass normalized frequency versus normalized NCD values where the crystallization process was done in fridge at 15 °C and with/ without following the treatment procedure.

In order to know which factor affects the enantioselectivity of chiral MOF, whether low temperature (15 °C) or the used of cleaning procedure, we have repeated the same experiments as mentioned before, but here two different series of vials were prepared: the first one is using glassware by following the treatment procedure and the second one is using glassware cleaned by classical method (ethanol and water). The data shows that the treatment procedure using NaOH is working properly at low temperature because the average of nNCD value is quite low (+80[mdeg]) in comparison to the experiment done by classical cleaning process (+259 [mdeg]). Generally, we have found a dramatic temperature effect on the enantioselectivity of chiral MOF. When performing the treatment procedure at different temperature (15 °C ,RT or slightly higher) gives different results:

At 28 °C the ratio of Λ and Δ enantiomers were not affected which signifies the presence of Λ enantiomer in excess. The obtained results might be due to the presence of a chiral structure that is robust enough to resist to the harsh conditions treatment procedure. However, at 15 °C, no excess of Λ enantiomer is obtained, it means that the unknown chiral object is still present but not active at this temperature.

II.7.c. Studying the effect of external forces on the ratio of Λ and Δ enantiomers

II.7.c.1. Crystallization in the presence of magnetic field

In these experiments we study the effect of weak (less than 290 mT) and strong (12 T) external magnetic field on the preferred handedness of chiral MOF crystals obtained by slow diffusion.

II.7.c.1.a. Low Field

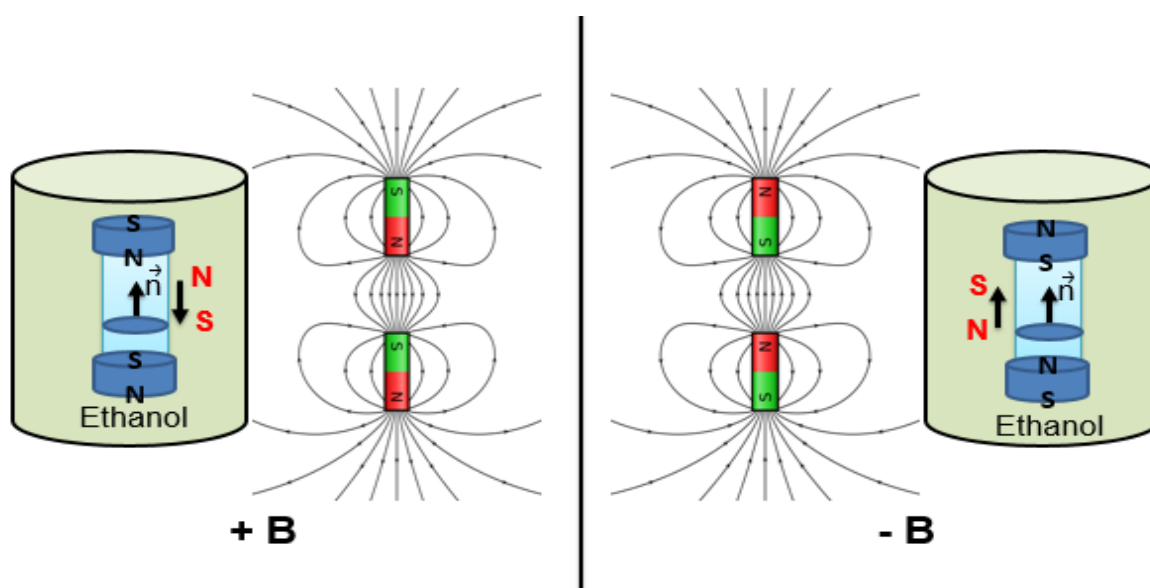


Figure II-27 crystallization process by slow diffusion of ethanol at the interface with changing orientation of the magnetic field.

To investigate this effect, our setup was built and presented in the section of general method (page 55). Figure II-27 in both sides (left and right) share an essential feature with only one difference which is the orientation of the field and it is seen clearly that the crystallization process will take place between these two small magnet where the direction of magnetic field is reversed. These experiments were performed at the very beginning of my PhD work. Accordingly, we use simplified cleaning procedure without using the optimized conditions because we thought from the beginning that the origin of excess comes from the external forces.

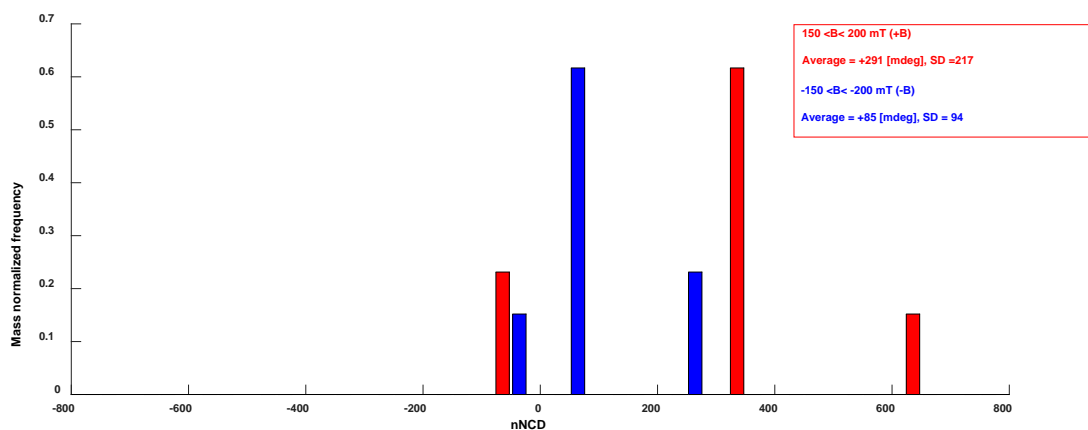


Figure II-28 Effect of using a small Neodymium magnets on the optical activity of chiral MOF.

This histogram represents the results obtained when the crystallization process occurred between two NdFeB magnets. From this experiment, we must realize that what is relevant is the difference between the average of nNCD obtained in +B and - B orientation of the field. However, reversing the sign of magnetic field didn't reverse the chirality of tris(oxalato)chromate(III) compound.

The possible reason for this result is inhomogeneity of the field which is represented clearly in Figure II-29.

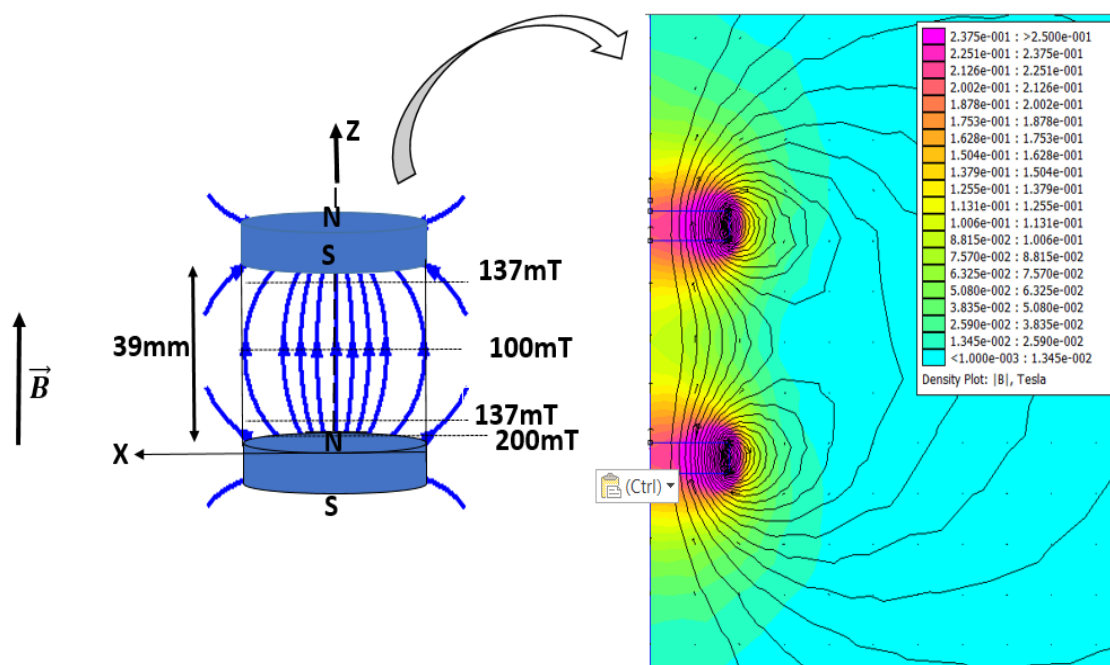


Figure II-29 Inhomogeneous magnetic field.

The left panel of Figure II-29 shows the intensity of the magnetic field between two NdFeB magnets measured using Gauss meter. The magnetic field varied strongly with slight

movements of the Gauss meter probe around the whole surface of the magnet. This is in agreement with the simulation performed using FEMM (Finite Element Method Magnet) (Figure II-29 right). This means that the crystallization conditions are not strictly the same for all samples.

In order to increase the homogeneity of the field between Neodymium magnets (NdFeB), the auxiliary iron tubes were utilized to ensure a uniform magnetization profile and to localize it inside the iron tube suppressing the fringe effect, which is due to the peripheral magnetic field outside of the magnet core is shown in the right panel of Figure II-29. After that, we have repeated the measurement of the intensity of magnetic field using this new setup. We have found that the intensity of the magnetic field became higher with less inhomogeneity of the field.

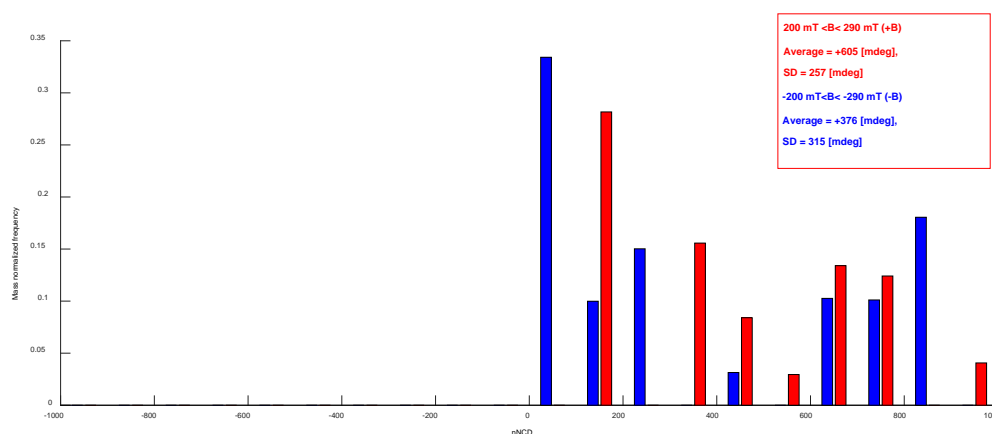


Figure II-30 Effect of using a small Neodymium magnets placed inside iron tubes on the enantioselectivity of chiral MOF.

Figure II-30 represents the obtained results when iron tubes were used in the experiment to improve the intensity and homogeneity of the magnetic field. By changing the orientation of the magnetic field, the average of nNCD does not vary much and the negative nNCD signals totally disappeared.

In general, we have found that there is no real effect of low magnetic field on the formation of enantiopure compounds with high dispersion of nNCD values along x-axis.

II.7.c.1.b. High Field

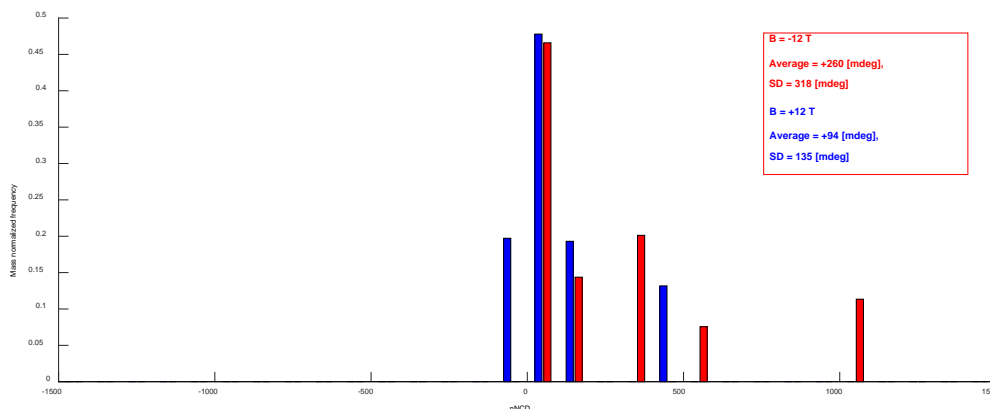


Figure II-31 High field effect on the optical activity of chiral MOF.

These experiments were performed under optimized conditions using a SCM that gives more homogenous and intense field compared to previous experiments. According to given results, when $B = +12$ T, the average of nNCD is equal to +94 [mdeg]. When $B = -12$ T, it is +260 [mdeg]. So that, there is the different effect of $+B$ and $-B$ on the enantioselectivity of chiral MOF, but in both cases the average of nNCD is positive due to the wide distribution which has a stronger influence on the final obtained results than the magnitude of the effect itself as it requires hundreds of experiments to confirm this. In addition, the conditions of this experiment are very difficult as each experiment requires 7 days for only three samples in the presence of ± 12 T to be done.

To improve statistics and reach definite results, the number of the samples was increased to 9 samples per experiment.

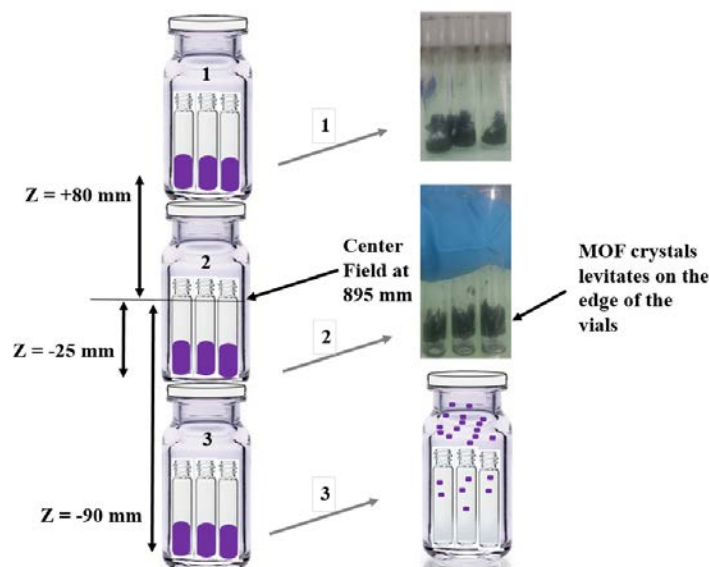


Figure II-32 Schematic illustration of the obtained crystals after running the crystallization process at the different position inside the SCM.

Figure II-32 shows the position of the crystals at the end of the crystallization process that is roughly after 7 days. The crystals were formed at different positions inside the vials either at the bottom, at the edges or randomly distributed in the whole surface of the big vial.

This unexpected observation is attributed to the effect of the gradient on the position of the vials with respect to the central field. Positive (negative) z values correspond to positions of each vial above (below) the central field.

In fact, we have an aqueous paramagnetic solution that contains manganese(II) chloride and ammonium tris(oxalato)chromate(III) dissolved in water. Actually, this paramagnetic solution, placed far from central field experienced a field gradient that leads to levitating this solution toward central field.

In vial 1, crystals were found to be at the bottom surface where the crystallization process occurred above the central magnetic field. In this case, the paramagnetic solution is attracted towards the central magnetic field.

In vial 2, crystals formed were seen on the whole side of the entire vials. However, in vial 3, crystals were found outside the small vials precisely in the large vial where the ethanol is placed. In both cases, the field gradient provided an upward force that led the paramagnetic solution to levitate towards the central magnetic field. In these two vials (2 & 3), we have found that the location of the crystals is dependent on its position with respect to the central field. As z value is increased, the field gradients becomes higher.

Accordingly, introducing a new perturbation on our experiment which is field gradient might change the symmetry analysis to become more complicated than for the Curie-de Gennes

conjecture. That's why we switched to study the effect of rotation as more than 24 experiments can be launched at the same time.

II.7.c.2. Crystallization in the presence of rotational force

In this part, we studied the effect of rotation using two different set-ups. In the first experiment, the rotation of the used rotatory plates did not meet our expectations; however, using a new set-up gave a better rotation in both direction.

II.7.c.2.a. Unstable Rotation

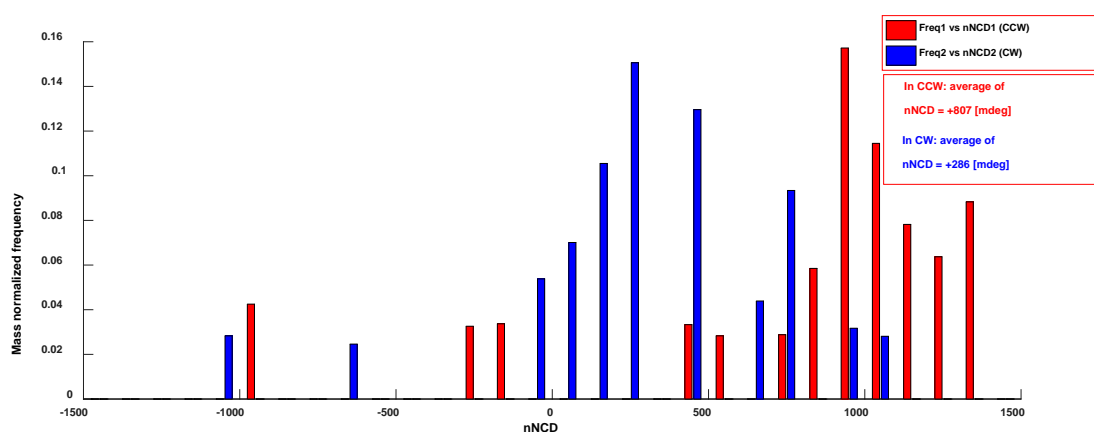


Figure II-33 Effect of the first rotatory plates in both direction (CW and CCW) on the enantioselectivity of chiral MOF.

It is clear from the figure shown above that the number of experiments is huge compared to the experiments done in the SCM. These experiments were performed using the classical method of cleaning procedure. In Figure II-33 the average of nNCD is positive in both directions of rotation, but there is a big difference between the values obtained in CW and CCW. Moreover, a random distribution and dispersion of nNCD values is still present. We expected that the possible reasons to have such results are: unstable rotation of the used rotatory plates during crystallization process, using plastic vials as it has possibility to store some kinds of bacteria [24], and not following the treatment procedure.

II.7.c.2.b. Orbital and stable Rotation

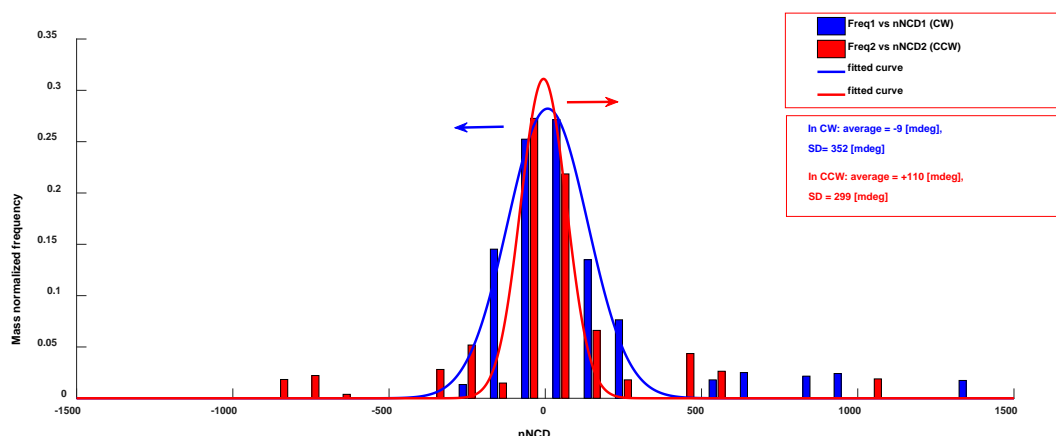


Figure II-34 Effect of rotation using new setup on the enantioselectivity of chiral MOF.

Despite the fact that the previous results were negative which calls for improvements, they were used as a source of inspiration to continue in that direction as we expected by getting rid of all obstacles that we faced in this experiment, we will be able to reach our objective.

Figure II-34 represents the results obtained after repeating the crystallization process in high speed of rotation using an optimized conditions. These experiments were performed using a new setup with better rotation in a dedicated fridge where we can set the temperature at 15 °C. As we can see clearly, there is still a random distribution of normalized NCD values; however, it is very small in comparison to previous experiments, and Gaussian distribution is centered at zero with a slight difference between CW and CCW experiments. The Gaussian distribution of CCW experiments is shifted to the right while for CW is shifted slightly to the left.

II.8. General Conclusion

In the first part of this chapter, the efforts was devoted to suppress the e.e. of Λ enantiomer to have blank experiments that will allow us to study the effect of external forces.

Interestingly, we have found that the optimized conditions for the crystallization process where there was no excess of any enantiomer over the other process which include low temperature (15 °C) crystallization and harsh treatment procedure through using concentrated sodium hydroxide solution and heating all glassware used for crystallization process twice into the oven at 250 °C for two hours. In fact, a large number of experiments were considered to lead us to draw this conclusion especially as the results were reproducible. Moreover, a significant

temperature effect on the enantioselectivity of the chiral MOF was observed. The origin of this temperature –dependent enantioselectivity might be due to the presence of unknown chiral object that are robust enough to resist the harsh conditions of the following treatment procedure (250°C and NaOH).

Moreover, the effect of temperature on the enantioselectivity has been described several times in the literature but with no comprehensive explanation to be reported. It is very difficult to give a definite or clear explanation, because the general mechanism might be very complicated [25], [26].

We have found that there is no real effect of low magnetic field on the formation of enantiopure compounds .

Moreover, growing enantiomerically enriched racemates of a chiral MOF in a SCM showed a different effect obtained after changing the orientation of magnetic field. However, a low number of experiments is not enough to determine the definite effect of magnetic field.

Increasing the number of samples to 9 per experiment by placing 3 big vials one over the other in the superconducting magnet introduced new source of perturbation on our system preventing us to continue in that direction.

Crystallization using high speed rotatory plates helped by launching more than 24 experiments at the same time.

In these experiments, we have found a slight difference between CW and CCW which means that there is a tendency yet there is a wide distribution of e.e..

In general, crystallization under the effect of external forces showed the possibility of controlling the optical activity of chiral MOF; however, high dispersion of nNCD values and the weakness of the expected effect make the Curie de-Gennes conjecture demonstration of this system can be very difficult to achieve.

Given the above statements, we turned ourselves to a new experiment where the amplification of the NCD signal toward measurable values were obtained by totally different means.

References

- [1] K. Akhbari and A. Morsali, "Thallium(I) supramolecular compounds: Structural and properties consideration," *Coord. Chem. Rev.*, vol. 254, no. 17, pp. 1977–2006, Sep. 2010.
- [2] J. Hafizovic *et al.*, "The Inconsistency in Adsorption Properties and Powder XRD Data of MOF-5 Is Rationalized by Framework Interpenetration and the Presence of Organic and Inorganic Species in the Nanocavities," *J. Am. Chem. Soc.*, vol. 129, no. 12, pp. 3612–3620, Mar. 2007.
- [3] E. Pardo *et al.*, "High Proton Conduction in a Chiral Ferromagnetic Metal–Organic Quartz-like Framework," *J. Am. Chem. Soc.*, vol. 133, no. 39, pp. 15328–15331, Oct. 2011.
- [4] D. L. Jaggard, A. R. Mickelson, and C. H. Papas, "On electromagnetic waves in chiral media," *Appl. Phys.*, vol. 18, no. 2, pp. 211–216, Feb. 1979.
- [5] C. Maxim, S. Ferlay, H. Tokoro, S.-I. Ohkoshi, and C. Train, "Atypical stoichiometry for a 3D bimetallic oxalate-based long-range ordered magnet exhibiting high proton conductivity," *Chem. Commun.*, vol. 50, no. 42, pp. 5629–5632, Apr. 2014.
- [6] C. Train *et al.*, "Strong magneto-chiral dichroism in enantiopure chiral ferromagnets," *Nat. Mater.*, vol. 7, no. 9, pp. 729–734, Sep. 2008.
- [7] R. Andrés, M. Gruselle, B. Malézieux, M. Verdaguer, and J. Vaissermann, "Enantioselective Synthesis of Optically Active Polymeric Homo- and Bimetallic Oxalate-Bridged Networks $[M_2(ox)_3]_n$," *Inorg. Chem.*, vol. 38, no. 21, pp. 4637–4646, Oct. 1999.
- [8] R. Andrés *et al.*, "Rational Design of Three-Dimensional (3D) Optically Active Molecule-Based Magnets: Synthesis, Structure, Optical and Magnetic Properties of $\{[Ru(bpy)_3]^{2+}, ClO_4^-, [MnIICrIII(ox)_3]^{-}\}_n$ and $\{[Ru(bpy)_2ppy]^+, [MIICrIII(ox)_3]^{-}\}_n$, with MII = MnII, NiII. X-ray Structure of $\{[\Delta Ru(bpy)_3]^{2+}, ClO_4^-, [\Delta MnIICrIII(ox)_3]^{-}\}_n$ and $\{[\Delta Ru(bpy)_2ppy]^+, [\Delta MnIICrIII(ox)_3]^{-}\}_n$," *Inorg. Chem.*, vol. 40, no. 18, pp. 4633–4640, Aug. 2001.
- [9] L. D. Barron, "Magnetic molecules: Chirality and magnetism shake hands," *Nat. Mater.*, vol. 7, no. 9, pp. 691–692, Sep. 2008.
- [10] R. S. Fishman, M. Clemente-León, and E. Coronado, "Magnetic Compensation and Ordering in the Bimetallic Oxalates: Why Are the 2D and 3D Series so Different?," *Inorg. Chem.*, vol. 48, no. 7, pp. 3039–3046, Apr. 2009.
- [11] M. Gruselle, R. Andres, B. Malezieux, M. Brissard, C. Train, and M. Verdaguer, "Optically active molecule-based magnets: enantioselective self-assembling, optical, and magnetic properties," *Chirality*, vol. 13, no. 10, pp. 712–714, 2001.
- [12] P. Curie, "Sur la symétrie dans les phénomènes physiques, symétrie d'un champ électrique et d'un champ magnétique," *J Phys Theor Appl*, vol. 3, no. 1, pp. 393–415, 1894.
- [13] L. Jun, Z. Feng-Xing, R. Yan-Wei, H. Yong-Qian, and N. Ye-Fei, "Thermal kinetic TG-analysis of metal oxalate complexes," *Thermochim. Acta*, vol. 406, no. 1, pp. 77–87, Nov. 2003.
- [14] K. Oa, N. Vd, K. Gi, and K. Lm, "Thermal analysis of ammonium trioxalatometallate complexes supported on titania and reducibility of their decomposition products," *Thermochim. Acta*, vol. 494, no. 1–2, pp. 35–39, 2009.
- [15] X. M. Dong and D. G. Gray, "Induced Circular Dichroism of Isotropic and Magnetically-Oriented Chiral Nematic Suspensions of Cellulose Crystallites," *Langmuir*, vol. 13, no. 11, pp. 3029–3034, May 1997.
- [16] "Applied Methods." [Online]. Available: http://www.diss.fu-berlin.de/diss/servlets/MCRFileNodeServlet/FUDISS_derivate_000000003525/04_5.pdf?hosts.

- [17] S. M. Kelly, T. J. Jess, and N. C. Price, "How to study proteins by circular dichroism," *Biochim. Biophys. Acta BBA - Proteins Proteomics*, vol. 1751, no. 2, pp. 119–139, Aug. 2005.
- [18] "CD." [Online]. Available: <http://www.friedli.com/research/phd/cd/chap3.html>.
- [19] A. ABU-SHUMAYS and J. J. DUFFIELD, "CIRCULAR DICHROISM-THEORY AND INSTRUMENTATION," *Anal. Chem.*, vol. 38, no. 7, p. 29A–58A, Jun. 1966.
- [20] A. Kaur, G. Hundal, and M. S. Hundal, "Spontaneous Resolution upon Crystallization of 3D, Chiral Inorganic Networks Assembled from Achiral, Polyoxometallate Units and Metal Ions," *Cryst. Growth Des.*, vol. 13, no. 9, pp. 3996–4001, Sep. 2013.
- [21] M.-P. Zorzano, S. Osuna-Esteban, M. Ruiz-Bermejo, C. Menor-Salván, and S. Veintemillas-Verdaguer, "Enantioselective Crystallization of Sodium Chlorate in the Presence of Racemic Hydrophobic Amino Acids and Static Magnetic Fields," *Challenges*, vol. 5, no. 1, pp. 1–18, 2014.
- [22] T. F. Bidleman *et al.*, "Chiral Chemicals as Tracers of Atmospheric Sources and Fate Processes in a World of Changing Climate," *Mass Spectrom.*, vol. 2, no. Spec Iss, 2013.
- [23] M. Górak and E. Żyłańczyk-Duda, "Application of cyanobacteria for chiral phosphonate synthesis," *Green Chem.*, vol. 17, no. 9, pp. 4570–4578, Sep. 2015.
- [24] I. G. Occhiuto *et al.*, "Aggregates of a cationic porphyrin as supramolecular probes for biopolymers," *J. Inorg. Biochem.*, vol. 153, pp. 361–366, Dec. 2015.
- [25] Xu, Wei, and Zhang, "Effect of Temperature on the Enantioselectivity in the Oxazaborolidine-Catalyzed Asymmetric Reduction of Ketones. Noncatalytic Borane Reduction, a Nonneglectable Factor in the Reduction System," *J. Org. Chem.*, vol. 68, no. 26, pp. 10146–10151, Dec. 2003.
- [26] H. Zhang and K. S. Chan, "Dramatic temperature effect in asymmetric catalysis in the enantioselective addition of diethylzinc to aldehydes," *J. Chem. Soc. [Perkin 1]*, no. 4, pp. 381–382, Jan. 1999.

Chapter III Magneto-electric Enantio-selective Catalysis

III. Abstract

*“Les cristaux liquides sont magnifique et mystérieux;
je les apprécie pour ces deux raisons .”
P. G. de-Gennes [1]*

Our work on this project brought us a confirmation of the Curie de-Gennes (CdG) conjecture. We generate enantiomeric excess up to 6×10^{-9} upon applying parallel magnetic and electric fields (4×10^5 VT/m) in biphenyl-based nematic liquid crystals.

This chapter is organized as follows:

- Atropisomerism of biphenyl system;
- estimation of the strength of the effect using atropisomeric biphenyl molecules
- general properties and motivation for using racemic atropisomeric based Nematic Liquid Crystals (NLC)
- fabrication of NLC cells using different alignment methods
- description of the optical setup used for magneto-electric optical measurements
- main results
- general conclusion.

III.1. Atropisomerism of Biphenyl System

There are many possible molecules that might be used to observe a Curie de-Gennes conjecture effect. To achieve this objective, atropisomeric biphenyl derivatives were chosen. This type of molecules have axial chirality because of the biphenyl moiety, which do not have a chiral center, but instead has an axis of chirality rotation that transforms one enantiomer into the other, an effect called atropisomerism. Atropisomerism has been reviewed by C. Wolf [2]. It can be

defined as conformational isomerism in which the conformers (atropisomers) can be isolated as separate chemical species [3]. The isolation of these conformers is closely related to the height of the energy barrier of the internal rotation around the C-C single bond between two phenyl rings (rotational barrier) [3], [4].

In the lowest energy state of biphenyl molecules, the two phenyl rings are not coplanar because of steric hindrance, but rotated out of planarity around the bond that connects them (typically $30^\circ - 40^\circ$). This means that the biphenyl molecule in its ground state is axially chiral and the amount of steric hindrance determines the rotational barrier. For example, in unsubstituted biphenyl, this barrier is about 2 kcal/mol [4] and the left and right handed enantiomers interconvert rapidly at room temperature, making it impossible to separate them. With bulky substituents in the ortho position, the rotational barrier becomes much larger, and one can separate the two enantiomers.

III.2. Estimation of the Strength of the Effect with an Atropisomeric Model

Following is the estimation of the magnitude of the CdG effect with a simple model for atropisomeric biphenyl molecule.

III.2.a. In the Absence of an Externally Applied Magnetic and Electric Fields

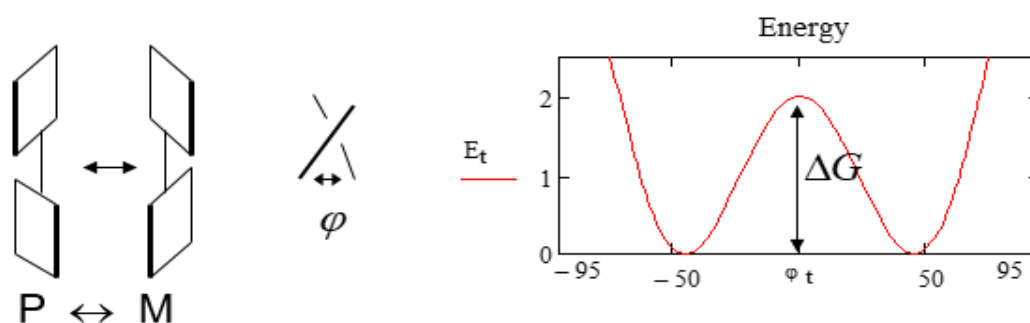


Figure III-1 Energy profile versus rotation angle of biphenyls when E and B are equal to zero.

Biphenyl derivatives can exist in two conformations, either P or M. Figure III-1 (left) represents the dynamic chirality along the biaryl axis. To simplify, small squares are used in place of phenyl rings (Figure III-1 (left)).

In the absence of magnetic and electric fields (Figure III-1 (right)), the forward reaction proceeds at the same rate as the reverse reaction ($k_P = k_M$) and both enantiomers (P and M) are present with no preference of one enantiomer over the other, (Equation III-1) i.e. the biphenyl mixture is racemic.

$$k_P = k_M = \frac{kT}{h} e^{\frac{\Delta G}{kT}} = k_0 \quad \text{Equation III-1}$$

III.2.b. In the Presence of Magnetic and Electric Fields

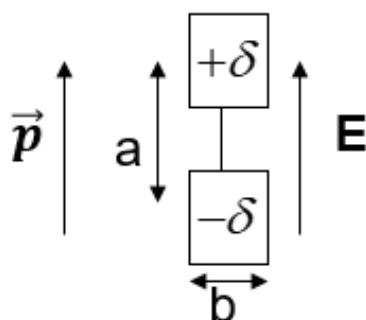


Figure III-2 Effect of an external electric field on biphenyl molecules.

Now we consider the effect of an external electric field on the molecule as shown in Figure III-2. The electronic charge in the aromatic rings of the biphenyl responds to the applied external electric field with the upper ring becoming positively charged and the lower one negatively charged. The induced electric dipole is then:

$$p = \delta a = \alpha E \quad \text{Equation III-2}$$

Where δ is the magnitude of the charge ($\delta = +\delta = |-\delta|$), a the distance between the separated positive and negative charges and α the polarizability which is defined as the ratio between electric dipole (p) of the biphenyl and the electric field (E) [5].

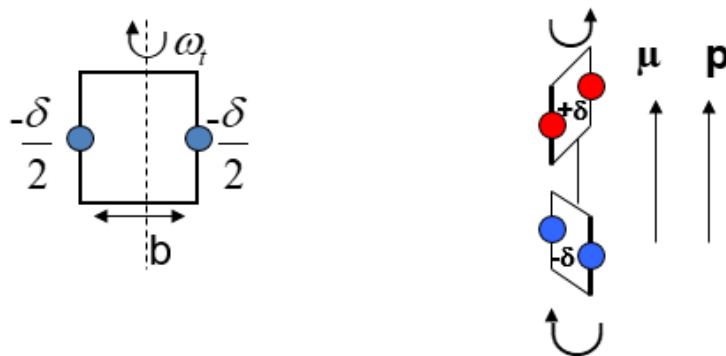


Figure III-3 Effect of an external magnetic and electric fields on biphenyl molecules.

Because of thermal excitation, the two phenyl rings will perform a torsional oscillation around the connecting C-C bond, with a characteristic frequency ω_t (Figure III-3). This internal rotational motion of the charged phenyl rings will generate a transient magnetic moment μ given by:

$$\mu = \sum_i q_i \mathbf{r}_i \times \mathbf{v}_i \quad \text{Equation III-3}$$

Where \mathbf{r}_i is the position of the electric charge q_i relative to the rotation axis and \mathbf{v}_i is the instantaneous velocity of the charges.

In Figure III-3 (right side) we have two phenyl rings connected by C-C single bond, each one rotated in opposite direction, the upper phenyl ring rotates in CCW direction and the lower one rotates CW. From the geometry of this figure and following the definition of transient magnetic moment μ , we obtained the expression of the magnitude of μ :

$$\mu = 2 \left(\frac{+\delta}{2} \right) \frac{b}{2} \left(+\omega_t \frac{b}{2} \right) + 2 \left(\frac{-\delta}{2} \right) \frac{b}{2} \left(-\omega_t \frac{b}{2} \right) = \frac{\delta \omega_t b^2}{2} \quad \text{Equation III-4}$$

In this equation, ω_t is the internal torsional frequency of biphenyl, $b/2$ is the position of electric charge relative to the rotation axis. δ is the magnitude of the induced charge ($\delta = +\delta = |-\delta|$). The first term in Equation III-4 comes from to the upper phenyl ring in Figure III-3 which is represented by two small red balls with the appropriate sign for partial charge and angular velocity, the second term comes from the lower phenyl ring. Note that the sign of the transient magnetic moment depends on whether the upper phenyl twists CW or CCW.

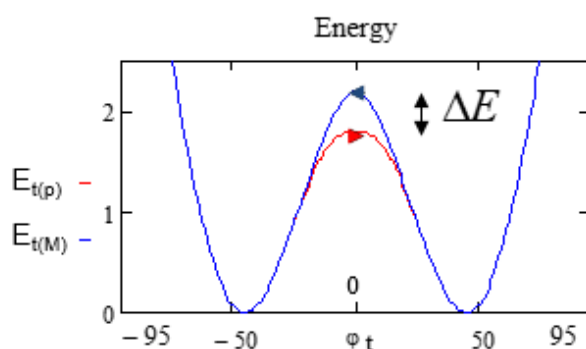


Figure III-4 Energy profile versus rotation angle of biphenyls in the presence of a time-noninvariant enantiomorphous influence.

The magnetic transition dipole moment, in an external magnetic field, leads to a transition Zeeman energy difference. This difference, that only exists under the combined effect of parallel electric and magnetic fields, alters the rotation barrier profile for biphenyl twisting. The distance ΔE between red and blue pathways as illustrated in Figure III-4 represents the energy

difference between the transition barriers for P→M and M→P twist. One enantiomer will be formed faster because of the lower transition barrier (curve with red arrow). So, although the P and M enantiomers remain strictly degenerate in the presence of parallel E and B fields, the reciprocity of the energy barrier between the two enantiomer is lost due to the effect of collinear E and B fields[6]. Because of this, $k_{P \rightarrow M} \neq k_{M \rightarrow P}$ and an e.e. can develop. In analogy with chemical catalysis, which also changes transition energies, we call this phenomenon magneto-electric enantioselective catalysis. ΔE is equal to:

$$\Delta E = 2\mu \cdot B = \frac{\alpha \omega_t b^2}{a} E \cdot B \quad \text{Equation III-5}$$

This conclusion is significant, since it implies a breakdown of microscopic reversibility and open the possibility of asymmetric synthesis under kinetic control [7]. Note that at thermodynamic equilibrium, one would still have e.e. = 0, because the two enantiomers remain degenerate. However, away from equilibrium, an e.e. can exist. The maximum value of this e.e. in this simple model is approximatively given by:

$$e. e._{max} \approx \frac{\Delta E}{2kT} = \frac{\alpha \omega_t b^2}{2a kT} E \cdot B \quad \text{Equation III-6}$$

With a magnetic field of 2 T and an electric field to 2×10^5 V/m, the estimated e.e. of biphenyl molecules will be 3.4×10^{-10} [8-9]. A priori, this value is too low to be detectable by optical rotation measurements, or any other known method to measure e.e.. Therefore, the NLC mixture of molecules containing biphenyl core constitute the ideal system to perform this experiment. Since in this experiment, we do not measure circular dichroism, but optical rotation, and the collective effect, expressed by the Helical twisting power (HTP) which amplifies the optical rotation of the very small magneto-electrically induced e.e. (explained in page 81). That's why, performing the experiment on biphenyl molecules in their NLC phase, allows us to use the large Helical Twisting Power (HTP) of nematic medium to bring the resulting optical rotation to measurable levels.

III.3. General Properties and Motivation for using Racemic Atropisomeric Based Nematic Liquid Crystals

There are three distinct types of liquid crystals (LCs): thermotropic, lyotropic and polymeric. Among these, thermotropic LCs have been the most extensively studied. This type of LCs can exist in three different phases: nematic, smectic and cholesteric. Furthermore, it exhibits various

liquid crystalline (mesomorphic) phases as a function of temperature [10]. Our demonstration focuses on nematic LC (NLC) based on rod-like shaped biphenyl derivatives (Figure III-5). The presence of asymmetric groups or substituents (CN, pentyl and pentoxy) in these molecules is to vary the intermolecular interactions hence to favor the formation of NLC phases [11].

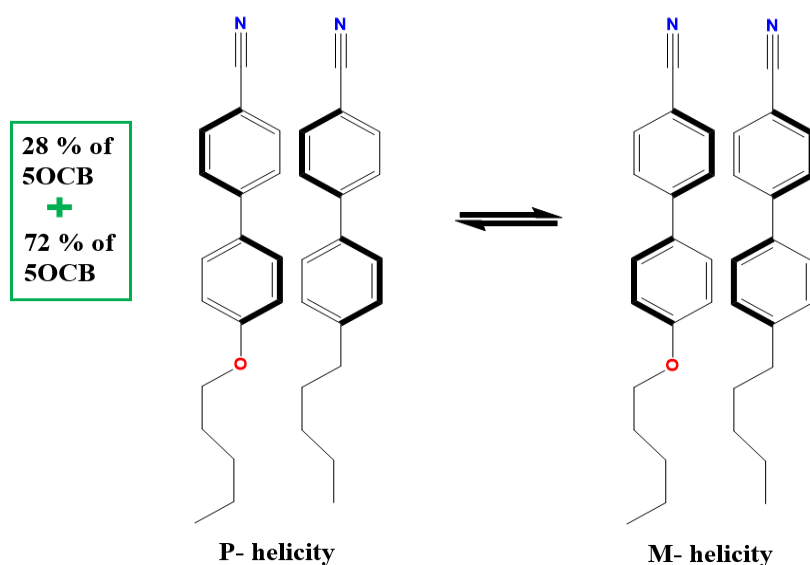


Figure III-5 Eutectic mixture of liquid crystals 72 % of 5CB and 28 % 5OCB (where 5CB and 5OCB denotes the abbreviation of these molecules) and their opposite signs twisting angle (φ).

Figure III-5 represents the system chosen for an experimental demonstration of the Curie de-Gennes (CdG) conjecture which is described as molecules containing: a core consisting of two phenyl rings, a linear aliphatic flexible tail such as pentyl or pentoxy at one end, and polar cyano group at the other end [5].

Our reasons to choose such molecules are the followings:

- Axial chiral biphenyls undergo enantiomerization via rotation about the pivotal aryl-aryl bond, which is basically depends on the type of substituent in their ortho position. Our molecules have a small energy barrier to rotation (E_a) due to absence of substituted groups in their ortho positions [3]; this means that the rotation about the central bond will occur rapidly at room temperature.
- A polar terminal group gives rise to a high positive parallel dielectric permittivity and thus a positive dielectric anisotropy ($\Delta\epsilon = \epsilon_{\text{parallel}} - \epsilon_{\text{perpendicular}}$), which are essential to achieve parallel alignment of the long axis of molecules with an applied field [12]. Furthermore, the conjugation of the molecule caused by a polar group leads to increased nematic-isotropic (N-I) values, viscosity, and birefringence.

- Because of the pentyl or pentoxy groups present at the other end of the molecules, the eutectic mixture composed of 72% pentylcyanobiphenyl (5CB) and 28% pentoxycyanobiphenyl (5OCB) exists in a NLC phase in a wide temperature range (18-43°C) that encompasses room temperature [13]–[15]. As demonstrated below, the CdG effect from the biphenyl core is expected to be very small and requires a way to amplify the effect into a detectable regime. For this, we use the capacity of low concentrations of chiral dopants in a NLC to transform it into a chiral nematic phase with a large optical rotation. This ability of the nematic phase to transform itself into chiral nematic phase in presence of a chiral dopant by forming supramolecular helices of the rod-like molecules is quantized by the helical twisting power (HTP or β) of the NLC system [16]. The HTP is equal to $\frac{1}{p \cdot c \cdot e.e.}$ where p is the resulting pitch in μm , c is the chiral species concentration and $e.e.$ its enantiomeric excess. The HTP of the commercial mixture of twisted biphenyl derivatives named E7 is ranging between $21.1 \text{ L} \cdot (\text{mol} \cdot \mu\text{m})^{-1}$ and $37.7 \text{ L} \cdot (\text{mol} \cdot \mu\text{m})^{-1}$ [17], [18]. Our mixture being in its NLC at room temperature will allow us to perform the magneto-electric optical measurements without introducing a cooling or heating device in the measurement set-up and still benefit from its HTP to amplify the optical response of the weakly chiral medium.

III.4. General and Experimental Methods

III.4.a. Typical Structure of Sandwich type LC cell

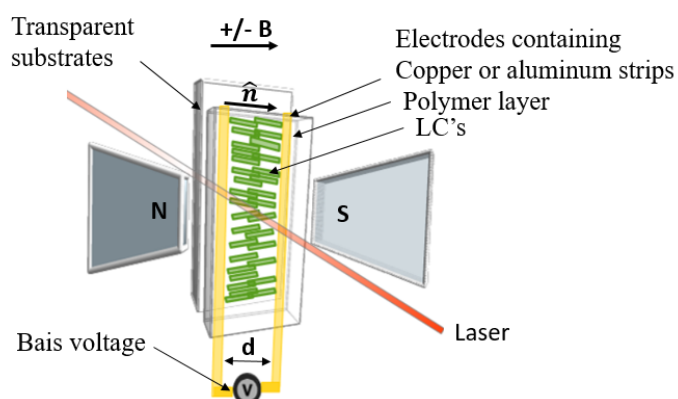


Figure III-6 Ideal structure of a homogeneously aligned nematic liquid crystal cells.

Figure III-6 represents the ideal structure of a homogeneously aligned NLCs inside sandwich-type cells. This cell consists of two transparent glass plates covered with a thin polyvinyl

alcohol polymer layer (PVA) either on both or one of them. Copper or Mylar strips are used as electrodes and at the same time are used as spacers to fix the LC layer thickness (Mylar strips containing a polyester foil with an aluminum coating on it). The thickness of copper electrodes is 25 μm and that of the Mylar electrodes is 8 μm . The typical electrode separation is 5 mm (d). The objective is to align the directors of NLC molecules (\hat{n}) along the short axis of the cell. Achieving this alignment will govern the choice of the fabrication method.

III.4.b. Fabrication of Liquid Crystal Cells using Different Methods

A variety of different LC aligning techniques have been proposed and developed. However, parallel liquid crystal alignment by means of substrate surface treatment was not described very well in the literature. I had to go through trial and error approaches to adapt the process. In this section, I will describe the fabrication procedures for the main methods (mechanical rubbing and uniform magnetic field) used to align LC parallel to the glass substrate.

III.4.b.1. Mechanical Rubbing

The conventional and most widely used approach is the rubbing method. The glass substrates covered with a thin polymer films like PVA are rubbed by a piece of a special type of cloth either manually or by a rubbing machine [19]. This procedure permits to generate grooves in the direction of rubbing and align the polymer chains. The rod-like LC molecules will align along this direction. The rubbing strength is an important factor for the quality of the obtained LC alignment. The quality of these cells were evaluated using a polarized light microscope and according to this observation we decide whether the cell is good enough to check the magneto-electric induced optical activity or not.

III.4.b.1.a. On Glass using Diamond Papers

The first method used to fabricate LC cells was done using the following procedure:

1. The large piece of glass was cut into smaller rectangular glass pieces. They were cleaned with distilled water, ethanol and acetone.

2. The substrates were rubbed along the long axis of the glass (vertically) using a diamond paper (1 micron grain size). The glass substrates were cleaned with distilled water, ethanol and acetone.
3. Two glass substrates were spaced by 8 μm Mylar stripes. The cells were pressed together by adding 1kg on them. After that, cyanolite glue along the long axis on the cell.
4. When the glue has hardened, the hot eutectic mixture of 72 % 5CB and 28% 5OCB in its isotropic phase was filled into the cells by capillary action.

This procedure is different to what has been described in the literature because there is no polymer layer on the glass plates and the rubbing process is performed directly on the glass substrates.

III.4.b.1.b. On PVA Polymer Layer using Optical Tissue

In this part, a new procedure of alignment of LCs on the glass substrate was performed using PVA polymer that was rubbed by optical tissue along the short axis and the procedure is as follows:

1. Cleaning of soda lime glass plates using concentrated solution of sodium hydroxide (14 mol /L) for 30 min followed by several rinsing's in distilled water then in acetone and ethanol (see in page 53).
2. Dip coating of glass plates in PVA (99% hydrolyzed) solution prepared by dissolution of 2.04 g of PVA in 200 ml of de-ionized water [20] followed by slow pulling and vertical drying of water.
3. After deposition of PVA on the glass substrate, it was heated to a temperature of 150 °C for 30 minutes in order to anneal the thin layer of PVA. Crystallinity of the PVA layer is necessary for an efficient alignment effect to occur [21].
4. Afterwards, the coated glass plates were rubbed with a piece of optical tissue under fixed pressure (15 g/cm²) and the direction is unidirectional (rubbing in one direction) or bidirectional (back and forth directions).
5. The large pieces of glass were then cut into small pieces. This process ensured that all single pieces of glass had the same alignment layer and rubbing direction.
6. The two glass substrates of LCs can be prepared differently; one glass plate is always rubbed and the other can be rubbed, uni- or bi-directionally, or unrubbed with both

substrates being covered with PVA polymer. These substrates are spaced by 8 μm Mylar stripes.

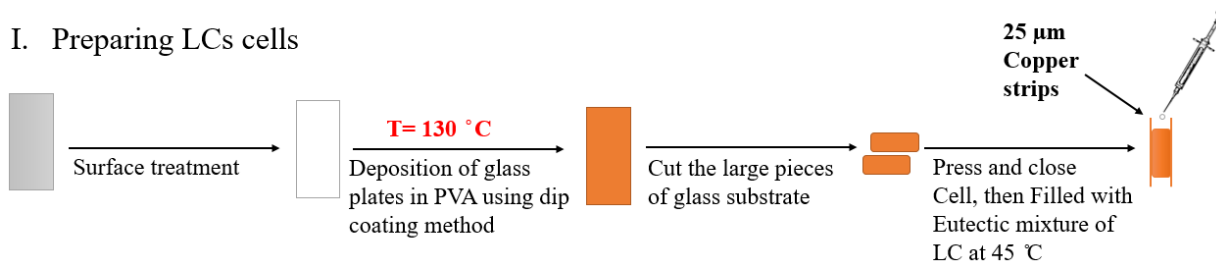
7. In order to make one panel of a cell, the cells were pressed very well by adding 1kg on it. After that cyanolite glue was added where these cells are pressed.
8. After one hour of drying, the eutectic mixture of 72 % 5CB & 28% 5OCB was introduced into the sandwich cells by capillary suction at 40° C to facilitate the flowing of isotropic liquid inside the cell.

Many attempts with the rubbing method failed. The quality of the prepared LC cells was not good, with only partial or non-homogeneous alignment, light scattering and no clear birefringence. Definitely, Curie-de Gennes conjecture effect was not tested for such type of cells.

III.4.b.2. Magnetic Field Alignment

It was demonstrated that the alignment of LC molecules can be achieved by exposing a LC cell (coated with uniform PVA polymer) to a static magnetic field whilst cooling slowly from the isotropic to the nematic phase [22]. Their alignment in the nematic phase remains stable even after the field is switched off.

I. Preparing LCs cells



II. LCs alignment in a static magnetic field

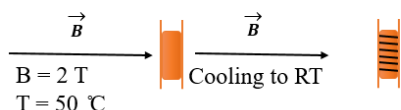


Figure III-7 Liquid crystals alignment using a static magnetic field .

Figure III-7 represents the method used to fabricate LCs cells, but instead of rubbing with optical tissue we have used a static magnetic field to align the LC molecules. Additionally, a 25 μm copper strips is used in place of 8 μm Mylar strips because preparing thicker cells will give a larger optical rotation.

After preparing cells filled with the eutectic mixture of LCs and *no rubbing*, the cells were slowly cooled over 30 minutes from the isotropic to the nematic phase in a magnetic field of 2 T parallel to the substrate and the short axis of the cell. Under the effect of a magnetic field of 2 T, heating the cells up to 50 °C to allow the transition of the liquid crystal phase into isotropic phase, then slowly cooling to room temperature gave a NLC phase where the director of liquid crystal molecules is observed to be homogeneously aligned parallel to the magnetic field direction (Figure III-7 (II)).

III.4.c. Experimental Setup

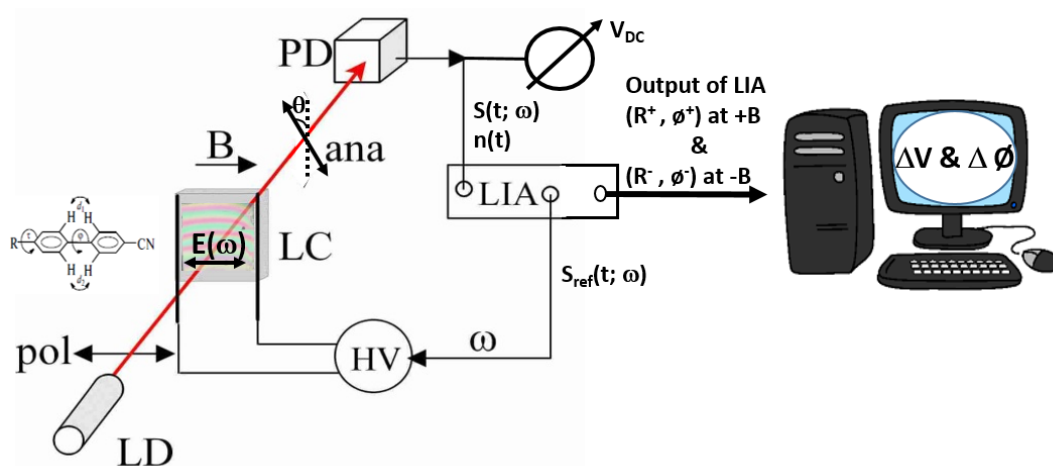


Figure III-8 Experimental setup to detect the optical transmission and optical rotation of nematic biphenyl liquid crystals, consisting of laser diode (LD), polarizer (pol), liquid crystal cell (LC), analyzer (ana), photodiode (PD), and a lock-in amplifier (LIA). The electric field was generated with a high voltage (HV) amplifier, the magnetic field with an electromagnet.

The optical transmission and magneto-electrically induced optical rotation of the biphenyl nematic liquid crystals (ϕ) are measured by the set-up shown in Figure III-8.

All measurements were performed using different strengths of the magnetic and electric fields where the maximum applied magnetic field is 2.3 T and the maximum electric field is 1.6×10^5 V/m. The light source is laser diode (LD) at a wavelength of 632 nm. A polarizer is placed after the laser diode to make its output linearly polarized. The LC cells (sample), filled with biphenyl-based NLC, were placed between the polarizer and analyzer. They were fabricated with LC director aligned along the short axis because the electric field will anyway tend to align the biphenyl molecules with their long axis parallel to E. The magnetic and electric fields are applied collinear (parallel and anti-parallel) to the short axis of the cell.

If the LC molecules are homogeneously aligned, when the polarizer is parallel to the short axis of the cell, and the analyzer perpendicular to this direction, no signal is detected by the photodiode. Nonetheless, the alignment methods that we performed to align the LC molecules between two slides of glass substrates do not form a completely homogeneous liquid crystal cells, so we directed the laser spot to the best zone where the LCs are well aligned characterised by a low transmission between crossed polarizers. The ratio of the transmitted light intensity between the situations with parallel and crossed polarizers was typically between 4 and 8.

For a given magnetic field, the electric field is alternated with a typical frequency of 35 Hz. The resulting modulation of the photo-diode signal is phase-sensitively detected by a vector lock-in amplifier and stored in a computer. Then the magnetic field is reversed and the vector lock-in signal is measured again. The vector difference between the lock-in signals for the two magnetic field polarities is then calculated (magnitude (ΔV) and phase ($\Delta\theta$)). We will refer R as the signal ΔV . It represents a variation in the optical transmission that is bilinear in the electric and magnetic fields, which we interpret as magneto-electrically induced optical rotation. The value of the average transmitted intensity is also measured (V_{DC}). The ratio $\Delta V/ V_{DC}$ is proportional to the magneto-electrically induced rotation angle ($\Delta\theta$).

After that, the values of e.e. corresponding to the observed optical rotation were calculated using the following steps:

- A magneto-optic device called a Faraday rotator was inserted directly before the LC cell. In this device, the light is propagating through a transparent medium which is exposed to a small longitudinal alternating magnetic field [23]. The polarization direction of the light after the Faraday rotator is periodically rotated. Through this method we found that the optical rotation sensitivity of our setup is roughly 2 V/rad with a LC sample in place.
- The e.e. can be calculated from the known HTP for rigid chiral biphenyl derivatives, which is equal to 20 L.(mol.μm)⁻¹, The concentration of biphenyl molecules in the NLC is equal to 4 L.(mol.μm)⁻¹ and so, using the e.e. = $\frac{1}{p.c.HTP}$ formula, gives an e.e. of 2 x 10⁻⁴ for a 90° optical rotation over 25 μm sample thickness (i.e. pitch equal to 50 μm) and 57.3 value is used to convert radian to degree.

$$e.e._{measured} = \frac{\Delta V}{2V/rad} \cdot \frac{57.3^\circ}{90^\circ} 2 \times 10^{-4} \quad \text{Equation III-7}$$

III.5. Results and Discussion

III.5.a. Mechanical rubbing

III.5.a.1. On Glass using Diamond Papers

III.5.a.1.a. Observation Under Microscope

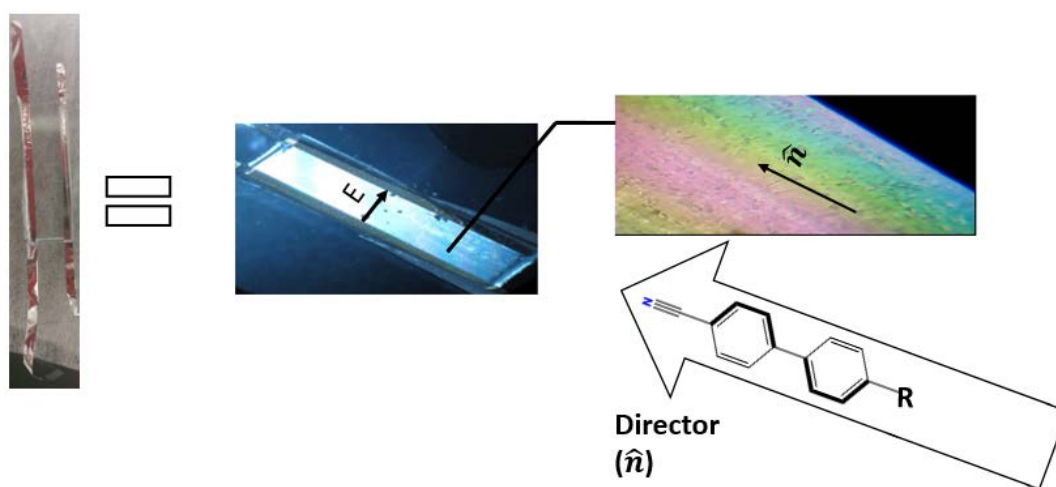


Figure III-9 Polarized optical microscope images of the cell filled with eutectic mixture of LCs and rubbed along long axis (longitudinally rubbed).

Figure III-9 showed the first observation for the optical appearance of the NLCs between the crossed polarizers of an optical polarizing microscope. The anisotropic molecular shape and alignment structure of nematic liquid crystals give them birefringence, and the optical axis is determined by the director of the nematic LC (\hat{n}). The first impression formed upon looking at the above figure says that this cell should have a good director alignment because it is optically clear and no birefringence scattering is shown which encouraged us to be test under the effect of EB. The change in color across the cell is because the cell does not have the same thickness in all its parts.

III.5.a.1.b. Optical Measurements under the Effect of Magnetic and Electric Fields

Nonetheless, the alignment of the LC under the effect of magnetic and electric field was unstable which led to drifting and fluctuating of ΔV and V_{DC} with time. They became better

and more homogeneous after cooling LC's from isotropic to nematic phase in the presence of magnetic field. However, it remained still somewhat unstable, with still a slow drift of ΔV . According to these results, we have found that it is better to use PVA polymer layer rather than rubbing the glass directly using abrasive diamond paper because nematic liquid crystal generally has good wettability on PVA surface. Moreover, we have found that the directors of LC tend to align along the direction of their filling (long axis) [24]. However, the expected effect will be bigger when the long axis of the biphenyls is parallel to the electric field.

III.5.a.2. On PVA Polymer Layer using Optical Tissue

III.5.a.2.a. Observation Under Microscope

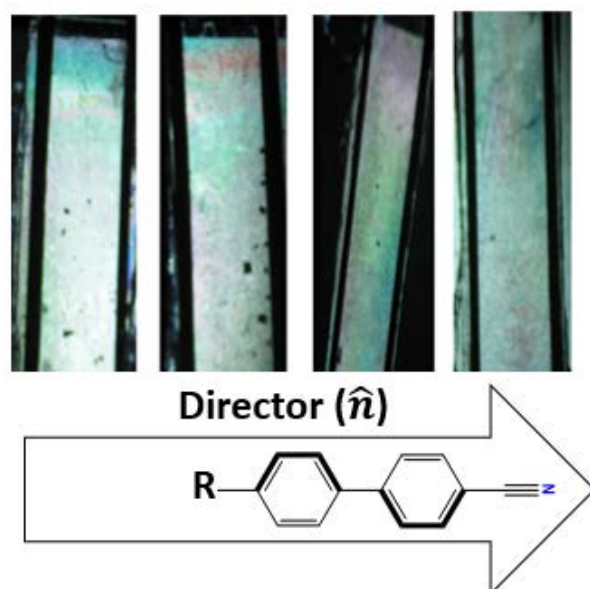


Figure III-10 Crossed polarized optical microscope images of the cell filled with eutectic mixture of LCs and rubbed along short axis.

Microscopic images of nematic liquid crystal cells between crossed polarizers are shown in figure III-10. These cells consist of two glass plates covered with polyvinyl alcohol (PVA) and rubbed horizontally either unidirectional or bidirectional along the short axis using optical tissue. The Mylar strips with thickness $8 \mu\text{m}$ act as electrode for applying the in-plane electric field. Little light scattering and a clear birefringence appeared in the figure shown above. The presence of holes in some cells may be due to air flow inside the cell when filling them.

As previously mentioned, the liquid crystal tend to align along the direction of flowing of LCs. For that reason, we faced some difficulties to get well aligned LCs along short axis (opposite to the previous cell) although we were able to produce visually good cells little light scattering.

III.5.a.2.b. Optical measurements under the Effect of Magnetic and Electric Fields

In this part, we will show the main obtained results for optical rotation measurements on LC cells prepared using the same fabrication method with slight difference.

The first cell consists of two glass plates, one of them is covered with PVA and rubbed in one direction along short axis. When this cell was subjected to an electric field, an unexpected linear electric field response was observed at zero magnetic field. In terms of symmetry, uniform or constant electric field alone cannot affect the equality of the equilibrium populations in a racemic mixture [25]. We expected that the origin of this signal might come from the rubbing in one direction, as this could introduce an in-plane polar preferential direction in the alignment of the LC molecules/domains. For this reason, the new cells with bidirectional rubbing were prepared. Actually, we have found that these cells were better than the previous one because we did not notice a large electric field induced signal in the absence of magnetic field. However, the general evaluation of these measurements is that there is no reproducible significant effect of electric and magnetic fields on the optical rotation of the LC.

The possible reason behind these results might be due to the fact that the rubbing method allows the formation of deep grooves on the glass substrates which facilitate the strong anchoring of LCs molecules on these grooves preventing LCs to assume a helical conformation; in other words it is very difficult to induce a chiral nematic phase inside such LC cells.

Moreover, using this method obliged us to use very thin spacers because only very thin cells enforce the LC molecule to align parallel to the walls. When the cell is too thick, the walls lose their influence, and the LC become polycrystalline. So, instead of making grooves, we have aimed at finding a new method to align the molecules. This was realized by using a static magnetic field and uniform smooth unrubbed glass substrates, as described below. In parallel, modifications of the LabVIEW program was done to simplify and facilitate averaging, compensate for drift and plot results.

III.5.b. Static Magnetic Field

Although the mechanical rubbing alignment technique is simple, it has many disadvantages such as the generation of dust, mechanical defects, and electrostatic charges. In addition, uniform rubbing for the whole surface of glass substrates is quite difficult to be achieved [19], [22], [26].

This is why we have switched to a new method of aligning LCs which is using a static magnetic field instead of rubbing. This technique is an alternative approach for the achievement of high quality liquid crystal alignment. In this section, we will show the magneto-electric induced optical activity measurements for one cell where the LCs molecules are aligned using this method.

III.5.b.1. Evolution of Averaging R and in Time

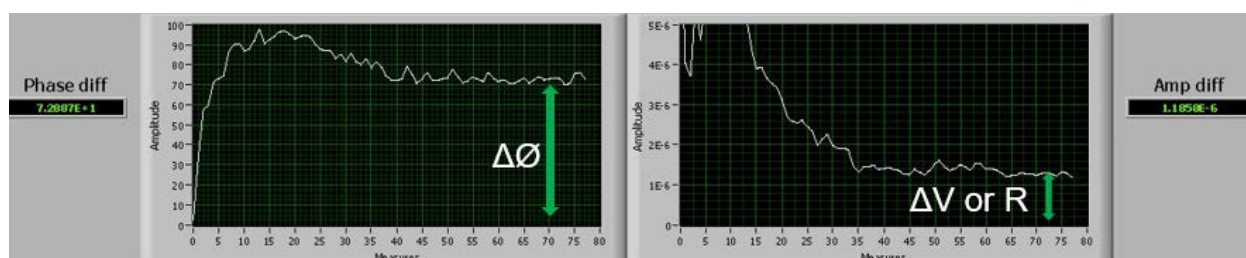


Figure III-11 Evolution of the averaging of $\Delta\phi$ and R in time.

The LabVIEW program connected to our setup facilitates the work on this particular experiment. Figure III-11 shows the evolution of the average phase ($\Delta\phi$) and amplitude (R) of the magneto-electrically induced optical rotation in time, as the number of fields cycles increases. A cycle corresponds to a measurement with + B, followed by a measurement with -B. The averaging time for each cycle is equal to 140 seconds. Slow drift was compensated by using sequences of +B,-B,-B,+B,+B, -B,..... Because of random fluctuations within the LC, it takes considerable averaging (typically one hour) before a stable and reproducible signal is obtained as shown in the figure above.

III.5.b.2. Frequency Dependence

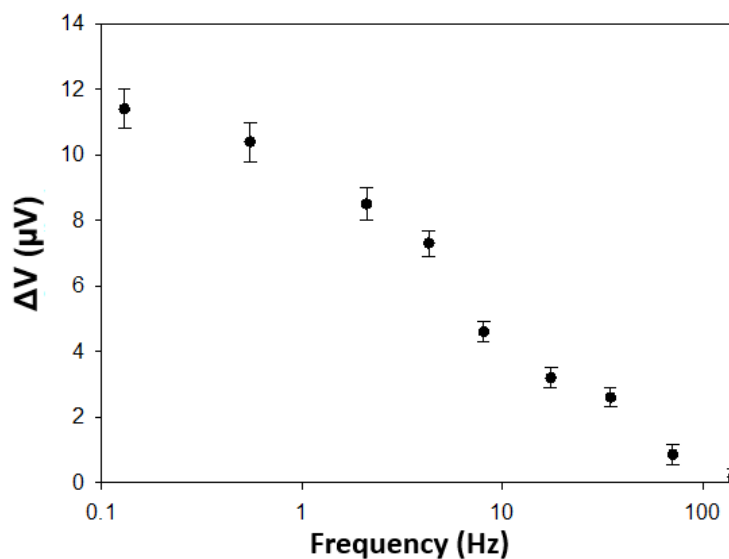


Figure III-12 Frequency dependence of the magneto-electrically induced optical rotation (R) in the nematic phase of eutectic mixture of LC at $V_{HV} = 500\text{V}$, $B = 2.3\text{ T}$

Figure III-12 shows the results for the measured magneto-electrically induced optical rotation signal in a magnetic field aligned NLC cell as a function of the electric field frequency. There are two aspects that determine the dynamics of our experiment. The e.e. generated is intrinsically a non-equilibrium one, and one should expect that it vanishes in the zero frequency limit. We cannot confirm this experimentally, the noise becoming very large at low frequency. The upper frequency limit for the generated e.e. should be of the order of $\omega_r \approx kT/\Delta G$ i.e. extremely high. However, the LC as a whole cannot adapt this fast to the generation of e.e.. A typical timescale for collective reorientation of LC molecules is 20 ms, so one would expect the observed OR to disappear above 50 Hz. This is consistent with our results.

III.5.b.3. Linear Dependence of the Combined E and B on the e.e. of NLCs

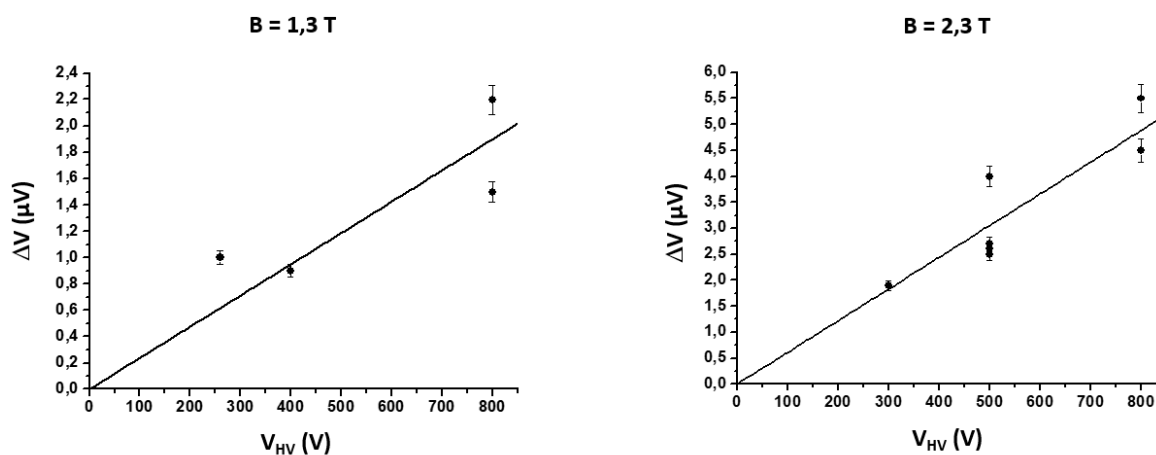


Figure III-13 ΔV is Linearly dependence on the combined B and V_{HV} at an electric field frequency of 37 Hz

Figure III-13 shows the results for the measured magneto-electrically induced optical rotation signal in a magnetic field aligned NLC cell. The two plots show the variation of ΔV as function of the high voltage (V_{HV}) where the magnetic fields are constant at 1.3 and 2.3 T respectively. We have found a linear relation between ΔV and product of B and V_{HV} . But, to present the results more effectively, we processed the calibration of ΔV to denote the vertical axis by label of e.e. using Equation III-7 and the horizontal axis is denoted by $B \cdot V_{\text{HV}}/d$ to have E.B in VT/m. The results in Figure III-13 were obtained at 37 Hz. Because of the observed frequency dependency, we need to rescale our signal to the low frequency limit (see Figure III- 12). We have used a scaling factor of 5 for this correction.

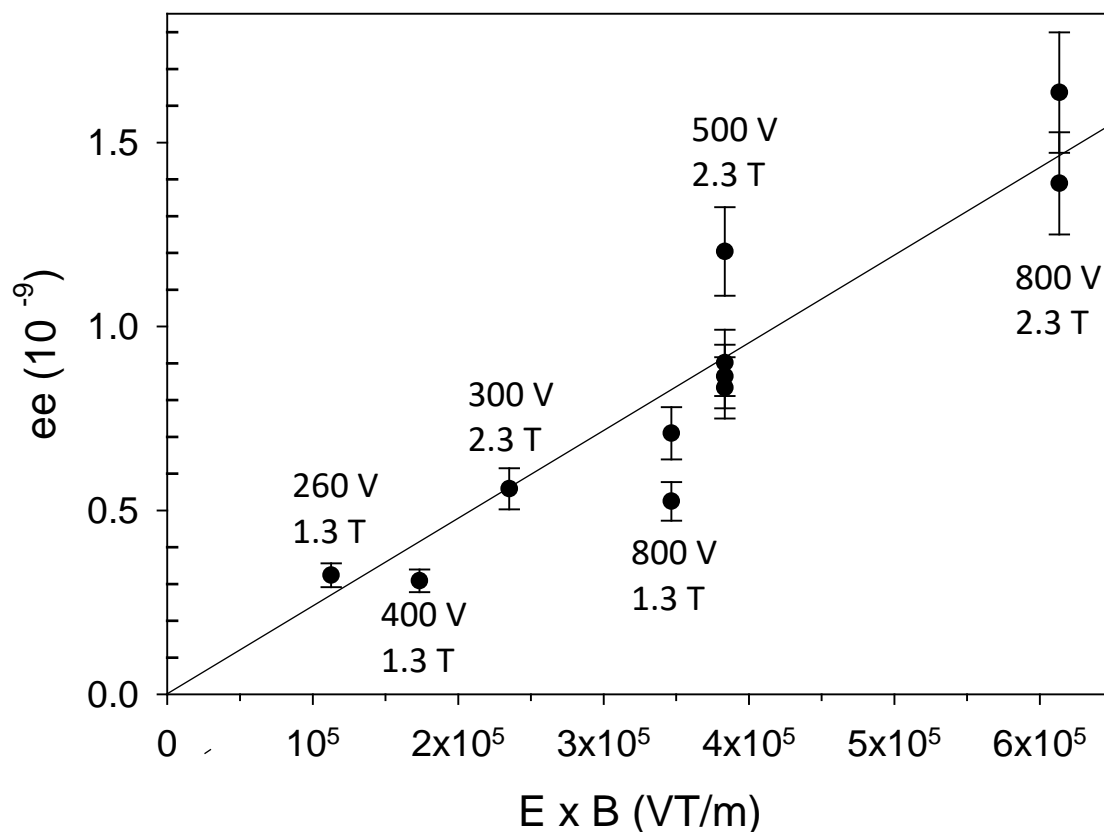


Figure III-14 Enantiomeric excess of the biphenyl derivatives (NLCs) as function of $E \cdot B$, with a linear fit to the data.

From Figure III-14 we can see clearly that there is a linear dependence between e.e. and the product of E and B with a value for the e.e. of 1.4×10^{-9} at 6×10^5 VT/m. The phenomenological model predicted (Eq. III-6) that the e.e. will be equal to 5.1×10^{-10} for $E \cdot B = 6 \times 10^5$ V.T/m i.e. within one order of magnitude of the experimentally observed result. In view of the simplicity of the model, this agreement is considered satisfactory. These results provide a demonstration of the Curie de-Gennes conjecture. However, the inhomogeneity of the LCs alignment of the cells is currently preventing us to get the same results in all zones of the same cell.

It should be noted that there are other optical effects bilinear in E and B , namely the Magneto-electric Linear Birefringence (MELB) [27] and the Magneto-Electric Jones Birefringence (MEJB) [28].

Regarding to the MELB, the general equation for this effect is:

$$\Delta n_{ME}(\theta, \lambda) = k_{ME}(\lambda) \lambda E B \sin \theta \quad \text{Equation III-8}$$

The θ is the angle between the two external fields (E and B), In our case E is perfectly parallel to B so, MELB vanishes.

MEJB is given by:

$$\Delta n_J = n_{+45^\circ} - n_{-45^\circ} = k_J \lambda E \cdot B \quad \text{Equation III-9}$$

Where λ is the wavelength, E and B are externally applied parallel electric and magnetic fields respectively. So that, this effect is proportional to the product of E and B (Equation III-9), and therefore, maximal if E and B are parallel to each other, which is CdG conjecture case. However, Δn_J corresponds to a linear birefringence between the polarization under 45° and -45° with respect to external fields. As our polarization is close to 45° , this makes the MEJB very small. Moreover, the magnitude of the two birefringence's is estimated to be less than 10^{-17} m/(V.T) [25], so for our fields and sample thickness, the maximum dephasing, even if the polarization configuration would be maximal for these two effects, would be 10^{-9} rad which is much smaller than the observed 10^{-6} rad.

III.6. General Conclusion and perspectives

Several empirical approaches were used to obtain aligned nematic biphenyl based LC cells without light scattering. Optically clear and non-scattering cells were obtained using a rubbing method. However, when these cells were subjected to magnetic and electric fields, no significant effect of Curie de-Gennes conjecture was observed.

Using a static magnetic field technique to align LCs inside the cells in place of rubbing method allow us to amplify the effect by preparing a thicker cells 25 μm in place of 8 μm .

It gave us the most convincing results regarding Curie de-Gennes conjecture demonstration.

We have experimentally observed for the first time e.e. of biphenyl-based NLCs derivatives induced by (anti)parallel combination of magnetic and electric fields.

To insure the validity of our results, we have considered the other effects bilinear in E and B for instance Magnetolectric Jones Birefringence (MEJB). But our experimental configuration and the expected magnitude of such effects cannot explain our observations.

However, we still need to confirm our demonstration of the CdG conjecture using optimized conditions and get more reliable results.

References

- [1] P. G. de Gennes and J. Prost, *The Physics of Liquid Crystals*. Clarendon Press, 1995.
- [2] C. Wolf, *Dynamic Stereochemistry of Chiral Compounds*. 2007.
- [3] A. Collet, J. Crassous, J.-P. Dutasta, and L. Guy, *Molécules chirales: Stéréochimie et propriétés*, CNRS. EDP Science, 2006.
- [4] S. Shil and A. Misra, "Electric field induced tuning of molecular conformation to acquire spintronics property in biphenyl systems," *RSC Adv.*, vol. 3, no. 34, pp. 14352–14362, Aug. 2013.
- [5] C. V. Brown, "Physical Properties of Nematic Liquid Crystals," in *Handbook of Visual Display Technology*, J. Chen, W. Cranton, and M. Fihn, Eds. Springer Berlin Heidelberg, 2012, pp. 1343–1361.
- [6] L. D. Barron, "True and false chirality and absolute asymmetric synthesis," *J. Am. Chem. Soc.*, vol. 108, no. 18, pp. 5539–5542, Sep. 1986.
- [7] L. D. Barron, "Can a Magnetic Field Induce Absolute Asymmetric Synthesis?," *Science*, vol. 266, no. 5190, pp. 1491–1492, 1994.
- [8] Y. Takei, T. Yamaguchi, Y. Osamura, K. Fuke, and K. Kaya, "Electronic spectra and molecular structure of biphenyl and para-substituted biphenyls in a supersonic jet," *J. Phys. Chem.*, vol. 92, no. 3, pp. 577–581, Feb. 1988.
- [9] P. G. Cummins, D. A. Dunmur, and D. A. Laidler, "The Dielectric Properties of Nematic 4'-n-pentylcyanobiphenyl," *Mol. Cryst. Liq. Cryst.*, vol. 30, no. 1–2, pp. 109–123, Jan. 1975.
- [10] Iam-choon. Khoo, *Liquid Crystals*. Wiley, 2007.
- [11] D. G. McDonnell *et al.*, "Liquid crystal thiol compounds," Jun. 1994.
- [12] M. A. Osman, "Nematic Liquid Crystals with High Positive Dielectric Anisotropy," *Z. Für Naturforschung B*, vol. 34, no. 8, pp. 1092–1095, 2014.
- [13] D. S. Hulme, E. Peter Raynes, and K. J. Harrison, "Eutectic mixtures of nematic 4'-substitued 4-cyanobiphenyls," *J. Chem. Soc. Chem. Commun.*, vol. 0, no. 3, pp. 98–99, 1974.
- [14] M. Villanueva-García, N. Huerta-Salazar, A. Martínez-Richa, and J. Robles, "Theoretical study of the experimental behavior of two homologous series of liquid crystals," *ARKIVOC*, vol. 2003, no. 11, Dec. 2003.
- [15] G. W. Gray and S. M. Kelly, "Mesomorphic Transition Temperatures and Viscosities for Some Cyano-biphenyls and -p-terphenyls with Branched Terminal Alkyl Groups," *Mol. Cryst. Liq. Cryst.*, vol. 104, no. 3–4, pp. 335–345, Mar. 1984.
- [16] A. Ferrarini, S. Pieraccini, S. Masiero, and G. P. Spada, "Chiral amplification in a cyanobiphenyl nematic liquid crystal doped with helicene-like derivatives," *Beilstein J. Org. Chem.*, vol. 5, Oct. 2009.
- [17] N. Katsonis, E. Lacaze, and A. Ferrarini, "Controlling chirality with helix inversion in cholesteric liquid crystals," *J. Mater. Chem.*, vol. 22, no. 15, pp. 7088–7097, Mar. 2012.
- [18] R. Eelkema and B. L. Feringa, "Amplification of chirality in liquid crystals," *Org. Biomol. Chem.*, vol. 4, no. 20, pp. 3729–3745, Oct. 2006.
- [19] Xiangyi Nie, "Anchoring Energy and Pretilt Angle Effects on Liquid Crystal Response Time," *doctoral dissertation*.
- [20] Y. Cui, R. S. Zola, Y.-C. Yang, and D.-K. Yang, "Alignment layers with variable anchoring strengths from Polyvinyl Alcohol," *J. Appl. Phys.*, vol. 111, no. 6, p. 063520, Mar. 2012.

- [21] J. M. Geary, J. W. Goodby, A. R. Kmetz, and J. S. Patel, "The mechanism of polymer alignment of liquid-crystal materials," *J. Appl. Phys.*, vol. 62, no. 10, pp. 4100–4108, Nov. 1987.
- [22] M. I. Boamfa, S. V. Lazarenko, E. C. M. Vermolen, A. Kirilyuk, and T. Rasing, "Magnetic Field Alignment of Liquid Crystals for Fast Display Applications," *Adv. Mater.*, vol. 17, no. 5, pp. 610–614, Mar. 2005.
- [23] "Encyclopedia of Laser Physics and Technology - Faraday rotators." Online available: https://www.rp-photonics.com/faraday_rotators.html.
- [24] "A Radial Molecular Orientation Using a Flow-Induced Aligning Method in a Nematic Liquid Crystal Cell," *Jpn. J. Appl. Phys.*, vol. 34, no. 8R, p. 4129, Aug. 1995.
- [25] L. D. Barron, "Fundamental Symmetry Aspects of Molecular Chirality," in *New Developments in Molecular Chirality*, P. G. Mezey, Ed. Springer Netherlands, 1991, pp. 1–55.
- [26] F. Nemoto, I. Nishiyama, Y. Takanishi, and J. Yamamoto, "Anchoring and alignment in a liquid crystal cell: self-alignment of homogeneous nematic," *Soft Matter*, vol. 8, no. 45, pp. 11526–11530, Nov. 2012.
- [27] T. Roth and G. L. J. A. Rikken, "Observation of magnetoelectric linear birefringence," *Phys. Rev. Lett.*, vol. 88, no. 6, p. 063001, Feb. 2002.
- [28] T. Roth and G. L. J. A. Rikken, "Observation of magnetoelectric jones birefringence," *Phys. Rev. Lett.*, vol. 85, no. 21, pp. 4478–4481, Nov. 2000.

General conclusion (EN)

The Curie de-Gennes conjecture describes the generation of an enantiomeric excess (e.e.) by a falsely chiral influence away from thermodynamic equilibrium. We have described in this thesis our efforts to confirm experimentally this Curie de-Gennes conjecture. In chapters II and III, we discuss illustrations and explanations of the motivation, the reasons for the chosen targets and how these targets have been tested under the influence of external forces.

✓ The enantioselective crystallization of a chiral metal-organic framework:

Crystallization from aqueous solutions of the metal-organic framework (MOF) $(\text{NH}_4)_4[\text{MnCr}_2(\text{ox})_6] \cdot 4\text{H}_2\text{O}$ yields a random distribution of Λ and Δ crystals with an unexplained excess of the Λ enantiomer in most of the crystallization processes. The origins of the observed enantiomeric excess might come from the combination of earth rotation or magnetic field, coupled to crystallization at the air-solution interface. After several crystallization process performed under a high speed of rotation or in high magnetic field, the same excess was observed for all conditions. So, at this stage, no real effect of these forces was observed and the proposed reason is the presence of an unknown chiral bias that enhances the formation of the Λ enantiomer that hides any effect of external forces. Accordingly, we have thoroughly searched for other possible origins of the observed excess in order to get rid of them and test again the effect of external forces. After a large number of crystallization experiments of this MOF under different conditions, we have found that performing crystallization process at 15 °C after a harsh cleaning procedures (250°C and NaOH) yields both enantiomers with equal ratio. Subsequently, the effect of external forces was tested again using these optimized conditions. Crystallization in high magnetic field gives a different average of circular dichroism values upon changing the orientation of magnetic field. However, a low number of experiments does not allow to identify unambiguously the effect of the magnetic field because the dispersion of the results is very important and calls for an impressive accumulation of experiments which is not reachable given the limited number of crystallizations that can be done at once.

Crystallization of this MOF using high speed rotatory plates gives much better statistics, by launching more than 24 experiments at the same time. Herein, a small difference between CW and CCW rotation in the average of circular dichroism values was observed. However again, this was not statistically relevant, despite the large number of crystallizations. We conclude that a Curie de-Gennes conjecture demonstration is difficult to be achieved in this system. Therefore we

have switched to a another experiment that might confirm the Curie de-Gennes conjecture by totally different means.

✓ **Magneto-electric enantio-selective catalysis in a Nematic Liquid Crystal (NLCs):**

We present a simple quantitative model how parallel electric and magnetic fields can induce a very small enantiomeric excess (e.e.) away from equilibrium in atropisomeric biphenyl molecules. This e.e. is too small to be detected with practical laboratory electric and magnetic fields. However, the large helical twisting power (HTP) of chiral biphenyls in nematic liquid crystals enables the detection of this expected e.e. by optical rotation measurements. Before doing these optical measurements, the molecules should be well aligned inside the LC cells. Accordingly, the LC cells were fabricated using different alignment methods which are mechanical rubbing and static magnetic field poling. When the cells prepared using rubbing methods were used to measure the magneto-electric induced optical rotation, no significant effect of electric and magnetic fields on the optical rotation of the LC molecules was observed. Among the possible reasons, one of them was that a strong anchoring on the cell walls does not allow to obtain a chiral nematic LC phase. Therefore, a static magnetic field was used to align the LC inside the cells instead of using the rubbing method. Additional advantages of this method over the rubbing method are the ability to prepare a thicker cells (25 μm) which allow to amplify the Curie de-Gennes conjecture effect and the absence of possible contamination that may come from the optical tissue. A dedicated setup for the detection of magneto-electrically induced optical rotation was constructed. The magneto-electric induced optical measurements for the cells prepared using the magnetic field alignment method gave us the most reliable results, for the time being, where an e.e was observed experimentally for the first time upon applying (anti)parallel combination of magnetic and electric fields. This excess was linearly dependent on the product of E and B and within one order of magnitude of the predicted value. In view of the simplicity of the phenomenological model, this agreement is satisfactory. This experiment therefore tentatively confirms the Curie de Gennes conjecture.

Conclusion Générale (FR)

La conjecture de Curie de-Gennes décrit la génération d'un excès énantiomérique (e.e.) par une influence faussement chirale à l'écart de l'équilibre thermodynamique. Nous avons décrit dans cette thèse notre contribution pour confirmer expérimentalement cette conjecture de Curie de-Gennes. Dans les chapitres II et III, nous avons discuté des illustrations et des explications de notre motivation à ce sujet, les raisons de choix des molécules et comment ces molécules ont été testées sous l'influence de forces externes.

✓ La cristallisation énantiosélective d'un métal organique chiral $(\text{NH}_4)_4[\text{MnCr}_2(\text{ox})_6]\cdot 4\text{H}_2\text{O}$

La cristallisation à partir de solutions aqueuses du cadre organométallique (MOF) $(\text{NH}_4)_4[\text{MnCr}_2(\text{ox})_6]\cdot 4\text{H}_2\text{O}$ donne une distribution aléatoire des cristaux Λ et Δ avec un excès inexplicable de l'énantiomère Λ dans la plupart des processus de cristallisation.

Les origines de l'excès énantiomérique observé pourraient provenir de la combinaison de la rotation terrestre ou du champ magnétique, couplée avec la cristallisation à l'interface solvant/vapeur d'éthanol.

Après plusieurs processus de cristallisation effectués sous une grande vitesse de rotation ou dans un champ magnétique élevé, le même excès a été observé à toutes les conditions. Donc, aucun effet réel de ces forces n'a été observé et la raison proposée est la présence d'un biais chirale inconnu qui améliore la formation de l'énantiomère Λ qui masque tout effet des forces externes.

En conséquence, nous avons soigneusement recherché d'autres origines possibles de l'excès observé afin de nous en débarrasser et de tester à nouveau l'effet des forces externes. Après un grand nombre d'expériences de cristallisation de cette molécule dans différentes conditions, nous avons constaté que le procédé de cristallisation à 15 ° C après des procédures de nettoyage sévères (250 ° C et NaOH) donne les deux énantiomères avec un rapport égal.

Par la suite, l'effet des forces externes a été testé de nouveau en utilisant ces conditions optimisées. La cristallisation dans un champ magnétique élevé donne une moyenne différente de valeurs de dichroïsme circulaire en changeant l'orientation du champ magnétique. Cependant, un faible nombre d'expériences ne permet pas d'identifier sans ambiguïté l'effet du champ magnétique car la dispersion des résultats est très importante et nécessite une accumulation impressionnante d'expériences qui n'est pas atteignable compte tenu du nombre limité de cristallisations réalisables immédiatement.

La cristallisation de cette molécule à l'aide de plaques rotatives à grande vitesse donne de meilleures statistiques, en lançant plus de 24 expériences en même temps. Ici, une petite différence entre la rotation CW et CCW dans la moyenne des valeurs de dichroïsme circulaire a été observée. Cependant, encore une fois, ceci n'était pas statistiquement pertinent, malgré le grand nombre de cristallisations. Nous concluons qu'une démonstration de conjecture de Curie de-Gennes est difficile à réaliser dans ce système. Nous sommes donc passés à une autre expérience qui pourrait confirmer la conjecture de Curie de-Gennes par des moyens totalement différents.

✓ **L'équilibre atropisomérique des biphenyls sous l'influence d'un champ électrique colinéaire au champ magnétique**

Nous présentons un modèle quantitatif simple de façon que les champs électriques et magnétiques parallèles puissent induire un très petit excès énantiomérique (e.e.) loin de l'équilibre dans les molécules de biphenyle atropisomères.

Cet excès énantiomérique est trop petit pour être détecté avec des champs électriques et magnétiques utilisés au laboratoire.

Un arrangement supramoléculaire hélicoïdal des molécules de biphenyls dans la phase nématique augmentera le signal lié à la présence d'un e.e. à un niveau mesurable.

Avant de faire ces mesures optiques, les molécules doivent être bien alignées à l'intérieur des cellules à cristaux liquides.

En conséquence, les cellules à cristaux liquides ont été fabriquées en utilisant différents procédés d'alignement qui sont le frottement mécanique et l'application d'un champ magnétique statique. Lorsque les cellules préparées en utilisant des méthodes de frottement ont été utilisées pour mesurer la rotation optique induite magnéto-électrique, aucun effet significatif des champs électriques et magnétiques sur la rotation optique des molécules cristaux liquides n'a été observé. Parmi les raisons possibles, l'une d'elles était qu'un ancrage fort sur les parois cellulaires ne permettait pas d'obtenir une phase nématique chirale de cristaux liquides.

Par conséquent, un champ magnétique statique a été utilisé pour aligner les cristaux liquides à l'intérieur des cellules au lieu d'utiliser la méthode de frottement. Des avantages supplémentaires de cette méthode par rapport à la méthode de frottement sont la capacité à préparer des cellules plus épaisses (25 μm) qui permettent d'amplifier l'effet de conjecture de Curie de-Gennes et l'absence de contamination possible provenant du tissu optique.

Une configuration dédiée à la détection de la rotation optique induite magnéto-électrique a été construite. Les mesures optiques induites magnéto-électriques pour les cellules préparées en

utilisant la méthode d'alignement de champ magnétique nous ont donné les résultats les plus fiables, pour la première fois, où un e.e. a été observé pour la première fois en appliquant une combinaison (anti) parallèle des champs. Cet excès dépend linéairement du produit de E et B et d'un ordre de grandeur de la valeur prédite. Compte tenu de la simplicité du modèle phénoménologique, cet accord est satisfaisant. Cette expérience confirme donc provisoirement la conjecture de Curie de Gennes.

Perspectives (EN)

Our observation of magneto-electrically induced optical rotation in nematic LC is very promising but clearly needs to be consolidated on other samples. Therefore, up until 11th of October, we were trying to find the suitable conditions to demonstrate Curie de-Gennes conjecture experimentally. To this aim, a new mixture of nematic LC has been ordered from INSTEC company (USA) to obtain the more homogeneous mixtures. Unfortunately, due to complicated delivery procedure, it took two months to be delivered, prior to the final defense.

A more accurate translation of the optical rotation into an e.e. needs to be found. This could be done by inducing a biphenyl e.e. with circularly polarized light illumination in the biphenyl absorption band.

The dynamics of the e.e. generation needs to be studied in more detail, in particular, its non-equilibrium character needs to be confirmed by measurements at very low frequencies. This will only be possible with a much more stable LC sample.

The influence of temperature on the dynamics and the value of the e.e. should be investigated. Improve the model that was developed by Dr. Geert Rikken, in particular, the magnetic transition moment needs to be calculated with a more realistic molecular model. To reach this objective, a collaboration with Prof. A. Milet at Département de Chimie Moléculaire (DCM), Université Grenoble-Alpes is currently developed to perform DFT calculations under electric and magnetic fields. Implement the effect of electric field in the calculation is relatively straightforward whereas the effect of magnetic field is more difficult to be taken into account. A better agreement between the experiment and the calculated e.e. would be a good sign of the robustness of our experimental demonstration.

Perspectives (FR)

Notre observation de la rotation optique induite sous l'effet des champs magnétiques et électriques en LC nématique est très prometteuse mais doit clairement être consolidée sur d'autres échantillons. Par conséquent, jusqu'au 11 octobre, nous avons essayé de trouver les conditions appropriées pour démontrer expérimentalement la conjecture de Curie de-Gennes. Dans ce but, d'autres types de LC nématiques ont été commandés auprès de la société INSTEC située aux Etats-Unis pour obtenir les mélanges les plus homogènes et malheureusement, en raison d'une procédure de livraison compliquée, ce mélange a été livré juste deux jours avant la date de la soutenance.

Une traduction plus précise de la rotation optique en un e.e. doit être trouvée. Cela pourrait être fait en induisant un e.e. biphényle avec une illumination de la lumière polarisée circulairement dans la bande d'absorption du biphényle.

La dynamique de la génération d'e.e. doit être étudiée avec plus de détails, en particulier, son caractère de non-équilibre doit être confirmé par des mesures à très basses fréquences. Cela ne sera possible qu'avec un échantillon de cristaux liquides beaucoup plus stable.

L'influence de la température sur la dynamique et la valeur d'e.e. devrait être étudiée.

Améliorer le modèle qui a été développé par le Dr Geert Rikken, en particulier, le moment de transition magnétique doit être calculé avec un modèle moléculaire plus réaliste. Pour atteindre cet objectif, une collaboration avec le Prof. A. Milet au Département de Chimie Moléculaire (DCM), l'Université Grenoble-Alpes est actuellement développée pour effectuer des calculs DFT sous champs électriques et magnétiques. Un meilleur accord entre l'expérience et l'e.e. calculée serait un bon signe de la robustesse de notre démonstration expérimentale.

